9-21-2015 12:00 AM

Influence of Waves on Groundwater Flows and Geochemistry in a Sandy Nearshore Aquifer: A Combined Field and Modelling Study

Spencer S. Malott
The University of Western Ontario

Supervisor
Clare Robinson
The University of Western Ontario

INFLUENCE OF WAVES ON GROUNDWATER FLOWS AND GEOCHEMISTRY IN A SANDY NEARSHORE AQUIFER: A COMBINED FIELD AND MODELLING STUDY

(Thesis format: Integrated Article)

by

Spencer <u>Malott</u>

Graduate Program in Civil and Environmental Engineering

A thesis submitted in partial fulfillment
of the requirements for the degree of
Master of Engineering Science

The School of Graduate and Postdoctoral Studies
The University of Western Ontario
London, Ontario, Canada

© Spencer Malott 2015

Abstract

Waves are known to influence the flux of pollutants to coastal waters via groundwater discharge. This study combines field measurements with numerical groundwater modelling to evaluate the influence of a period of intensified wave conditions (wave event) on nearshore groundwater flows and geochemistry in a sandy freshwater beach. Comprehensive vertical nested pressure transducer data obtained over a 2.5 day isolated wave event reveal the development of transient groundwater flow recirculations through the nearshore aquifer combined with enhanced water exchange across the sediment-water interface (i.e., beach face). The wave-induced groundwater flows were simulated in FEFLOW using a phase-averaged wave setup approach to represent waves acting on the sediment-water interface. The time-varying measured and simulated hydraulic gradients match well indicating that consideration of wave setup alone, rather than instantaneous (phase-resolved) wave effects, is able to adequately capture wave-induced perturbations in nearshore groundwater flows. Additionally, the impact of the wave-induced groundwater flows on geochemical conditions near the sediment-water interface is illustrated by redox and pH fluctuations over the wave event. The observed fluctuations may considerably impact the fate of reactive pollutants discharging and also recirculating through a nearshore aquifer.

In addition to the importance of the phase-averaged effect of waves, the phase-resolved effects of waves also need to be understood to better predict the fate of chemical and microbial constituents close to the sediment-water interface. Additional high frequency field measurements indicate that the phase-resolved effects of waves account for considerably larger fluxes of water and associated constituents exchanged across the sediment-water interface than the phase-averaged flux. Despite the large magnitude, the flux generated by phase-resolved wave effects is rapidly reversing in direction and thus is not expected to considerably influence dissolved constituents due to its short residence time, estimated to be between < 1 and 70 seconds. However, the exchange of particulates may be important as their transport is strongly governed by attachment and detachment processes. It is proposed that the rapid water exchange processes near the sediment-water interface control the fate and transport of particulate organic matter and fecal bacteria and thus are important for regulating nutrient and microbial coastal water quality.

Co-Authorship Statement

The candidate is responsible for the gathering and analyzing of data in addition to writing the drafts of all chapters of this thesis. Dr. Clare Robinson developed the initial framework for this research, provided assistance with fieldwork and numerical modelling in addition to providing revisions and suggestions for improvement of this thesis. The co-authorship breakdown of Chapters, 3 and 4 are as follows:

Chapter 3: Dynamic groundwater flows and geochemistry in a sandy coastal aquifer

Authors: Spencer Malott, Denis O'Carroll, Clare Robinson

Contributions:

Spencer Malott: Developed field deployment strategy, built field equipment, analyzed and interpreted field data, performed numerical simulations, wrote draft of manuscript

Denis O'Carroll: Aided in field monitoring, provided revisions to draft

Clare Robinson: Initiated research topic, aided in field monitoring, made suggestions for numerical simulations, provided revisions to draft

Chapter 4: Importance of Phase-Averaged versus Phase-Resolved Effects of Waves for Contaminant Transport in Coastal Aquifers

Authors: Spencer Malott, Clare Robinson

Contributions:

Spencer Malott: Developed field deployment strategy, built field equipment, analyzed and interpreted field data, performed numerical simulations, wrote draft of manuscript

Clare Robinson: Initiated research topic, aided in field monitoring, provided revisions to draft

Acknowledgments

Table of Contents

List of Figures

List of Appendices

Chapter 1

1   Introduction

1.1   Background

Increases in urban, industrial and agricultural development has led to the degradation of groundwater quality in many coastal areas [*Bowen, et al.*, 2007; *International Joint Commission*, 2011; *Kornelsen and Coulibaly*, 2014]. In areas where groundwater quality is degraded groundwater discharge can be an important pathway for delivering chemical pollutants (e.g., nutrients, heavy metals, organic compounds, radionuclides) to coastal surface waters. Pollutants delivered by groundwater have been shown to impact nearshore water quality and ecosystem health [*Burnett, et al.*, 2003; *Johannes*, 1980; *Slomp and Van Cappellen*, 2004]. Evaluating the delivery of groundwater pollutants to coastal waters is difficult to quantify because both discharge and pollutant concentrations in aquifers exhibit high spatial and temporal variability [*Winter*, 1999]. Additionally, many chemicals undergo transformations along their subsurface transport pathway prior to being discharged [*Slomp and Van Cappellen*, 2004]. A holistic understanding of the pollution source and the relevant hydrological and reactive processes is therefore required in order to predict the ultimate loading rates to coastal waters.

Forcing from tides and waves results in the recirculation of large quantities of coastal water through the beach aquifer [*Geng, et al.*, 2014; *Robinson, et al.*, 2007b; *Xin, et al.*, 2010]. The subsequent mixing of groundwater and surface water has been shown to strongly influence geochemical conditions (e.g., pH and redox) in the nearshore aquifer. Geochemical processes occurring near the sediment-water interface strongly control the exit conditions and thus discharge fluxes for various pollutants including nutrients, trace elements, and industrial compounds [*Anwar, et al.*, 2014; *Beck, et al.*, 2010; *Lee, et al.*, 2014; *Robinson, et al.*, 2009; *Santos, et al.*, 2009; *Spiteri, et al.*, 2008]. Therefore, to be able to predict the fate and ultimate flux of pollutants to receiving coastal waters there is a need to understand the impact of coastal forcing on the hydrological and geochemical processes in nearshore aquifers and their complex interactions.

While the influence of tides on the groundwater flow and geochemical conditions in coastal aquifers has been well studied [e.g., *Kuan, et al.*, 2012; *Robinson, et al.*, 2007a; *Robinson, et al.*, 2007b; *Santos, et al.*, 2009] knowledge on the influence of waves is limited. Waves present a set of challenges that makes the impacts more difficult to quantify. For instance, waves are temporally variable in height and frequency [*Boufadel, et al.*, 2007; *Xin, et al.*, 2014]. They are also often present with other forcing (e.g., tides) making their effects difficult to isolate. Nevertheless, waves are an important form of coastal forcing common to nearly all coastlines worldwide. Waves breaking near the shore cause an upward tilt in the phase-averaged (i.e., mean) water surface. This increase in the water surface elevation above the still water level (SWL) is referred to as wave setup [*Longuet-Higgins and Stewart*, 1964]. Studies have shown that the onshore pressure gradient associated with wave set up drives recirculation of water across the sediment-water interface and through the beach aquifer. Wave driven groundwater recirculation through the nearshore aquifer has been shown to enhance groundwater discharge and strongly impacts the transport of reactive and conservative constituents within the beach aquifer [e.g., *Anwar, et al.*, 2014; *Bakhtyar, et al.*, 2013; *Boufadel, et al.*, 2007; *Geng, et al.*, 2014; *Robinson, et al.*, 2014; *Xin, et al.*, 2010]. To date, studies investigating the effects of waves on nearshore groundwater flows and solute transport have been numerical or laboratory-based and consequently, there is an absence of field data that quantifies the effects of waves on beach groundwater processes. As most research is conducted in marine settings, quantification of wave effects is difficult due to the various complex forcing that act on different temporal and spatial scales. For example, groundwater processes in marine beaches are influenced by tides, waves as well as density differences between the fresh and saline waters. A freshwater setting like the Great Lakes does not have tides or density variations, thus it is an ideal setting to isolate the effects of waves on nearshore groundwater flows and geochemistry.

Although waves occur at a high frequency studies suggest it is the phase-averaged effects of waves that ultimately drive the groundwater recirculation flow pattern [e.g., *Xin, et al.*, 2010] due to the dampening effect of sediment beds [*Masselink and Puleo*, 2006]. However, the high frequency (i.e., phase-resolved) effects of waves are still important for processes occurring at or near to the SWI where dampening is minimal. Here

groundwater velocities in the shallow sediment may be several orders of magnitude larger than those of the phase-averaged recirculations [e.g., *Horn, et al.*, 1998; *Turner and Masselink*, 1998]. These large and rapidly reversing velocities have been linked to sediment transport and beachface morphology [*Baldock, et al.*, 2001; *Masselink and Puleo*, 2006]; however, there has yet to be any effort to understand their influence on the behaviour of pollutants at the sediment-water interface. For instance, the large velocities and high frequency water exchange driven by the phase-resolved effects of waves may control the fate of particulates such as organic matter (OM) and fecal bacteria (e.g., *E. coli*, enterococci) for which mechanisms such as straining and attachment govern their transport behaviour in porous media [*Huettel, et al.*, 1996; *Phillips, et al.*, 2011]. The physical and chemical processes controlling the fate of OM and fecal bacteria in beaches are important for understanding the transport and transformation of dissolved chemicals (e.g., nutrients, trace metals) in addition to regulating nearshore water quality, respectively. It is therefore necessary to develop an understanding of the underlying flow processes near the SWI to be able to evaluate how they may impact the transport of these particulate constituents.

1.2   Research Objectives

This thesis aims to develop a better understanding of how waves, in particular wave events, alter the groundwater flow dynamics and geochemical conditions within a beach aquifer. The knowledge gained from this research should provide insight into the fate of dissolved and particulate constituents known to be important for ecological and recreational water quality. This thesis is divided into two objectives. The first objective is to evaluate the effects of wave setup on the nearshore groundwater flows and geochemistry in the field at a freshwater Great Lakes beach. A comprehensive field investigation is paired with numerical simulations using FEFLOW [*Diersch,* 2005] to serve as the first form of field-scale validation for using the phase-averaged wave setup approach for modelling coastal groundwater processes. The second objective is to evaluate the relative importance of the phase-resolved and the phase-averaged behaviour of wave-induced groundwater flows near the SWI. The understanding generated is expected to provide insight into the role of phase-resolved wave action in controlling the

behaviour of constituents found near the SWI such as particulate OM and microbial bacteria. This study will ultimately introduce the importance of high-frequency wave effects near the SWI, a concept often only considered by those studying sediment dynamics, to researchers interested in contaminant transport in coastal aquifers.

1.3 Thesis Outline

This thesis is written in "Integrated Article Format". A brief description of each chapter is presented below.

Chapter 1: Introduces the topic and states the research objectives.

Chapter 2: Reviews relevant work related to the role of groundwater – coastal water interaction on the fate of groundwater pollutants. Specific emphasis is given to the effects of waves.

Chapter 3: Details the field methodology, numerical model development and provides analysis of field data and numerical simulations. The results are used to demonstrate the effect of wave setup on the groundwater flows and geochemistry in the beach aquifer. Implications for the fate of groundwater pollutants are discussed.

Chapter 4: Details field methodology, data analysis and provides in-depth discussion of implications of work. The results highlight the difference in the phase-averaged vs. phase-resolved effects of waves. The relative importance of both approaches is discussed in the context of dissolved and particulate constituents.

Chapter 5: Summarizes findings and provides recommendations for future work.

1.4 References

Anwar, N., C. Robinson, and D. A. Barry (2014), Influence of tides and waves on the fate of nutrients in a nearshore aquifer: Numerical simulations, *Adv. Water Resour.*, *73*, 203-213, doi: 10.1016/j.advwatres.2014.08.015.

Bakhtyar, R., A. Brovelli, D. A. Barry, C. Robinson, and L. Li (2013), Transport of variable-density solute plumes in beach aquifers in response to oceanic forcing, *Adv. Water Resour.*, *53*, 208-224, doi 10.1016/j.advwatres.2012.11.009.

Baldock, T. E., A. J. Baird, D. P. Horn, and T. Mason (2001), Measurements and modeling of swash-induced pressure gradients in the surface layers of a sand beach, *Journal of Geophysical Research: Oceans (1978–2012)*, *106*, 2653-2666, doi: 10.1029/1999JC000170.

Beck, A. J., J. K. Cochran, and S. A. Sañudo-Wilhelmy (2010), The distribution and speciation of dissolved trace metals in a shallow subterranean estuary, *Mar. Chem.*, *121*, 145-156, doi: 10.1016/j.marchem.2010.04.003.

Boufadel, M. C., H. Li, M. T. Suidan, and A. D. Venosa (2007), Tracer studies in a laboratory beach subjected to waves, *J. Environ. Eng-ASCE*, *133*, 722-732, doi: 10.1061/(asce)0733-9372(2007)133:7(722).

Bowen, J., K. Kroeger, G. Tomasky, W. Pabich, M. Cole, R. Carmichael, and I. Valiela (2007), A review of land–sea coupling by groundwater discharge of nitrogen to New England estuaries: Mechanisms and effects, *Appl. Geochem.*, *22*, 175-191, doi: 10.1016/j.apgeochem.2006.09.002.

Burnett, W. C., H. Bokuniewicz, M. Huettel, W. S. Moore, and M. Taniguchi (2003), Groundwater and pore water inputs to the coastal zone, *Biogeochemistry*, *66*, 3-33, doi: 10.1023/B:BIOG.0000006066.21240.53.

Geng, X., M. C. Boufadel, Y. Xia, H. Li, L. Zhao, and N. L. Jackson (2014), Numerical study of wave effects on groundwater flow and solute transport in a laboratory beach, *J. Contam. Hydrol.*, 37-52, doi: 10.1016/j.jconhyd.2014.07.001.

Horn, D. P., T. E. Baldock, A. J. Baird, and T. E. Mason (1998), Field measurements of swash induced pressures within a sandy beach, *Coastal Engineering Proc.*, *1*, doi: 10.9753/icce.v26.%25p.

Huettel, M., W. Ziebis, and S. Forster (1996), Flow-induced uptake of particulate matter in permeable sediments, *Limnol. Oceanogr.*, *41*, 309-322, doi: 10.4319/lo.1996.41.2.0309.

International Joint Commission (2011), 15th Biennial Report on Great Lakes Water Quality, Ottawa.

Johannes, R. (1980), Ecological significance of the submarine discharge of groundwater, *Marine. Ecol.- Prog. Ser.*, *3*, 365-373.

Kornelsen, K. C., and P. Coulibaly (2014), Synthesis review on groundwater discharge to surface water in the Great Lakes Basin, *J. Great Lakes Res.*, *40*, 247-256, doi: 10.1016/j.jglr.2014.03.006.

Kuan, W. K., G. Jin, P. Xin, C. Robinson, B. Gibbes, and L. Li (2012), Tidal influence on seawater intrusion in unconfined coastal aquifers, *Water Resour. Res.*, *48*, doi: 10.1029/2011WR010678.

Lee, J., C. Robinson, and R.-M. Couture (2014), Effect of groundwater–lake interactions on arsenic enrichment in freshwater beach aquifers, *Environ. Sci. Technol.*, *48*, 10174-10181, doi: 10.1021/es5020136.

Longuet-Higgins, M. S., and R. Stewart (1964), Radiation stresses in water waves; a physical discussion, with applications, paper presented at Deep Sea Research and Oceanographic Abstracts, Elsevier.

Masselink, G., and J. A. Puleo (2006), Swash-zone morphodynamics, *Continental shelf research*, *26*, 661-680, doi: 10.1016/j.csr.2006.01.015.

Phillips, M. C., H. M. Solo-Gabriele, A. J. Reniers, J. D. Wang, R. T. Kiger, and N. Abdel-Mottaleb (2011), Pore water transport of enterococci out of beach sediments, *Marine pollution bulletin*, *62*, 2293-2298, doi: 10.1016/j.marpolbul.2011.08.049.

Robinson, C., A. Brovelli, D. Barry, and L. Li (2009), Tidal influence on BTEX biodegradation in sandy coastal aquifers, *Adv. Water Resour.*, *32*, 16-28, doi: 10.1016/j.advwatres.2008.09.008.

Robinson, C., B. Gibbes, H. Carey, and L. Li (2007a), Salt-freshwater dynamics in a subterranean estuary over a spring-neap tidal cycle, *J. Geophys. Res.-Oceans*, *112*, doi: 10.1029/2006jc003888.

Robinson, C., L. Li, and D. Barry (2007b), Effect of tidal forcing on a subterranean estuary, *Adv. Water Resour.*, *30*, 851-865, doi: 10.1016/j.advwatres.2006.07.006.

Robinson, C., P. Xin, L. Li, and D. A. Barry (2014), Groundwater flow and salt transport in a subterranean estuary driven by intensified wave conditions, *Water Resour. Res.*, *50*, 165-181, doi: 10.1002/2013WR013813.

Santos, I. R., W. C. Burnett, T. Dittmar, I. G. Suryaputra, and J. Chanton (2009), Tidal pumping drives nutrient and dissolved organic matter dynamics in a Gulf of Mexico subterranean estuary, *Geochem. Cosmochim. Acta*, *73*, 1325-1339, doi: 10.1016/j.gca.2008.11.029.

Slomp, C. P., and P. Van Cappellen (2004), Nutrient inputs to the coastal ocean through submarine groundwater discharge: controls and potential impact, *J. Hydrol.*, *295*, 64-86, doi: 10.1016/j.jhydrol.2004.02.018.

Spiteri, C., C. P. Slomp, M. A. Charette, K. Tuncay, and C. Meile (2008), Flow and nutrient dynamics in a subterranean estuary (Waquoit Bay, MA, USA): field data and reactive transport modeling, *Geochem. Cosmochim. Acta*, *72*, 3398-3412, doi: 10.1016/j.gca.2008.04.027.

Turner, I. L., and G. Masselink (1998), Swash infiltration-exfiltration and sediment transport, *J. Geophys. Res.-Oceans*, *103*, 30813-30824, doi: 10.1029/98JC02606.

Winter, T. C. (1999), Relation of streams, lakes, and wetlands to groundwater flow systems, *Hydrogeology Journal*, *7*, 28-45, doi: 10.1007/s100400050178.

Xin, P., C. Robinson, L. Li, D. A. Barry, and R. Bakhtyar (2010), Effects of wave forcing on a subterranean estuary, *Water Resour. Res.*, *46*, doi: 10.1029/2010WR009632.

Xin, P., S. S. J. Wang, C. Robinson, L. Li, Y. G. Wang, and D. Barry (2014), Memory of past random wave conditions in submarine groundwater discharge, *Geophys Res. Lett.*, *41*, 2401-2410, doi: 10.1002/2014GL059617.

Chapter 2

2   Literature Review

2.1   Introduction

This chapter provides a review of prior research on groundwater-coastal water interactions with specific emphasis on the impact of waves and their implications for the fate of pollutants commonly found in coastal aquifers. Methods of quantifying groundwater–surface water interactions are also discussed. While much of the previous research in this study area has been completed for marine (i.e., salt water) coastlines many of the concepts are transferrable to large inland freshwater seas such as the Laurentian Great Lakes Basin. Herein, the term coastal water refers to both marine waters and inland freshwater seas.

2.1.1   Groundwater discharge to coastal waters

Groundwater discharge is an important part of the hydrologic cycle since it ultimately provides recharge to coastal waters [*Winter, et al.*, 1998]. Groundwater discharge contributes to the water budget of coastal waters indirectly by supplying base-flow to tributaries and directly through seepage across the groundwater-coastal water interface [*Burnett, et al.*, 2001; *Hoaglund, et al.*, 2002; *Moore*, 2010; *Taniguchi, et al.*, 2002]. Direct discharge occurs when the elevation of the water table in the coastal aquifer is higher than the adjacent coastal water level [*Burnett, et al.*, 2003]. The aquifer must also be hydraulically connected to the coastal water body [*Cherkauer and Zvibleman*, 1981] which is the case for permeable beach shorelines. It is now widely recognized that groundwater discharge is an important pathway for delivering pollutants (e.g., nutrients, trace metals, organic compounds, radionuclides) to coastal waters [*Charette and Sholkovitz*, 2006; *Moore*, 1996; *Robinson, et al.*, 2009; *Valiela, et al.*, 1992]. However, unlike pollutant loading associated with riverine discharge, the diffuse and patchy nature of groundwater discharge makes it much more difficult to quantify [*Burnett, et al.*, 2006].
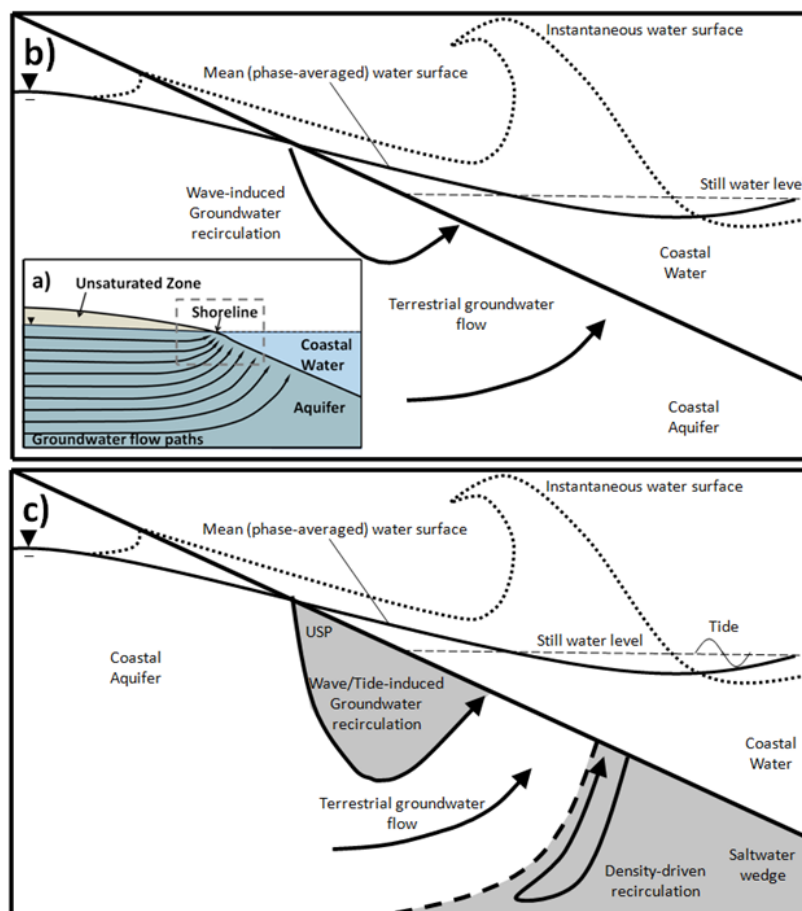
Figure 2-1 A conceptual diagram of (a) an unconfined coastal aquifer also showing the main groundwater flow processes in a (b) freshwater and (c) marine coastal setting. The grey fill in (c) represents salt water within the upper saline plume (USP) and saltwater wedge. The saline formations are not present in freshwater coastal aquifers. The tidal signal would also not be present in a freshwater setting.

Burnett, et al. [2003] estimate that direct groundwater discharge accounts for approximately 6% of the total discharge to the oceans worldwide; however, the assumptions required to make these types of large scale estimates carry a great deal of uncertainty. In the Great Lakes Basin direct groundwater discharge is still poorly quantified. While several studies have attempted to quantify direct discharge through modelling of regional scale aquifer systems [e.g., *Feinstein, et al.*, 2010; *Hoaglund, et al.*, 2002], *Grannemann, et al.* [2000] suggest that most groundwater within the Great Lakes Basin discharges from shallow local flow systems. Nevertheless, studies estimate that in

Lake Michigan, direct discharge accounts for up to 2.6% of the total water budget [*Kornelsen and Coulibaly*, 2014]. Lake Michigan however has the largest area of permeable shoreline [*Grannemann and Weaver*, 1999] and thus the percentage for the overall Great Lakes Basin may be slightly less. While direct groundwater discharge seems to be of little importance from a water budget perspective, pollutant concentrations are often elevated in coastal aquifers due to high population densities near coastlines [*Bowen, et al.*, 2007; *Eckhardt and Stackelberg*, 1995; *Wickham, et al.*, 2002]. Consequently, the contribution of groundwater as a pollutant source to coastal waters rivals that of riverine sources [*Santos, et al.*, 2008; *Slomp and Van Cappellen*, 2004; *Taniguchi, et al.*, 2002].

Groundwater discharge is not entirely terrestrially sourced, rather it includes all water that discharges across the sediment-water interface (SWI). Shorelines are exposed to various coastal forcing (e.g., tides and waves) that cause considerable amounts of water to be recirculated across the SWI [*Burnett, et al.*, 2003; *Santos, et al.*, 2012]. Consequently, the total groundwater discharge rate is often higher than the terrestrial flow of groundwater through the coastal aquifer. For example, a numerical study by *Xin, et al.* [2010] showed that recirculating water from tides and waves made up 61% of the groundwater discharge. Similarly, a field study by *Cable, et al.* [1997] showed that groundwater discharge may contain up to 80 − 90% recirculated water. The forcing conditions present at marine coastlines are different to that of freshwater coastlines. Marine settings experience tidal fluctuations, wave action and density driven flow (Figure 2-1c) [*Robinson, et al.*, 2006]. The salinity structure in a marine beach aquifer consists of an upper saline plume (USP) formed by wave and tide-induced infiltration and a convectively driven saltwater wedge (Figure 2-1c). Conversely, freshwater settings such as the Great Lakes are only exposed to waves and gradual seasonal fluctuations (Figure 2-1b) [*Crowe and Meek*, 2009]. Regardless of the setting, the recirculating water has a unique chemical composition in comparison to the terrestrial groundwater. The subsequent mixing of the two chemically unique sources of water sets up an important geochemical reaction zone – the reactive processes that occur in this zone are important for controlling the fate of groundwater pollutants such as nutrients [*Anwar, et al.*, 2014; *Kroeger and Charette*, 2008; *Slomp and Van Cappellen*, 2004], trace metals [*Beck, et al.*,

2007; *Lee, et al.*, 2014], and organic compounds [*Robinson, et al.*, 2009] in coastal aquifers. These processes are discussed further in Section 2.3 and 2.4.

2.2 Beach Groundwater Dynamics

Beaches serve as an interface between groundwater and surface water [*Crowe and Meek*, 2009; *Horn*, 2002]. The hydrological and geochemical processes occurring at this interface are important for regulating the fate of pollutants in the coastal aquifer. It is therefore imperative to develop an understanding of the fundamental processes of beach groundwater dynamics in order manage pollutant loading to coastal waters. The groundwater regime of a beach aquifer is an unconfined flow system (Figure 2-1a) with groundwater flow occurring in both saturated and unsaturated zones [*Horn*, 2002]. Unconfined conditions dictate that the water table, also referred to as the phreatic surface, is located below grade and its elevation is free to fluctuate in response to hydrologic conditions (e.g., precipitation, evaporation etc.) and various coastal processes (tides, waves, seasonal lake level changes) [*Crowe and Meek*, 2009; *Kang, et al.*, 1994; *Nielsen*, 1990]. The water table is defined as the location where the pore pressures are equal to atmospheric pressure, beneath which, the pore pressures increase linearly with depth [*Turner*, 1998]. Under typical conditions, the water table slopes towards the adjacent coastal water, eventually intersecting the sand surface. This intersection point between the water table and SWI properly defines the location of the shoreline [*Nielsen*, 1989] and is often referred to as the exit point [e.g., *Cartwright, et al.*, 2006; *Turner*, 1993]. Immediately above the water table, a zone of saturation exists called the capillary fringe. Here, groundwater is held under negative capillary forces within the porous media. Water may also enter the unsaturated zone from above via aerial precipitation or by wave/tide driven infiltration.

Figure 2-1a shows the steady-state groundwater flow pattern through a homogeneous beach aquifer during calm surface water conditions. Landward of the shoreline, groundwater flow is generally assumed to be horizontal in homogeneous aquifers [*Schwartz and Zhang*, 2003]. Near the shoreline, flow becomes 2-dimensional with groundwater discharging vertically (upwards) [*Turner*, 1998; *Winter, et al.*, 1998]. The maximum groundwater discharge occurs directly adjacent to the shoreline and decreases

exponentially offshore [*Taniguchi, et al.*, 2002]. The nearshore groundwater flow behaviour becomes much more complex with the introduction of coastal forcing from tides and waves (Figure 2-1b, c). These forcing produce dynamic fluctuations in water table elevation in addition to recirculation of coastal water across the SWI (See section 2.3).
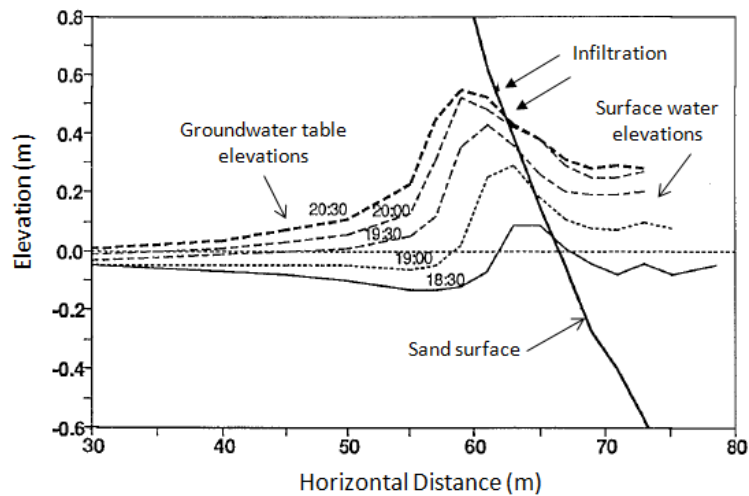
Figure 2-2 Response of the groundwater table elevation in a coastal aquifer subject to waves. Figure adapted from [*Kang, et al.*, 1994]

Like any aquifer system, the beach aquifer water table fluctuates in response to a variety of natural (e.g., precipitation, drought, etc.) and anthropogenic (e.g., pumping) influences. However, the most frequent and dynamic water table fluctuations occur near the shoreline where tides and waves cause infiltration and drainage into and out of the aquifer respectively [*Kang, et al.*, 1994; *Nielsen*, 1990]. The increase in the mean water surface elevation results in a local increase in the beach groundwater table elevation due to infiltrating seawater [*Nielsen*, 1990]. A beach acts as a non-linear, low-pass filter and thus the increase in water table elevation, whether it be at the tidal or wave frequency, is attenuated with increasing landward distance resulting in a local reversal of the terrestrial hydraulic gradient [*Kang, et al.*, 1994; *Nielsen*, 1990; *Robinson, et al.*, 1998]. This behaviour is illustrated in Figure 2-2. The direction and slope of the water table is important for controlling the movement of contaminant plumes in coastal aquifers [*Heiss, et al.*, 2014].

2.3   Effects of Waves on Coastal Aquifers

2.3.1   Wave setup and groundwater recirculation

Waves are a complex coastal forcing that affect nearly all shorelines worldwide to some extent. Studies have shown that wave-driven recirculation can contribute as a significant component of groundwater discharge. For instance, numerical simulations by *Xin, et al.* [2010] showed wave setup alone contributed up to 49% of groundwater discharge. The wave-induced recirculation also enhances mixing between groundwater and coastal water in the beach aquifer [e.g., *Li, et al.*, 1999; *Robinson, et al.*, 2014; *Xin, et al.*, 2010] and in turn may strongly regulate the loading of pollutants to coastal waters [*Anwar, et al.*, 2014].

Incident waves break in a nearshore region called the surf zone which causes a dissipation of radiation stresses in the water column. This produces a positive (upward) slope in the phase-averaged (mean) water surface extending from the wave breaking point to the average wave run up limit (Figure 2-1b, c) [*Li and Barry*, 2000; *Longuet-Higgins*, 1983]. This phenomenon is referred to as wave setup [*Longuet-Higgins and Stewart*, 1964; *Nielsen*, 2009]. Conversely, offshore of the surf zone, shoaling waves cause an increase in water column radiation stress producing a negative (downward) slope in the phase-averaged water surface [*Li and Barry*, 2000; *Longuet-Higgins and Stewart*, 1964] – this is referred to as wave set-down. The upward sloping gradient associated with wave setup produces a mean-onshore pressure gradient that drives groundwater recirculations through the beach aquifer (Figure 2-1b, c). At marine coastlines the groundwater recirculation is also tidally and convectively driven due to the density gradient between the saline surface water and fresh groundwater and thus the extent of the recirculation is typically larger than that of freshwater coastlines. Nevertheless, studies have shown wave-induced groundwater recirculations in large inland water bodies such as the Great Lakes are important [e.g., *Lee, et al.*, 2014].

Sediment beds such as those of permeable coastal shorelines act as low-pass filters, effectively attenuating high-frequency pressure gradients imposed on the beach face by waves [*Masselink and Puleo*, 2006]. Consequently, it is the lower frequency, phase-

averaged behaviour that drives the bulk groundwater recirculation through the beach. *Longuet-Higgins* [1983] was the first to demonstrate the phase-averaged effects of wave setup on the groundwater flows beneath a permeable sloping beach through laboratory experiments. He proposed an analytical solution to the hydraulic head distribution and subsequent groundwater flows through the beach produced by wave setup and qualitatively evaluated this solution through tracer dye experiments. Later, numerical simulations by *Li and Barry* [2000] showed that the extent of the recirculation zone is regulated by the height of the beach water table relative to the wave setup limit. For example, a high water table acts to counterbalance the intrusion of the wave-induced recirculation whereas a low water table does the opposite, allowing for the development of a larger recirculation zone. Until recently, wave setup had mainly been studied with regards to its potential impact on the stability of natural coastal systems (e.g., wetlands, sand dunes) and engineered structures (e.g., piers and harbours) [*Dean and Walton Jr.*, 2008]. In recent years, studies have shown the effects of wave setup and the subsequent groundwater recirculations on the fate and transport of nearshore groundwater chemicals via laboratory experimentation [*Boufadel, et al.*, 2007] and numerical simulations [*Geng, et al.*, 2014; *Li, et al.*, 1999; *Robinson, et al.*, 2006; *Robinson, et al.*, 2014; *Xin, et al.*, 2010; *Xin, et al.*, 2014].

Numerical simulations by *Li, et al.* [1999] suggested that wave setup has the potential to contribute to the release of large fluxes of chemicals over short periods of time into coastal waters. Waves have also been shown to be important for solute transport within beach aquifers causing increased dispersion in addition to modification of the discharge pathway leading to increased residence time of conservative solute plumes [*Bakhtyar, et al.*, 2013; *Boufadel, et al.*, 2007; *Geng, et al.*, 2014]. While most studies evaluating the impacts of waves on groundwater discharge and solute transport utilize a steady wave condition, in reality, waves are a non-steady forcing. Waves are often temporally variable exhibiting 'event' type behaviour where a peak wave height is reached in response to a storm [e.g., *Cartwright, et al.*, 2004]. To address this, *Robinson, et al.* [2014] performed numerical simulations at a field-scale marine beach to observe the impact of wave events on groundwater flow patterns and salt transport in the USP and saltwater wedge. They simulated events where the wave height gradually grew to a peak (maximum offshore

wave height = 7 m) and then declined back to pre-event conditions. The observed groundwater recirculations and salt influx into the aquifer grew in response to the wave height. Although the groundwater flows quickly returned to pre-event conditions following the wave event, the salt distribution was much slower to respond. This suggests that although the duration of a wave event may be short, it could have long lasting impacts on the geochemical conditions of coastal aquifers. *Xin, et al.* [2014] also explored the effects of variable wave conditions on groundwater discharge and salt transport in response to a year-long time series of random offshore wave heights. Their findings are consistent with *Robinson, et al.* [2014] adding that the antecedent conditions are important for evaluating the impact of a wave event.

There is a significant lack of field data regarding groundwater flow and geochemical dynamics of nearshore aquifers in response to wave events. This is likely because isolating the effects of waves at a marine beach where there are numerous competing factors (i.e., tides and density driven flow) is difficult to do. Although the wave setup approach has been used to simulate wave induced recirculation it has yet to be validated by field data. Freshwater settings such as the Great Lakes provide an ideal setting to address this gap in the research as the lack of tides and density effects means that changes in groundwater flows and geochemistry can be directly attributed to waves alone.

2.3.2 Swash – groundwater interaction

The swash zone is the part of the beachface where fluid coverage is intermittent due to the uprush and backwash of waves (i.e., swash). Although the bulk groundwater flow through the beach is driven by the phase-averaged wave setup, the groundwater velocities in the shallow sediments beneath the swash zone driven by the phase-resolved effects of waves are considerably larger than the phase-averaged. For instance, *Turner and Masselink* [1998] estimated swash-driven phase-resolved velocities measured in the field to be up to $O(10^2)$ larger than the average velocities calculated using a simple one-dimensional modified Boussinesq equation. Another unique feature of swash-driven groundwater flow is that it rapidly (i.e., within a single swash cycle) reverses between large fluxes of both infiltration and exfiltration [e.g., *Baldock, et al.*, 2001]. Consequently, the total volume of water filtered though the shallow aquifer may be

considerably larger than the phase-averaged (i.e., net) wave-induced volume. While these high frequency effects are attenuated in the aquifer, they may have important implications for particulates and colloids such as particulate organic matter (POM) and fecal bacteria (e.g., *E. coli,* enterococci) exchanged across the SWI as their transport through porous media tends to be retarded by straining and attachment [*Díaz, et al.*, 2010; *Huettel, et al.*, 1996; *Whitman, et al.*, 2014] (see Section 2.4). To the author's knowledge, *Heiss, et al.* [2014] present the only study that has proposed that swash-scale processes may be important for the biogeochemical conditions near the SWI of coastal aquifers. They measured high frequency moisture dynamics in response to swash overtopping the unsaturated zone and used these measurements to calculate infiltration rates. From their findings, *Heiss, et al.* [2014] inferred that the moisture dynamics and subsequent water table response have important implications for transport of reactive constituents in the beach aquifer; however, this was not quantified.

2.4   Influence of Beach Groundwater Dynamics on Pollutant Discharge

2.4.1   Nutrients cycling and transport

This section provides a brief overview of the key processes controlling the fate and transport of nutrients (nitrate [NO_3^-], phosphate [PO_4^{3-}] and ammonium [NH_4^+]) in nearshore aquifers. Understanding the flux of nitrogen (N) and phosphorus (P) to coastal waters is particularly important for the sustainability of phytoplankton populations, which require an N/P ratio of 16:1, otherwise known as the Redfield ratio. Changes in this ratio may also lead to algae blooms and eutrophication impacting the ecological structure and biodiversity of coastal ecosystems [*Howarth, et al.*, 2000; *Howarth*, 1988; *Valiela, et al.*, 1990]. The fate of nutrients and their ultimate discharge to coastal waters depends greatly on the prevailing redox conditions along their subsurface transport pathway [*Slomp and Van Cappellen*, 2004]. Tides and waves deliver surface water into the aquifer bringing with it considerable quantities of dissolved oxygen (DO) and organic matter (OM). The availability of the these constituents strongly influence geochemical conditions and can lead to strong geochemical (pH and redox) gradients forming near the SWI [*Anschutz, et al.*, 2009; *McLachlan, et al.*, 1985; *Robinson, et al.*, 2007a; *Santos, et al.*, 2009]. These

gradients have been shown to regulate the ultimate flux of N and P to coastal waters with geochemical pathways including denitrification and nitrification leading to transformation and mass loss/production of chemical species [*Anwar, et al.*, 2014; *Kroeger and Charette*, 2008; *Slomp and Van Cappellen*, 2004; *Spiteri, et al.*, 2008]. The nutrients in coastal aquifers are derived from two primary sources: (1) from terrestrially derived contamination (e.g., agriculture, septic systems) and (2) from OM delivered into the aquifer via coastal forcing. For the latter source, remineralization (i.e., decomposition) of OM converts organic N and P back to their dissolved inorganic forms (e.g., ammonium and phosphate) [*Anschutz, et al.*, 2009; *Charbonnier, et al.*, 2013; *McLachlan, et al.*, 1981]. This process also regulates the redox conditions in the nearshore aquifer as remineralization consumes oxygen and other electron acceptors leading to anoxic/reducing conditions. Nutrients derived from surface water OM remineralization or terrestrial sources may be released to coastal waters via groundwater discharge; however, their transport depends on the chemical transformations that may occur along the groundwater flow path [*Slomp and Van Cappellen*, 2004]. For instance NH_4^+ may be removed via nitrification in oxic groundwater leading to the formation of NO_3^-. Conversely, under anoxic conditions NO_3^- may be removed through denitrification [*Anwar, et al.*, 2014; *Kroeger and Charette*, 2008; *Slomp and Van Cappellen*, 2004; *Spiteri, et al.*, 2008]. PO_4^{3-} can also undergo important geochemical processes in coastal aquifers whereby its transport is attenuated through adsorption to ferric (hydr)oxides that precipitate along redox boundaries set up near the SWI [*Charette and Sholkovitz*, 2002].

In addition to affecting the geochemical conditions in a nearshore aquifer, tide and wave-driven groundwater recirculation has also been shown to increase the residence time of chemicals including nutrients discharging through the nearshore aquifer. This has been observed through increased dispersion and the movement of the terrestrial discharge zone further offshore [e.g., *Bakhtyar, et al.*, 2013; *Geng, et al.*, 2014]. The resulting increase in residence time is important for the fate of terrestrially derived nutrients as it may correspond to increased transformation or removal of chemical species within the aquifer prior to discharge.

2.4.2 Microbial contaminants

Beaches, whether marine or freshwater, provide significant recreational and tourism benefits. The water quality at beaches is often impaired due to high levels of fecal contaminants (e.g., from wastewater outfall, birds, dogs etc.). Understanding the drivers behind water quality is important for beach managers to effectively ensure public safety for beach users. Microbial beach water quality is typically assessed through the detection of fecal indicator bacteria (FIB, e.g., *E. coli,* enterococci) in the surface water [*Health Canada*, 2012]. Their occurrence positively correlates with the presence of harmful pathogens known to cause gastrointestinal illness in humans [*Cabelli, et al.*, 1982]. While the occurrence of FIB in surface waters had long been considered to come primarily from point sources (*e.g.,* storm water outfall, sewage discharge etc), it is now well established that FIB are present in large concentrations in beach sands [*Alm, et al.*, 2003; *Whitman, et al.*, 2014]. Beach sands therefore act as a reservoir of bacteria and have been identified as a potential source for surface waters if mobilized [*Ge, et al.*, 2010; *Yamahara, et al.*, 2007].

Numerous chemical, microbial and physical processes including waves play an important role in the accumulation and ultimate fate of FIB in the shallow groundwater and sand at beaches where concentrations are typically elevated by several orders of magnitude relative to surface waters [*Edge and Hill*, 2007; *Gast, et al.*, 2015; *Phillips, et al.*, 2014; *Whitman and Nevers*, 2003]. Recent field studies by *Russell, et al.* [2012] and *Gast, et al.* [2015] showed wave-induced infiltration is a means of delivering surface water-derived FIB into beach sands. Conversely, studies have shown that the FIB concentrations in shallow surface water is often related to the adjacent sand quality suggesting that FIB may be released back to coastal waters under certain conditions [*Alm, et al.*, 2003; *Beversdorf, et al.*, 2007; *Ge, et al.*, 2010]. While it is suspected groundwater discharge may be a potential pathway for transporting FIB from beach sand into receiving coastal waters [*Boehm, et al.*, 2004; *Gast, et al.*, 2015; *Russell, et al.*, 2012] the transport of FIB through sand is affected by sediment interactions including straining as well as attachment to sand grains, biofilms, OM and the air-water interface [*Díaz, et al.*, 2010; *Russell, et al.*, 2012; *Whitman, et al.*, 2014]. Mechanistic understanding of the underlying

physical flow processes in the nearshore groundwater and associated sand is needed to understand why and under what conditions FIB accumulates and is subsequently released from the sand reservoir. For instance, the large groundwater velocities and water exchange through the shallow sediments induced by the phase-resolved effects of waves may not only be important for delivering FIB into the sand but also releasing it back to coastal waters.

2.5 Quantifying Wave-Induced Groundwater – Coastal Water Interactions

Groundwater – coastal water interactions have been successfully quantified using several techniques such as nested piezometers, pressure sensors, seepage meters, natural tracers and numerical groundwater modelling. Although certain techniques are more suited for evaluating regional (e.g. tracers, modelling) as opposed to localized groundwater discharge (e.g. seepage meters, nested piezometers), it is widely acknowledged that accurate characterization of groundwater-coastal water interactions requires several techniques to be used to cross validate results [*Burnett, et al.*, 2006; *Kalbus, et al.*, 2006].

2.5.1 Hydraulic head based measurements

Using the principle that groundwater discharge has a considerable vertical flow component, multi-level piezometer nests can be used to measure vertical head gradients below the SWI [*Burnett, et al.*, 2006; *Robinson, et al.*, 2007a; *Turner*, 1998]. Estimation of the groundwater seepage flux can be calculated using the one-dimensional Darcy's Law (Equation 1):

$$q = -K\frac{dh}{dz} \quad (1)$$

Where q is the Darcian flux [LT^{-1}], K is the hydraulic conductivity of the soil, and *dh/dz* is the head gradient. Head elevations within piezometers are often monitored using a tape measure; however, manually measuring hydraulic heads can be time consuming, especially with a large number of piezometers. Therefore, it is common to install pressure sensors, which automatically measure the head level at a specified frequency. Pressure sensors are considerably more costly than manual measurements; however they produce

results over a wide range of temporal resolutions to a high degree of accuracy. Nested pressure sensors have also been directly buried [e.g., *Turner and Masselink*, 1998; *Turner and Nielsen*, 1997] and installed in screened PVC casings (Figure 2.3) [e.g., *Gibbes, et al.*, 2007]. Similar to nested piezometers, nested pressure sensors measure a head gradient and therefore the vertical groundwater seepage flux can also be quantified using Darcy's law (Equation 1). It is worth noting that piezometers and pressure sensors are a trusted method for determining localized groundwater discharge; however, their accuracy depends on obtaining a representative value of the hydraulic conductivity, which can vary over several orders of magnitude. Consequently, these discrete methods may suffer from spatial variability in subsurface geology [*Burnett, et al.*, 2006].

2.5.2   Direct measurements

The most direct measurement method of localized groundwater discharge is with a seepage meter [*Lee*, 1977], where a bottomless steel drum is embedded in the sea/lakebed and vented to a deflated collection bag into which groundwater seeps into or out of (Figure 2.3). The bag should be partially prefilled with water and periodically checked. Any change in volume represents infiltration or exfiltration across the SWI. More advanced systems such as a heat pulse meter have since been implemented to replace the tedious bag collection method [*Taniguchi and Fukuo*, 1993]. Seepage meters are advantageous since knowledge of the hydraulic conductivity is not required. Seepage meters however should not be used in areas subject to wave action or strong currents because these can lead to artifacts in seepage volume [*Kalbus, et al.*, 2006; *Shinn, et al.*, 2002]. In addition, the application of seepage meters is limited to offshore where they remain submerged and thus they cannot provide any estimates of exchange fluxes across the swash zone or intertidal zone where submergence is intermittent.
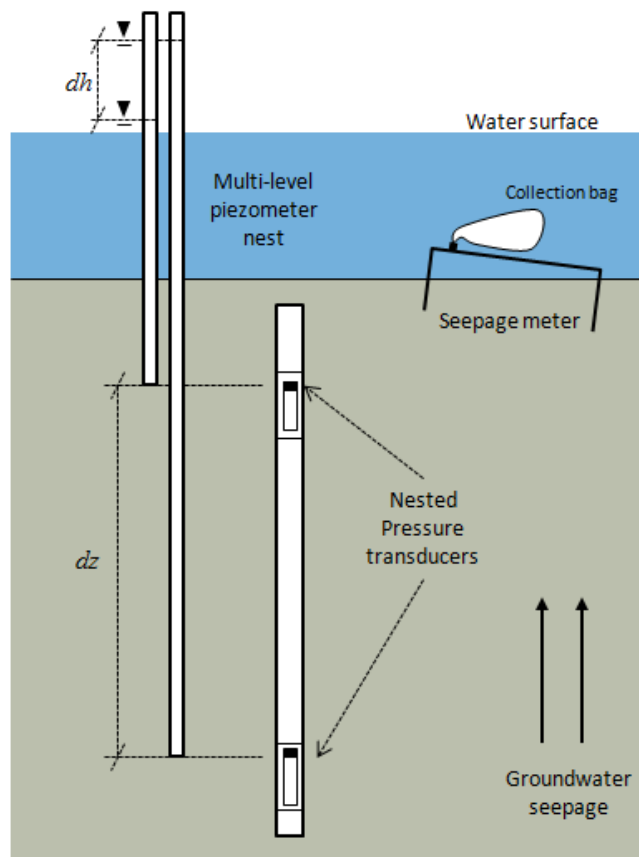
Figure 2-3 Common techniques for quantifying vertical groundwater seepage

2.5.3   Geophysical and geochemical tracers

Tracers for estimating groundwater discharge can be categorized as either geophysical or geochemical [*Burnett, et al.*, 2006]. Geophysical techniques use physical characteristics of the groundwater and subsurface sediments whereas geochemical techniques use chemical properties of the groundwater and surface water end members. In general, tracer techniques are used for larger spatially and temporally scaled monitoring regimes as the small scale variability tends to be smoothed over time and space [*Burnett, et al.*, 2001]. A brief discussion of select tracers is presented below.

Two common geophysical tracers used to assess groundwater discharge are (1) temperature and (2) the bulk electrical resistivity (ER) of the seafloor [*Anderson*, 2005; *Befus, et al.*, 2013; *Burnett, et al.*, 2006; *Schmidt, et al.*, 2007]. Temperature can be used to estimate vertical groundwater discharge based on the thermal gradient between

groundwater and surface water end members [*Anderson*, 2007; *Rau, et al.*, 2010]. Temperature – depth profiles can be fit to type-curves for different groundwater velocities based on the assumption of one-dimensional conduction – advection heat transport [*Taniguchi*, 1993]. Other temperature-based methods such as thermal imaging have also been used to qualitatively delineate zones of groundwater discharge [*Banks, et al.*, 1996; *Deitchman and Loheide*, 2009]. In the summer months, discharge zones appear cooler than the ambient air and surface water temperatures and vice versa in the winter. Similarly, the use of ER is another qualitative geophysical technique that has been used to assess the salinity structure in the subsurface for which qualitative information about groundwater discharge patterns can be inferred [*Befus, et al.*, 2013]. ER is most useful in marine environments where resistivity difference between seawater and fresh groundwater is high.

Many naturally occurring geochemical tracers such as radionuclides (e.g., ^{226}Ra, ^{222}Rn) are used for determining groundwater discharge rates since concentrations are typically much higher in groundwater than in coastal water [*Burnett, et al.*, 2006]. To properly assess the relationship between the occurrence of the tracer and a quantitative groundwater discharge estimate, all sources and sinks must be identified which can be an arduous task. ^{222}Rn, which has a half life of 3.8 days [*Moore*, 2010] has been proven on many occasions to be a suitable tracer for estimating groundwater discharge to coastal waters [e.g., *Burnett and Dulaiova*, 2003; *Cable, et al.*, 1996; *Corbett, et al.*, 2000; *Lambert and Burnett*, 2003]. In order to link the concentration of ^{222}Rn in the surface water to groundwater discharge a groundwater end member concentration must be known. Then a mass balance approach can be used whereby a nearshore inventory is supplied by benthic activity and groundwater discharge and is subject to losses through atmospheric evasion and offshore mixing [*Burnett and Dulaiova*, 2003]. However, there is still a great deal of uncertainty with regards to how to properly assess a suitable end member concentration as heterogeneities in geology and geochemistry in the subsurface results in spatial and temporal variation of radon concentrations [*Dulaiova, et al.*, 2008].

2.5.4   Numerical groundwater flow modelling

Validated numerical models can be an efficient, cost effective approach for investigating hydrological and biogeochemical processes occurring in nearshore aquifers. Depending on the modelling objective, different scales are used (i.e., regional vs. local). Several regional scale three-dimensional models have been developed to assess the regional contribution of groundwater discharge to coastal waters [e.g., *Feinstein, et al.*, 2010; *Hoaglund, et al.*, 2002]. These models are highly sophisticated and require large amounts of information for model construction and calibration. Different numerical modelling software including FEFLOW [*Diersch*, 2005], MODFLOW [*McDonald and Harbaugh*, 1988], SUTRA [*Voss*, 1984], MARUN [*Boufadel, et al.*, 1999] etc. employing different mathematical methods (e.g., finite difference, finite element) are available and have been used to solve various groundwater and contaminant transport scenarios in coastal aquifers.

Numerical models used to evaluate groundwater discharge from nearshore aquifers in addition to the influence of dynamic coastal forcing on a nearshore aquifer often use simplified two-dimensional vertical slice cross sections [e.g., *Geng and Boufadel*, 2015; *Robinson, et al.*, 2007b; *Xin, et al.*, 2010]. This type of model has also been used to assess the fate of reactive chemical constituents in nearshore aquifers exposed to tides and waves [e.g., *Anwar, et al.*, 2014; *Robinson, et al.*, 2009; *Spiteri, et al.*, 2008]. The simulated interaction between groundwater and surface water is governed by the boundary conditions and the parameter values assigned in the model. The landward boundary of a two-dimensional nearshore groundwater model domain is generally assigned as either a constant head [e.g., *Geng, et al.*, 2014; *Lee, et al.*, 2014] or constant flux boundary [e.g., *Abarca, et al.*, 2013; *Robinson, et al.*, 2007b]. This boundary is important because it controls the terrestrial groundwater discharge though the aquifer which has been shown to counterbalance the extent of the groundwater recirculation and subsequent mixing induced by tide and wave forcing [*Robinson, et al.*, 2007c; *Robinson, et al.*, 2014]. The boundary condition applied along the SWI is used to simulate the effect of tides and/or waves on groundwater flow dynamics in the aquifer. Numerous approaches have been used to simulate the effects of waves on nearshore groundwater

dynamics. For instance, studies have used both the phase-averaged and phase-resolved approach to generate a boundary condition to simulate the effect of waves. The most computationally intensive and complex approach involves the implementation of the phase-resolved, time-varying specified heads along the SWI boundary that represent the forcing from instantaneous wave action. The BeachWin model [*Li, et al.*, 2002] was one of the first attempts to simulate the phase-resolved effects of waves on groundwater flows in a permeable nearshore aquifer. This model generates the seaward boundary condition by solving the shallow water wave equations. *Xin, et al.* [2010] used BeachWin to generate the boundary condition for their model investigating wave impacts on groundwater flow and salt transport dynamics in a nearshore aquifer. *Bakhtyar, et al.* [2009] simulated the hydrodynamics of waves using the Reynolds Averaged Navier Stokes (RANS) equations. This approach has since been used to generate the boundary condition for studies involving the impact of coastal forcing on solute transport in nearshore aquifers [*Bakhtyar, et al.*, 2012; *Bakhtyar, et al.*, 2013; *Geng and Boufadel*, 2015; *Geng, et al.*, 2014] and beach morphology [*Bakhtyar, et al.*, 2011]. While simulating the phase-resolved effects of waves may arguably produce the most accurate representation of field conditions, it requires considerable computational effort through the implementation of very small time steps and fine grid discretization.

Xin, et al. [2010] compared results from simulations using both the phase-resolved (instantaneous waves) and phase-averaged (wave setup only) boundary conditions. Their findings revealed similar water exchange rates as well as similar groundwater flow and solute transport in the nearshore aquifer suggesting that using the simplified, phase-averaged approach provides adequate performance despite its highly reduced computational demand. Use of the wave setup approach is also advantageous when simulating combined forcing (i.e., waves and tides together) due to its reduced computational demand [*Bakhtyar, et al.*, 2013]. Several studies have used a simple empirical wave setup formula for the boundary condition derived by *Nielsen* [2009]:

$$\bar{\eta} = \frac{0.4 H_{rms}}{1 + 10 \dfrac{D + \bar{\eta}}{H_{rms}}} \qquad (2)$$

where η (m) is the increase in mean water level above the still water level due to wave setup; H_{rms} (m) is the offshore root mean square wave height; and D (m) is the distance from the SWI to the still water level. This approach was adopted recently by *Robinson, et al.* [2014] and *Xin, et al.* [2014] to investigate the impacts of variable wave conditions on submarine groundwater discharge and salt transport through nearshore aquifers. *Anwar, et al.* [2014] also adopted this approach in their investigation of the effects of coastal forcing on nutrient dynamics. Although these studies used the findings from *Xin, et al.* [2010] to justify their use of the simplified wave setup approach in numerical simulations there has yet to be any field validation of this approach. It remains uncertain if it is reasonable to assume that the simplified wave setup approach can adequately capture the wave-induced groundwater flows given the complexity often observed in the field.
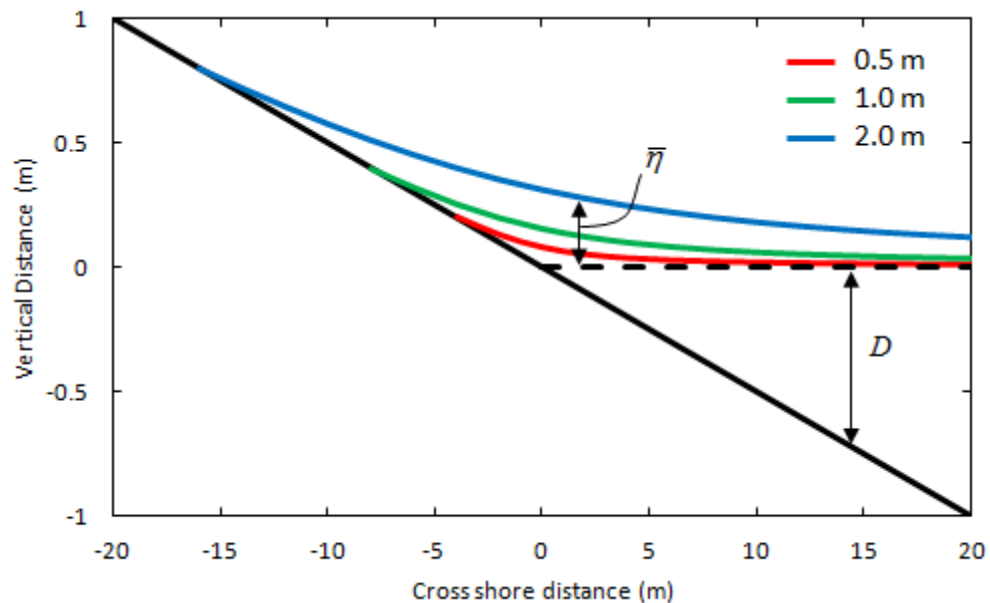
Figure 2-4 The mean water surface given by the solution of Equation 2 is shown for three different offshore wave heights. The solid black line and dashed black line represent the beach surface and still water level respectively

2.6 Summary

This chapter has described the importance of coastal groundwater discharge and the influence of coastal forcing, particularly waves, on the fate of pollutants in nearshore aquifers and their subsequent flux to coastal waters. A critical review of previous work reveals several research gaps that need to be addressed to better understand the effect of waves on the nearshore aquifer dynamics, and subsequently the fate of pollutants near the SWI in nearshore environments. While prior studies have numerically evaluated the impacts of waves on groundwater discharge and associated chemical fluxes, there has yet to be any field validation of the wave setup approach commonly used to specify the coastal boundary condition in these models. Chapter 3 of this thesis addresses the need to validate this simplified modelling approach using field data paired with numerical simulations. In addition there is currently limited overlap between research focused on the influence of waves on beachface sediment transport and those focused on understanding nearshore aquifer dynamics to better evaluate groundwater discharge and the fate of pollutants in nearshore aquifers. The latter of the two research communities is generally focused on the bulk movement of water and solutes driven by terrestrial groundwater flow and tide/wave-driven groundwater recirculation, where the former is focused on the high frequency effects of waves near to the SWI. The rapid and highly dynamic shallow groundwater-surface water exchange has been overlooked with respect to its significance for the behavior of pollutants near the SWI. Chapter 4 of this thesis aims to address this lack of understanding by comparing the phase-averaged and phase-resolved effects of waves in the field and assessing the relative importance of these effects for dissolved and particulate constituents in nearshore environments.

2.7 References

Abarca, E., H. Karam, H. F. Hemond, and C. F. Harvey (2013), Transient groundwater dynamics in a coastal aquifer: The effects of tides, the lunar cycle, and the beach profile, *Water Resour. Res.*, *49*, 2473-2488, doi: 10.1002/wrcr.20075.

Alm, E. W., J. Burke, and A. Spain (2003), Fecal indicator bacteria are abundant in wet sand at freshwater beaches, *Water research*, *37*, 3978-3982, doi: 10.1016/S0043-1354(03)00301-4.

Anderson, M. P. (2005), Heat as a ground water tracer, *Ground water*, *43*, 951-968, doi: 10.1111/j.1745-6584.2005.00052.x.

Anderson, M. P. (2007), Introducing groundwater physics, *Physics Today*, *60*, 42-47, doi: 10.1063/1.2743123.

Anschutz, P., T. Smith, A. Mouret, J. Deborde, S. Bujan, D. Poirier, and P. Lecroart (2009), Tidal sands as biogeochemical reactors, *Estuar. Coast. Shelf S.*, *84*, 84-90, doi: 10.1016/j.ecss.2009.06.015.

Anwar, N., C. Robinson, and D. A. Barry (2014), Influence of tides and waves on the fate of nutrients in a nearshore aquifer: Numerical simulations, *Adv. Water Resour.*, *73*, 203-213, doi: 10.1016/j.advwatres.2014.08.015.

Bakhtyar, R., D. A. Barry, and A. Brovelli (2012), Numerical experiments on interactions between wave motion and variable-density coastal aquifers, *Coast. Eng.*, *60*, 95-108, doi: 10.1016/j.coastaleng.2011.09.001.

Bakhtyar, R., A. Brovelli, D. A. Barry, and L. Li (2011), Wave-induced water table fluctuations, sediment transport and beach profile change: Modeling and comparison with large-scale laboratory experiments, *Coast. Eng.*, *58*, 103-118, doi: 10.1016/j.coastaleng.2010.08.004.

Bakhtyar, R., A. Brovelli, D. A. Barry, C. Robinson, and L. Li (2013), Transport of variable-density solute plumes in beach aquifers in response to oceanic forcing, *Adv. Water Resour.*, *53*, 208-224, doi: 10.1016/j.advwatres.2012.11.009.

Bakhtyar, R., A. Ghaheri, A. Yeganeh-Bakhtiary, and D. A. Barry (2009), Process-based model for nearshore hydrodynamics, sediment transport and morphological evolution in the surf and swash zones, *Applied Ocean Research*, *31*, 44-56, doi: 10.1016/j.apor.2009.05.002.

Baldock, T. E., A. J. Baird, D. P. Horn, and T. Mason (2001), Measurements and modeling of swash-induced pressure gradients in the surface layers of a sand beach, *Journal of Geophysical Research: Oceans (1978–2012)*, *106*, 2653-2666, doi: 10.1029/1999JC000170.

Banks, W. S., R. L. Paylor, and W. B. Hughes (1996), Using thermal-infrared imagery to delineate groundwater discharge, *Groundwater*, *34*, 434-443, doi: 10.1111/j.1745-6584.1996.tb02024.x.

Beck, A. J., Y. Tsukamoto, A. Tovar-Sanchez, M. Huerta-Diaz, H. J. Bokuniewicz, and S. A. Sanudo-Wilhelmy (2007), Importance of geochemical transformations in determining submarine groundwater discharge-derived trace metal and nutrient fluxes, *Appl. Geochem.*, *22*, 477-490, doi: 10.1016/j.apgeochem.2006.10.005.

Befus, K. M., M. B. Cardenas, D. V. Erler, I. R. Santos, and B. D. Eyre (2013), Heat transport dynamics at a sandy intertidal zone, *Water Resour. Res.*, doi: 10.1002/wrcr.20325.

Beversdorf, L., S. Bornstein-Forst, and S. McLellan (2007), The potential for beach sand to serve as a reservoir for Escherichia coli and the physical influences on cell die-off, *Journal of applied microbiology*, *102*, 1372-1381, doi: 10.1111/j.1365-2672.2006.03177.x.

Boehm, A. B., G. G. Shellenbarger, and A. Paytan (2004), Groundwater discharge: potential association with fecal indicator bacteria in the surf zone, *Environ. Sci. Technol.*, *38*, 3558-3566, doi: 10.1021/es035385a.

Boufadel, M. C., H. Li, M. T. Suidan, and A. D. Venosa (2007), Tracer studies in a laboratory beach subjected to waves, *J. Environ. Eng-ASCE*, *133*, 722-732, doi: 10.1061/(asce)0733-9372(2007)133:7(722).

Boufadel, M. C., M. T. Suidan, and A. D. Venosa (1999), A numerical model for density-and-viscosity-dependent flows in two-dimensional variably saturated porous media, *J. Contam. Hydrol.*, *37*, 1-20, doi: 10.1016/S0169-7722(98)00164-8.

Bowen, J., K. Kroeger, G. Tomasky, W. Pabich, M. Cole, R. Carmichael, and I. Valiela (2007), A review of land–sea coupling by groundwater discharge of nitrogen to New England estuaries: Mechanisms and effects, *Appl. Geochem.*, *22*, 175-191, doi: 10.1016/j.apgeochem.2006.09.002.

Burnett, W., P. Aggarwal, A. Aureli, H. Bokuniewicz, J. Cable, M. Charette, E. Kontar, S. Krupa, K. Kulkarni, and A. Loveless (2006), Quantifying submarine groundwater discharge in the coastal zone via multiple methods, *Science of the Total Environment*, *367*, 498-543, doi: 10.1016/j.scitotenv.2006.05.009.

Burnett, W. C., H. Bokuniewicz, M. Huettel, W. S. Moore, and M. Taniguchi (2003), Groundwater and pore water inputs to the coastal zone, *Biogeochemistry*, *66*, 3-33, doi: 10.1023/B:BIOG.0000006066.21240.53.

Burnett, W. C., and H. Dulaiova (2003), Estimating the dynamics of groundwater input into the coastal zone via continuous radon-222 measurements, *Journal of Environmental Radioactivity*, *69*, 21-35, doi: 10.1016/s0265-931x(03)00084-5.

Burnett, W. C., M. Taniguchi, and J. Oberdorfer (2001), Measurement and significance of the direct discharge of groundwater into the coastal zone, *Journal of Sea Research*, *46*, 109-116, doi: 10.1016/S1385-1101(01)00075-2.

Cabelli, V. J., A. P. Dufour, L. McCabe, and M. Levin (1982), Swimming-associated gastroenteritis and water quality, *Am. J. Epidemiol.*, *115*, 606-616.

Cable, J., W. Burnett, and J. Chanton (1997), Magnitudes and variations of groundwater seepage into shallow waters of the Gulf of Mexico, *Biogeochemistry*, *38*, 189-205.

Cable, J. E., W. C. Burnett, J. P. Chanton, and G. L. Weatherly (1996), Estimating groundwater discharge into the northeastern Gulf of Mexico using radon-222, *Earth and Planetary Science Letters*, *144*, 591-604, doi: 10.1016/S0012-821X(96)00173-2.

Cartwright, N., T. E. Baldock, P. Nielsen, D. S. Jeng, and L. Tao (2006), Swash-aquifer interaction in the vicinity of the water table exit point on a sandy beach, *Journal of Geophysical Research: Oceans (1978–2012)*, *111*, doi: 10.1029/2005JC003149.

Cartwright, N., L. Li, and P. Nielsen (2004), Response of the salt–freshwater interface in a coastal aquifer to a wave-induced groundwater pulse: Field observations and modelling, *Adv. Water Resour.*, *27*, 297-303, doi: 10.1016/j.advwatres.2003.12.005.

Charbonnier, C., P. Anschutz, D. Poirier, S. Bujan, and P. Lecroart (2013), Aerobic respiration in a high-energy sandy beach, *Mar. Chem.*, *155*, 10-21, doi: 10.1016/j.marchem.2013.05.003.

Charette, M. A., and E. R. Sholkovitz (2002), Oxidative precipitation of groundwater-derived ferrous iron in the subterranean estuary of a coastal bay, *Geophys Res. Lett.*, *29*, doi: 10.1029/2001gl014512.

Charette, M. A., and E. R. Sholkovitz (2006), Trace element cycling in a subterranean estuary: Part 2. Geochemistry of the pore water, *Geochem. Cosmochim. Acta*, *70*, 811-826, doi: 10.1016/j.gca.2005.10.019.

Cherkauer, D., and B. Zvibleman (1981), Hydraulic connection between Lake Michigan and a shallow ground-water aquifer, *Groundwater*, *19*, 376-381, doi: 10.1111/j.1745-6584.1981.tb03483.x.

Corbett, D. R., K. Dillon, W. Burnett, and J. Chanton (2000), Estimating the groundwater contribution into Florida Bay via natural tracers, 222Rn and CH4, *Limnol. Oceanogr.*, *45*, 1546-1557, doi: 10.4319/lo.2000.45.7.1546.

Crowe, A. S., and G. A. Meek (2009), Groundwater conditions beneath beaches of Lake Huron, Ontario, Canada, *Aquat. Ecosyst. Health Management*, *12*, 444-455, doi: 10.1080/14634980903354825.

Dean, R. G., and T. L. Walton Jr. (2008), WAVE SETUP - A State of Art Review, 26 pp, Florida Department of Environmental Protection and The Bureau of Beaches and Coastal Systems.

Deitchman, R. S., and S. P. Loheide (2009), Ground-based thermal imaging of groundwater flow processes at the seepage face, *Geophys Res. Lett.*, *36*, doi: 10.1029/2009GL038103.

Díaz, J., M. Rendueles, and M. Díaz (2010), Straining phenomena in bacteria transport through natural porous media, *Environmental Science and Pollution Research*, *17*, 400-409, doi: 10.1007/s11356-009-0160-2.

Diersch, H. (2005), *FEFLOW finite element subsurface flow and transport simulation system*.

Dulaiova, H., M. E. Gonneea, P. B. Henderson, and M. A. Charette (2008), Geochemical and physical sources of radon variation in a subterranean estuary—implications for groundwater radon activities in submarine groundwater discharge studies, *Mar. Chem.*, *110*, 120-127, doi: 10.1016/j.marchem.2008.02.011.

Eckhardt, D. A., and P. E. Stackelberg (1995), Relation of Ground-Water Quality to Land Use on Long Island, New York, *Groundwater*, *33*, 1019-1033, doi: 10.1111/j.1745-6584.1995.tb00047.x.

Edge, T. A., and S. Hill (2007), Multiple lines of evidence to identify the sources of fecal pollution at a freshwater beach in Hamilton Harbour, Lake Ontario, *Water Research*, *41*, 3585-3594, doi:10.1016/j.watres.2007.05.012.

Feinstein, D., R. Hunt, and H. Reeves (2010), Regional groundwater-flow model of the Lake Michigan Basin in support of Great Lakes Basin water availability and use studies, U. S. Geological Survey.

Gast, R. J., S. Elgar, and B. Raubenheimer (2015), Observations of transport of bacterial-like microspheres through beach sand, *Continental shelf research*, *97*, 1-6, doi: 10.1016/j.csr.2015.01.010.

Ge, Z., M. B. Nevers, D. J. Schwab, and R. L. Whitman (2010), Coastal loading and transport of Escherichia coli at an embayed beach in Lake Michigan, *Environ. Sci. Technol.*, *44*, 6731-6737, doi: 10.1021/es100797r.

Geng, X., and M. C. Boufadel (2015), Numerical study of solute transport in shallow beach aquifers subjected to waves and tides, *J. Geophys. Res.-Oceans*, *120*, 1409-1428, doi: 10.1002/2014JC010539.

Geng, X., M. C. Boufadel, Y. Xia, H. Li, L. Zhao, and N. L. Jackson (2014), Numerical study of wave effects on groundwater flow and solute transport in a laboratory beach, *J. Contam. Hydrol.*, 37-52, doi: 10.1016/j.jconhyd.2014.07.001.

Gibbes, B., C. Robinson, L. Li, and D. Lockington (2007), Measurement of hydrodynamics and pore water chemistry in intertidal groundwater systems, *J. Coastal Res.*, 884-894.

Grannemann, N. G., R. J. Hunt, J. R. Nicholas, T. E. Reilly, and T. C. Winter (2000), The Importance of Ground Water in the Great Lakes Region, *US Geological Survey Water-Water Resources Investigations Report 00-4008*.

Grannemann, N. G., and T. Weaver (1999), An annotated bibliography of selected references on the estimated rates of direct ground-water discharge to the Great Lakes, *U.S. Geological Surbey Water-Resrources Investigations Report*, *98-4039*.

Health Canada (2012), Guidelines for Canadian Recreational Water Quality edited by A. a. C. C. B. Water, Healthy Environments and Consumer Safety Branch, Minister of Health, Ottawa.

Heiss, J. W., W. J. Ullman, and H. A. Michael (2014), Swash zone moisture dynamics and unsaturated infiltration in two sandy beach aquifers, *Estuar. Coast. Shelf S.*, 20-31, doi: 10.1016/j.ecss.2014.03.015.

Hoaglund, J. R., G. C. Huffman, and N. G. Grannemann (2002), Michigan basin regional ground water flow discharge to three Great Lakes, *Groundwater*, *40*, 390-406, doi: 10.1111/j.1745-6584.2002.tb02518.x.

Horn, D. P. (2002), Beach groundwater dynamics, *Geomorphology*, *48*, 121-146, doi: 10.1016/S0169-555X(02)00178-2.

Howarth, R., D. Anderson, J. Cloern, C. Elfring, C. Hopkinson, B. Lapointe, T. Malone, N. Marcus, K. McGlathery, and A. Sharpley (2000), Nutrient pollution of coastal rivers, bays, and seas, *Issues in Ecology*, *7*, 1-15.

Howarth, R. W. (1988), Nutrient limitation of net primary production in marine ecosystems, *Annu. Rev. Ecol. Syst.*, *19*, 89-110, doi: 10.1146/annurev.es.19.110188.000513.

Huettel, M., W. Ziebis, and S. Forster (1996), Flow-induced uptake of particulate matter in permeable sediments, *Limnol. Oceanogr.*, *41*, 309-322, doi: 10.4319/lo.1996.41.2.0309.

Kalbus, E., F. Reinstorf, and M. Schirmer (2006), Measuring methods for groundwater–surface water interactions: a review, *Hydrology and Earth System Sciences*, *10*, 873-887.

Kang, H.-Y., P. Nielsen, and D. J. Hanslow (1994), Watertable overheight due to wave runup on a sandy beach, *Coastal Engineering Proc.*, *1*, 2115-2124, doi: 10.9753/icce.v24.%25p.

Kornelsen, K. C., and P. Coulibaly (2014), Synthesis review on groundwater discharge to surface water in the Great Lakes Basin, *J. Great Lakes Res.*, *40*, 247-256, doi: 10.1016/j.jglr.2014.03.006.

Kroeger, K., and M. Charette (2008), Nitrogen biogeochemistry of submarine groundwater discharge, *Limnol. Oceanogr.*, *53*, 1025-1039, doi: 10.4319/lo.2008.53.3.1025.

Lambert, M. J., and W. C. Burnett (2003), Submarine groundwater discharge estimates at a Florida coastal site based on continuous radon measurements, *Biogeochemistry*, *66*, 55-73, doi: 10.1023/B:BIOG.0000006057.63478.fa.

Lee, D. R. (1977), A device for measuring seepage flux in lakes and estuaries, *Limnology and Oeanography*, *22*, 8, doi: 10.4319/lo.1977.22.1.0140.

Lee, J., C. Robinson, and R.-M. Couture (2014), Effect of groundwater–lake interactions on arsenic enrichment in freshwater beach aquifers, *Environ. Sci. Technol.*, *48*, 10174-10181, doi: 10.1021/es5020136.

Li, L., and D. Barry (2000), Wave-induced beach groundwater flow, *Adv. Water Resour.*, *23*, 325-337, doi: 10.1016/S0309-1708(99)00032-9.

Li, L., D. Barry, C. Pattiaratchi, and G. Masselink (2002), BeachWin: modelling groundwater effects on swash sediment transport and beach profile changes, *Environ. Modell. Softw.*, *17*, 313-320, doi: 10.1016/S1364-8152(01)00066-4.

Li, L., D. Barry, F. Stagnitti, and J. Y. Parlange (1999), Submarine groundwater discharge and associated chemical input to a coastal sea, *Water Resour. Res.*, *35*, 3253-3259, doi: 10.1029/1999WR900189.

Longuet-Higgins, M. S. (1983), Wave set-up, percolation and undertow in the surf zone, *Proc. R. Soc. London*, *390*, 283-291, doi: 10.1098/rspa.1983.0132.

Longuet-Higgins, M. S., and R. Stewart (1964), Radiation stresses in water waves; a physical discussion, with applications, paper presented at Deep Sea Research and Oceanographic Abstracts, Elsevier.

Masselink, G., and J. A. Puleo (2006), Swash-zone morphodynamics, *Continental shelf research*, *26*, 661-680, doi: 10.1016/j.csr.2006.01.015.

McDonald, J., and A. Harbaugh (1988), MODFLOW, a modular 3D finite difference ground-water flow model, *US Geological Survey, Open File Report*, 83-875.

McLachlan, A., A. Dye, and B. Harty (1981), Simulation of the interstitial system of exposed sandy beaches, *Estuar. Coast. Shelf S.*, *12*, 267-278, doi: 10.1016/S0302-3524(81)80124-7.

McLachlan, A., I. G. Eliot, and D. J. Clarke (1985), Water filtration through reflective microtidal beaches and shallow sublittoral sands and its implications for an inshore ecosystem in Western-Australia, *Estuarine Coastal and Shelf Science*, *21*, 91-104, doi: 10.1016/0272-7714(85)90008-3.

Moore, W. S. (1996), Large Groundwater inputs revealed by Ra 226 enrichments, *Nature*, *380*, 612-614.

Moore, W. S. (2010), The effect of submarine groundwater discharge on the ocean, *Annu. Rev. Marine Sci.*, *2*, 59-88, doi: 10.1146/annurev-marine-120308-081019.

Nielsen, P. (1989), Wave setup and runup: an integrated approach, *Coast. Eng.*, *13*, 1-9, doi: 10.1016/0378-3839(89)90029-X.

Nielsen, P. (1990), Tidal dynamics of the water table in beaches, *Water Resour. Res.*, *26*, 2127-2134, doi: 10.1029/WR026i009p02127.

Nielsen, P. (2009), *Coastal and Estuarine Processes*, World Scientific Publishing Co. Pt2. Ltd., Singapore.

Phillips, M. C., Z. Feng, L. J. Vogel, A. J. Reniers, B. K. Haus, A. A. Enns, Y. Zhang, D. B. Hernandez, and H. M. Solo-Gabriele (2014), Microbial release from seeded beach sediments during wave conditions, *Marine pollution bulletin*, *79*, 114-122, doi: 10.1016/j.marpolbul.2013.12.029.

Rau, G. C., M. S. Andersen, A. M. McCallum, and R. I. Acworth (2010), Analytical methods that use natural heat as a tracer to quantify surface water–groundwater exchange, evaluated using field temperature records, *Hydrogeology Journal*, *18*, 1093-1110, doi: 10.1007/s10040-010-0586-0.

Robinson, C., A. Brovelli, D. Barry, and L. Li (2009), Tidal influence on BTEX biodegradation in sandy coastal aquifers, *Adv. Water Resour.*, *32*, 16-28, doi: 10.1016/j.advwatres.2008.09.008.

Robinson, C., B. Gibbes, H. Carey, and L. Li (2007a), Salt-freshwater dynamics in a subterranean estuary over a spring-neap tidal cycle, *J. Geophys. Res.-Oceans*, *112*, doi: 10.1029/2006jc003888.

Robinson, C., B. Gibbes, and L. Li (2006), Driving mechanisms for groundwater flow and salt transport in a subterranean estuary, *Geophys Res. Lett.*, *33*, doi: 10.1029/2005GL025247.

Robinson, C., L. Li, and D. Barry (2007b), Effect of tidal forcing on a subterranean estuary, *Adv. Water Resour.*, *30*, 851-865, doi: 10.1016/j.advwatres.2006.07.006.

Robinson, C., L. Li, and H. Prommer (2007c), Tide-induced recirculation across the aquifer-ocean interface, *Water Resour. Res.*, *43*, doi: 10.1029/2006WR005679.

Robinson, C., P. Xin, L. Li, and D. A. Barry (2014), Groundwater flow and salt transport in a subterranean estuary driven by intensified wave conditions, *Water Resour. Res.*, *50*, 165-181, doi: 10.1002/2013WR013813.

Robinson, M., D. Gallagher, and W. Reay (1998), Field observations of tidal and seasonal variations in ground water discharge to tidal estuarine surface water, *Groundwater Monitoring & Remediation*, *18*, 83-92, doi: 10.1111/j.1745-6592.1998.tb00605.x.

Russell, T. L., K. M. Yamahara, and A. B. Boehm (2012), Mobilization and transport of naturally occurring enterococci in beach sands subject to transient infiltration of seawater, *Environ. Sci. Technol.*, *46*, 5988-5996, doi: 10.1021/es300408z.

Santos, I. R., W. C. Burnett, J. Chanton, B. Mwashote, I. G. N. A. Suryaputra, and T. Dittmar (2008), Nutrient biogeochemistry in a Gulf of Mexico subterranean estuary and groundwater-derived fluxes to the coastal ocean, *Limnol. Oceanogr.*, *53*, 705-718, doi: 10.4319/lo.2008.53.2.0705.

Santos, I. R., W. C. Burnett, T. Dittmar, I. G. Suryaputra, and J. Chanton (2009), Tidal pumping drives nutrient and dissolved organic matter dynamics in a Gulf of Mexico subterranean estuary, *Geochem. Cosmochim. Acta*, *73*, 1325-1339, doi: 10.1016/j.gca.2008.11.029.

Santos, I. R., B. D. Eyre, and M. Huettel (2012), The driving forces of porewater and groundwater flow in permeable coastal sediments: A review, *Estuar. Coast. Shelf S.*, *98*, 1-15, doi: 10.1016/j.ecss.2011.10.024.

Schmidt, C., B. Conant Jr, M. Bayer-Raich, and M. Schirmer (2007), Evaluation and field-scale application of an analytical method to quantify groundwater discharge using mapped streambed temperatures, *J. Hydrol.*, *347*, 292-307, doi: 10.1016/j.jhydrol.2007.08.022.

Schwartz, F. W., and H. Zhang (2003), *Fundamentals of ground water*, Wiley New York.

Shinn, E. A., C. D. Reich, and T. D. Hickey (2002), Seepage meters and Bernoulli's revenge, *Estuaries*, *25*, 126-132, doi: 10.1007/BF02696056.

Slomp, C. P., and P. Van Cappellen (2004), Nutrient inputs to the coastal ocean through submarine groundwater discharge: controls and potential impact, *J. Hydrol.*, *295*, 64-86, doi: 10.1016/j.jhydrol.2004.02.018.

Spiteri, C., C. P. Slomp, M. A. Charette, K. Tuncay, and C. Meile (2008), Flow and nutrient dynamics in a subterranean estuary (Waquoit Bay, MA, USA): field data and reactive transport modeling, *Geochem. Cosmochim. Acta*, *72*, 3398-3412, doi: 10.1016/j.gca.2008.04.027.

Taniguchi, M. (1993), Evaluation of vertical groundwater fluxes and thermal properties of aquifers based on transient temperature-depth profiles, *Water Resour. Res.*, *29*, 2021-2026, doi: 10.1029/93WR00541.

Taniguchi, M., W. C. Burnett, J. E. Cable, and J. V. Turner (2002), Investigation of submarine groundwater discharge, *Hydrological Processes*, *16*, 2115-2129, doi: 10.1002/hyp.1145.

Taniguchi, M., and Y. Fukuo (1993), Continuous Measurements of Ground-Water Seepage Using an Automatic Seepage Meter, *Ground water*, *31*, 675-679, doi: 10.1111/j.1745-6584.1993.tb00601.x.

Turner, I. (1993), Water table outcropping on macro-tidal beaches: a simulation model, *Marine Geology*, *115*, 227-238, doi: 10.1016/0025-3227(93)90052-W.

Turner, I. L. (1998), Monitoring groundwater dynamics in the littoral zone at seasonal, storm, tide and swash frequencies, *Coast. Eng.*, *35*, 1-16, doi: 10.1016/S0378-3839(98)00023-4.

Turner, I. L., and G. Masselink (1998), Swash infiltration-exfiltration and sediment transport, *J. Geophys. Res.-Oceans*, *103*, 30813-30824, doi: 10.1029/98JC02606.

Turner, I. L., and P. Nielsen (1997), Rapid water table fluctuations within the beach face: Implications for swash zone sediment mobility?, *Coast. Eng.*, *32*, 45-59, doi: 10.1016/S0378-3839(97)00015-X.

Valiela, I., J. Costa, K. Foreman, J. M. Teal, B. Howes, and D. Aubrey (1990), Transport of groundwater-borne nutrients from watersheds and their effects on coastal waters, *Biogeochemistry*, *10*, 177-197, doi: 10.1007/BF00003143.

Valiela, I., K. Foreman, M. LaMontagne, D. Hersh, J. Costa, P. Peckol, B. DeMeo-Andreson, C. D'Avanzo, M. Babione, and C.-H. Sham (1992), Couplings of watersheds

and coastal waters: sources and consequences of nutrient enrichment in Waquoit Bay, Massachusetts, *Estuaries*, *15*, 443-457, doi: 10.2307/1352389.

Voss, C. I. (1984), A finite-element simulation model for saturated-unsaturated, fluid-density-dependent ground-water flow with energy transport or chemically-reactive single-species solute transport, US Geological Survey.

Whitman, R. L., V. J. Harwood, T. A. Edge, M. B. Nevers, M. Byappanahalli, K. Vijayavel, J. Brandao, M. J. Sadowsky, E. W. Alm, and A. Crowe (2014), Microbes in beach sands: integrating environment, ecology and public health, *Rev. Environ. Sci Bio/Tech.*, *13*, 329-368, doi: 10.1007/s11157-014-9340-8.

Whitman, R. L., and M. B. Nevers (2003), Foreshore sand as a source of Escherichia coli in nearshore water of a Lake Michigan beach, *Appl. Environ. Microbio.*, *69*, 5555-5562, doi: 10.1128/AEM.69.9.5555-5562.2003.

Wickham, J. D., R. V. O'Neill, K. H. Riitters, E. R. Smith, T. G. Wade, and K. B. Jones (2002), Geographic targeting of increases in nutrient export due to future urbanization, *Ecological Applications*, *12*, 93-106, doi: 10.1890/1051-0761(2002)012[0093:GTOIIN]2.0.CO;2.

Winter, T. C., J. W. Harvey, O. L. Franke, and W. M. Alley (1998), Ground Water and Surface Water: A Single Resource: USGS Survey Circular 1139, U.S. Geological Survey, Denver, CO.

Xin, P., C. Robinson, L. Li, D. A. Barry, and R. Bakhtyar (2010), Effects of wave forcing on a subterranean estuary, *Water Resour. Res.*, *46*, doi: 10.1029/2010WR009632.

Xin, P., S. S. J. Wang, C. Robinson, L. Li, Y. G. Wang, and D. Barry (2014), Memory of past random wave conditions in submarine groundwater discharge, *Geophys Res. Lett.*, *41*, 2401-2410, doi: 10.1002/2014GL059617.

Yamahara, K. M., B. A. Layton, A. E. Santoro, and A. B. Boehm (2007), Beach sands along the California coast are diffuse sources of fecal bacteria to coastal waters, *Environ. Sci. Technol.*, *41*, 4515-4521, doi: 10.1021/es062822n.

Chapter 3

3 Dynamic Groundwater Flows and Geochemistry in a Sandy Nearshore Aquifer Over a Wave Event

3.1 Introduction

Increasing urban, agricultural and industrial development continues to deteriorate groundwater quality in coastal areas worldwide [e.g., *Bowen, et al.*, 2007; *International Joint Commission*, 2011; *Valiela, et al.*, 1992]. It is widely recognized that groundwater discharge can be an important pathway for delivering contaminants to marine and inland (i.e., Laurentian Great Lakes) coastal waters [*Burnett, et al.*, 2003; *Haack, et al.*, 2005; *Johannes*, 1980; *Kornelsen and Coulibaly*, 2014; *Moore*, 2010]. The flux of groundwater contaminants to coastal waters depends on the ultimate groundwater contamination source, the subsurface contaminant transport pathways and residence time, and the geochemical conditions occurring along the discharge pathways [*Anwar, et al.*, 2014; *Slomp and Van Cappellen*, 2004].

Various coastal forcing, including tides and waves, lead to the recirculation of large quantities of coastal water across the sediment-water interface (SWI) [*Robinson, et al.*, 2007c; *Robinson, et al.*, 2014; *Xin, et al.*, 2010]. This not only alters groundwater discharge rates and exit concentrations for contaminants (i.e., due to dilution) but also the extent of mixing between recirculating coastal water and discharging terrestrial groundwater in a nearshore aquifer. As the recirculating water and terrestrial groundwater have distinct chemical compositions, mixing sets up important geochemical gradients (e.g., pH and redox) in the nearshore aquifer. Reactions occurring in this mixing zone, termed a subterranean estuary in marine settings [*Moore*, 1999], strongly regulate the ultimate discharge of trace elements [*Beck, et al.*, 2010; *Lee, et al.*, 2014; *O'Connor, et al.*, 2015], nutrients [*Charbonnier, et al.*, 2013; *Kroeger and Charette*, 2008; *Slomp and Van Cappellen*, 2004] and industrial contaminants [*Robinson, et al.*, 2009; *Westbrook, et al.*, 2005]. Therefore, understanding the influence of coastal forcing on water exchange across the SWI, and groundwater flows and geochemical conditions near the SWI is key

to unraveling the processes controlling the flux of groundwater contaminants to receiving coastal waters along permeable shorelines.

The impact of coastal forcing on nearshore groundwater flows and salt transport along permeable marine coastlines has been well studied [e.g. *Abarca, et al.*, 2013; *Cartwright, et al.*, 2004; *Heiss and Michael*, 2014; *Robinson, et al.*, 2009; *Xin, et al.*, 2010; *Xin, et al.*, 2015]. These coastlines are complex environments where nearshore groundwater processes, including its discharge to coastal waters, are strongly influenced by diurnal/semi-diurnal and spring-neap tidal fluctuations [*Abarca, et al.*, 2013; *Heiss and Michael*, 2014; *Robinson, et al.*, 2007b], waves [*Geng, et al.*, 2014; *Xin, et al.*, 2010], offshore storms [*Cartwright, et al.*, 2004; *Robinson, et al.*, 2014; *Xin, et al.*, 2014], seasonal oscillations [*Michael, et al.*, 2005], and density dependent flow effects [*Kuan, et al.*, 2012; *Werner, et al.*, 2013].

Numerous field studies have demonstrated the impact of tides on nearshore groundwater flows, and the fate and discharge of contaminants [e.g. *Abarca, et al.*, 2013; *Anschutz, et al.*, 2009; *Heiss and Michael*, 2014; *Robinson, et al.*, 2006; *Santos, et al.*, 2009]. In contrast, investigations of wave effects have generally been limited to laboratory experiments [*Boufadel, et al.*, 2007; *Longuet-Higgins*, 1983; *Sous, et al.*, 2013], numerical studies [*Bakhtyar, et al.*, 2012; *Robinson, et al.*, 2014; *Xin, et al.*, 2010; *Xin, et al.*, 2014] or combinations of both [*Bakhtyar, et al.*, 2011; *Geng and Boufadel*, 2015; *Geng, et al.*, 2014]. Waves produce high frequency (e.g. seconds) swash motion, which induces rapid infiltration/exfiltration across the beachface [*Heiss, et al.*, 2014; *Horn*, 2002; *Li and Barry*, 2000; *Turner and Masselink*, 1998; *Turner and Nielsen*, 1997]. In addition, waves modify the phase-averaged surface water level causing a downward tilt in the mean water surface offshore of the wave breaking point and an upward tilt in the mean water surface extending onshore of the wave breaking point to the average wave run-up limit (Figure 3-1) [*Li and Barry*, 2000; *Longuet-Higgins*, 1983]. These phenomena, known as wave setdown and setup, are respectively caused by an increase in water column radiation stresses due to wave shoaling, and a reduction in water column radiation stresses due to wave breaking [*Longuet-Higgins and Stewart*, 1964; *Nielsen*, 2009]. The hydraulic head distribution imposed on a permeable sloping beach face by

wave setup induces groundwater recirculations that extend from the average wave run-up limit to the average wave breaking point [*Li and Barry*, 2000; *Longuet-Higgins*, 1983].

Longuet-Higgins [1983] was the first to demonstrate groundwater recirculations due to phase-averaged wave motion (*i.e.* wave setup) on a laboratory sloping permeable beach. Numerical simulations by *Li and Barry* [2000] showed that the extent and strength of the recirculations are influenced by the landward water table height and the aquifer thickness. More recently, a laboratory study by *Boufadel, et al.* [2007], later numerically simulated by *Geng, et al.* [2014], illustrated that the wave-induced recirculations result in significant water exchange across the SWI beneath the surf and swash zones. In addition they observed that waves increase the trajectory length, residence time and spreading of conservative contaminants in the nearshore aquifer.
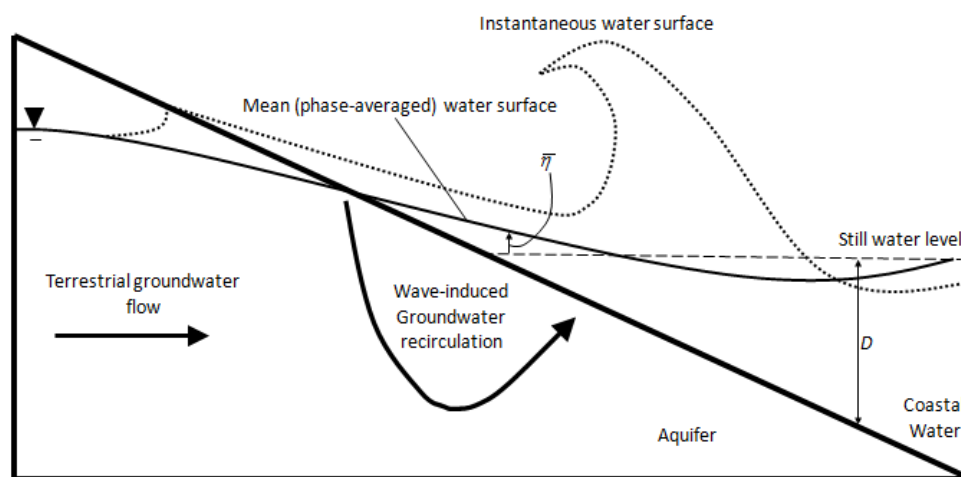
Figure 3-1 Conceptual diagram illustrating impact of waves on groundwater flows in nearshore aquifer. The still water level (black dashed line), instantaneous water surface due to waves (black dotted line), and mean (phase-averaged) water surface (black solid line) are shown.

Field-scale numerical investigations by *Xin, et al.* [2010] illustrated that simulation of the phase-averaged wave setup effect only, rather than instantaneous waves, adequately captures the main effects of waves on groundwater dynamics (i.e., similar water exchange rates, nearshore groundwater flows and salt distribution). Simulations by *Geng and Boufadel* [2015] made similar conclusions when applying a new net inflow technique

for the seaward boundary condition. This method varies slightly from the approach of *Xin, et al.* [2010] in that instead of applying average hydraulic heads at each location, they applied the mean inflow at each location. Using either of these averaged methods significantly reduces the computational demand compared with simulating individual waves which requires the use of very small time steps (< 0.1 s). Field data however is required to validate the simplified wave setup approach adopted in numerical studies [e.g., *Robinson, et al.*, 2014; *Xin, et al.*, 2014].

A modelling study by *Robinson, et al.* [2014] adopted the phase-averaged wave setup approach to examine the response of a marine nearshore aquifer to a period of intensified wave conditions (herein called a wave event). They demonstrated that while groundwater flows and water exchange rates are perturbed in direct response to wave height, they rapidly returned to initial conditions once the waves diminish. In contrast, the wave event may have a long lasting impact (order of weeks to months) on the salt distribution in the nearshore aquifer. While this numerical study illustrated the effect of wave events on salt transport in the nearshore aquifer, the impacts on geochemical conditions and ultimately the fate of reactive constituents in the nearshore aquifer is unknown. In addition to modifying salt transport, increased wave-induced infiltration will also cause influx of chemical species such as organic matter and oxygen into the aquifer. This may alter the pH and redox gradients, stimulate reactive processes (e.g., reductive dissolution of metal hydroxides and release of adsorbed constituents [*Lee, et al.*, 2014]) and in turn affect the fate of contaminants discharging through the aquifer. Varying geochemical conditions may also influence the survival of microbial bacteria (e.g., *E. coli* and enterococci) that are known to accumulate in shallow groundwater and sand near the shoreline [*Alm, et al.*, 2006; *Whitman, et al.*, 2014]. While temporal variations of pH and redox conditions in the shallow nearshore aquifer have been observed previously in response to spring-neap tidal fluctuations [*Robinson, et al.*, 2007a], the extent to which wave events affect these conditions remains unclear.

Prior investigations of wave effects have to date been restricted to laboratory and numerical experiments in part due to the complexity of measuring wave effects on dynamic marine shorelines where processes are complicated by tides and density-driven

flow. Permeable sandy shorelines also exist in large inland seas, such as the Laurentian Great Lakes. In contrast to the marine environment, nearshore aquifers in freshwater settings are not influenced by tides or density effects. Rather, the main coastal forcing affecting groundwater-coastal water interactions are waves [*Lee, et al.*, 2014] and long period lake level fluctuations driven by seasonal variability [*Crowe and Meek*, 2009]. While much of the knowledge regarding the influence of coastal forcing on groundwater dynamics is transferable between marine and freshwater settings, few studies have evaluated nearshore groundwater dynamics along permeable freshwater shorelines despite their potentially significant impact on groundwater discharge and associated contaminant fluxes to coastal waters. Permeable freshwater shorelines, such that exist on the Great Lakes, provide an ideal field setting to study wave effects since changes in the groundwater flows and geochemistry can be directly attributed to waves alone, rather than a combination of the many forcing present in the marine environment.

This study combines field measurements with numerical modeling to evaluate the influence of an isolated 2.5 day wave event on groundwater flow dynamics in a sandy freshwater beach aquifer. Groundwater flows and water exchange across the SWI over the wave event were simulated using a two-dimensional, variably saturated groundwater flow model implemented in FEFLOW [*Diersch*, 2005]. Field data was compared with model results to validate the wave setup approach adopted to simulate the effect of waves. Redox and pH was also measured continuously over the wave event to evaluate the impact of the wave-induced water exchange and groundwater flows on geochemical conditions and thus the dynamic nature of the shallow mixing and reaction zone near the SWI.

3.2 Methodology

3.2.1   Field site

A continuous 2.5 day field study was conducted from July 22-25, 2014 at Ipperwash Beach which is located on the southeastern shore of Lake Huron, ON Canada (43º12'46.6"N, 81º58'6.0"W, Figure 3-2). The beach is part of a 20 km stretch of sandy coastline with an extensive dune system rising several meters above the lake surface

[*Eyles and Meulendyk*, 2012]. There is a high frequency of wave events at the site due to its northwestern exposure coupled with regular strong winds from the north and west [*Bitton and Byrne*, 2002]. This makes it an ideal site for measuring the influence of a wave event on nearshore groundwater dynamics. The average beach slope (β), which changes in response to wave-driven erosion, is typically 0.035 landward of the still water shoreline and steepens to 0.18 around the shoreline. Particle size analysis performed on sand samples (n = 7) collected across the beach up to 2.5 m below the water table indicated that the beach is comprised of relatively homogeneous fine sand (Coefficient of Uniformity (C_u) = 2.18 and d_{50} = 0.16 mm). The saturated hydraulic conductivity was estimated to range from $7 - 15$ md^{-1} using the method of *Krumbein and Monk* [1943].
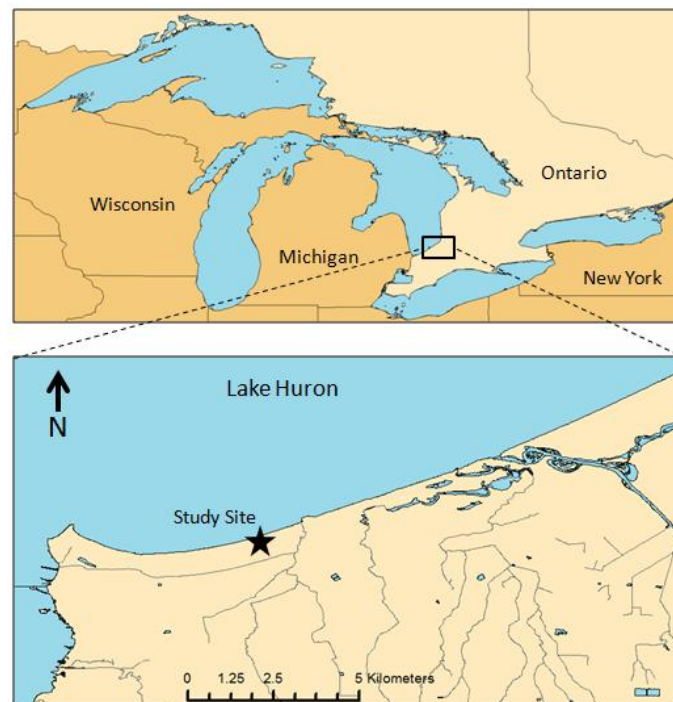
Figure 3-2 Map of the Laurentian Great Lakes region (upper map) and the location of the Ipperwash Beach study site (lower map).

3.2.2   Field methods

Wind speed and direction forecasts were used to predict a wave event *a priori*. Offshore wave data were obtained from a Fisheries and Oceans Canada buoy (C45149 Southern Lake H, www.meds-sdmm.dfo-mpo.gc.ca) located ~35 km directly offshore from the

field site. In advance of the wave event, a cross-shore monitoring transect was installed that extended from 60 m landward of the initial (still water level) shoreline position ($x =$ 0) to 30 m offshore (Figure 3-3a). Landward of the swash zone the elevation of the groundwater table was monitored using piezometers (ϕ 50 mm PVC pipe) spaced at 8 - 20 m intervals. As groundwater in the swash zone is not hydrostatic [*Sous, et al.*, 2013; *Turner*, 1998] fully slotted wells (ϕ 50 mm fully slotted PVC pipe) spaced at 2 - 3 m intervals were used to measure the water table in this zone. The mean water surface elevation in the lake, including the wave setup effect, was monitored using four stilling piezometers (ϕ 50 mm clear poly-carbonate tubing) spaced at 5 - 10 m intervals secured to rigid metal stakes hammered into the lake bed. Water level measurements were manually recorded every two hours during daylight hours over the wave event. In addition, the shoreline position and wave run-up limit were qualitatively tracked through time-lapse photography at five minute intervals while the site was occupied.

Nearshore groundwater flow dynamics were quantified by installing four nested vertical pressure measurement arrays along the transect (Figure 3-3b). Two arrays were installed lakeward of the initial shoreline ($x = 0.5$ m and $x = 6$ m) and two arrays were installed landward of the initial shoreline ($x = -1$ m and $x = -6$ m; Figure 3-3b). Each array consisted of two self-logging pressure transducers (In-Situ Inc. Level TROLL 700) located at different depths (1.25 m vertical separation). Transducers were installed in isolated, screened chambers inside ϕ 25 mm PVC casings (see *Gibbes, et al.* [2007]). The chambers were filled with water prior to inserting the pressure transducers to eliminate trapping air in the chamber. Transducers logged pressure and temperature at 0.1 Hz over the monitoring period with instantaneous pressures used to calculate time-series of vertical head gradients over the wave event. The average head values recorded by each pair of pressure transducers also provided continuous measurement of the groundwater table elevation or the mean lake water surface depending on the location of the array relative to the shoreline. Miniature nested piezometers (ϕ 10 mm) were installed in pairs (with openings spaced 1.25 m vertically) directly adjacent to each vertical pressure transducer array to provide manual validation of the transducer measurements. Pressure head gradients were obtained from the miniature nested piezometers by connecting each

pair to a differential manometer (see *Gibbes, et al.* [2007]). Manometer readings were recorded manually every two hours when the water levels were measured. Finally, four self-logging multi-parameter transducers (In-Situ Inc. TROLL 9500) were installed in screened ϕ 50 mm PVC casings 0.2 - 0.5 m below the SWI. The transducers logged oxidation-reduction potential (ORP) and pH once per minute over the monitoring period.
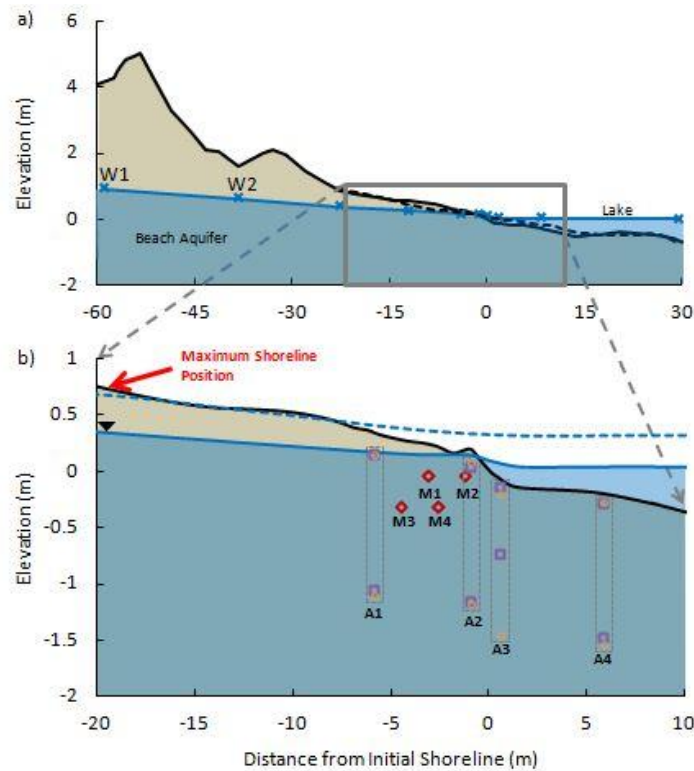
Figure 3-3 (a) Two-dimensional view of the cross-shore monitoring transect showing the initial sand surface (—), initial groundwater table and lake surface elevation (—), sand surface at $t = 17.5$ hours (— —) and stilling well and piezometer locations (×). (b) Layout of equipment installed around the initial shoreline location including miniature nested piezometer openings (□), self-logging pressure transducers (○), and multi-parameter water chemistry transducers (◊, M1-M4). The initial sand surface (—), groundwater table and lake surface elevation (—) and groundwater table and lake surface elevation at peak of wave event (— —, $t = 16$ hours) are also shown in. The x-z coordinate origin (0,0) is located at the initial shoreline location.

All equipment was installed using a hand sand auger. For equipment located below the water table a ϕ 90 mm external PVC casing system was used during installation to prevent collapse of the boring. A total station (Topcon GTS-239W) was used to obtain equipment locations and to conduct sand level surveys twice daily over the wave event. Equipment elevations were verified using a leveling telescope.

3.2.3   Numerical groundwater model

A two-dimensional variably saturated groundwater flow model was developed in FEFLOW [*Diersch*, 2005]. The model domain was made up of a finite element mesh consisting of 125,000 nodes (~ 0.2 m spacing) with refinements (~ 0.05 m spacing) around the water table and SWI. The model was 125 m long extending from 80 m onshore to 45 m offshore (Figure 3-4). The aquifer thickness was assigned as 11 m based on local well records indicating the presence of a clay layer at approximately this depth. The beach morphology was fixed over the simulation period with measured sand levels from the middle to end of the wave event used to set the beach slope. The simulated beach slope was $\beta = 0.04$ from $x = -23$ m to $x = 5$ m, and $\beta = 0.02$ from $x = 5$ m to $x = 45$ m.   Sand erosion was observed during the initial 12.5 hours of the wave event (particularly from $x = -5 - 0$ m) and additional simulations were performed to evaluate the effects of the non-planar beach morphology at the start of the wave event. The model domain was extended 20 m further offshore than the most lakeward stilling well with a flat beach slope ($\beta = 0$) to ensure that the offshore boundary (**DE**) did not influence groundwater flows in the nearshore area. Based on the particle size analysis, the aquifer was assumed to be homogeneous and isotropic with a saturated hydraulic conductivity K_s = 10 m d^{-1} and porosity $n = 0.3$. Unsaturated groundwater flow was resolved with the head-based form of the Richards equation [*Richards*, 1931] and the *van Genuchten* [1980] model with $\alpha = 14.5$ m^{-1} and $n = 2.68$ from *Carsel and Parrish* [1988] and an initial saturation $S_i = 0.1$. Additional simulations performed indicated that these parameter values did not considerably affect the wave-induced groundwater flows. See Appendix A for descriptions of the governing equations of saturated and unsaturated groundwater flow. It is important to note that no parameters were calibrated to improve the performance of the model. While this is often an important step in model

development, the objective of this study was to assess the validity of the phase-averaged wave setup approach used in previous studies [e.g., *Robinson et al.,* 2014; *Xin at al.,* 2014].
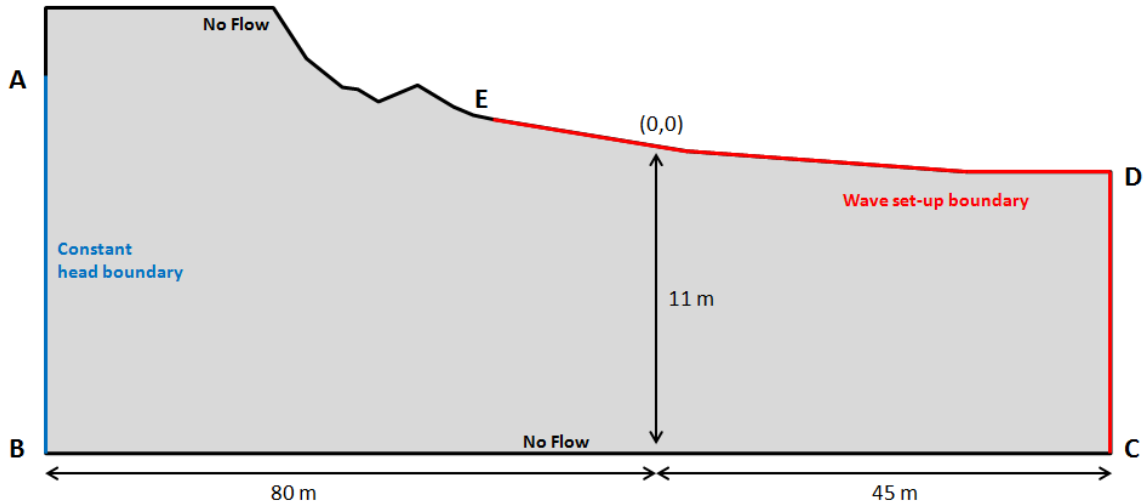
Figure 3-4 Numerical model domain with flow boundary conditions.

A constant head boundary condition was assigned to the landward model boundary **AB** based on measured groundwater table elevations. Aerial recharge and evaporation were assumed to be negligible over the monitoring period and therefore **AE** was specified as a no flux boundary. The bottom boundary **BC** was assumed to be impermeable and thus a no flux boundary was also applied. Using offshore wave height data (Figure 3-5), time-varying specified heads applied along the lakeward boundary **CDE** were derived by applying an empirical wave setup formula developed by *Nielsen* [2009]. This equation is given as:

$$\bar{\eta} = \frac{0.4 H_{rms}}{1 + 10 \dfrac{D + \bar{\eta}}{H_{rms}}} \qquad (1)$$

where η (m) is the increase in water level above the still water level due to wave setup; H_{rms} (m) is the offshore root mean square wave height; and D (m) is the distance from the SWI to the still water level, which varies as a function of location across the beach face (see Figure 3-1). This approach was adopted recently by *Robinson, et al.* [2014] and

Xin, et al. [2014]. The time varying head value for the furthest offshore node along **DE** was also assigned along the vertical offshore boundary **CD** as the groundwater at this location is assumed to be hydrostatic. As the wave height changed, the landward extent of the observed wave setup boundary varied from $x = 0$ to $x = -20$ m. The maximum landward extent of the wave setup boundary (referred to as wave setup limit) was constrained such that it could not exceed $0.4H_{rms}$ [*Nielsen*, 2009] at each time step. For a given time, nodes located landward of the wave setup limit were treated as no flux, whereas nodes below were submerged and the time-varying specified head boundary was applied. A seepage face boundary condition above the wave setup limit was not implemented because decoupling of the shoreline location with the exit point of the water table was not observed in the field. To verify this observation, simulations were performed with a seepage face boundary condition implemented; however, the size and duration of seepage face formation was negligible.
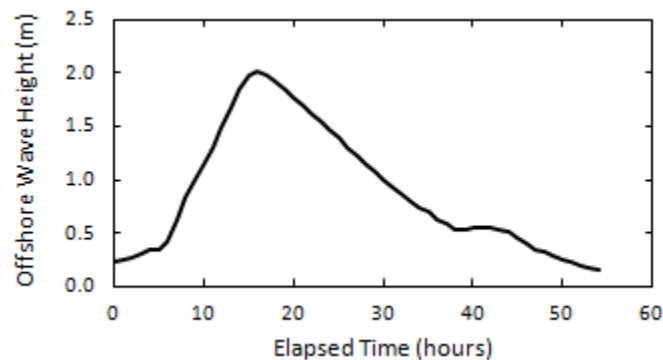
Figure 3-5 Time series of offshore wave height at the field site. Data was downloaded from the Department of Fisheries and Oceans Canada Buoy (C45149 Southern Lake H).

The model was first run to steady state using the boundary conditions assigned at $t = 0$ hours. The steady state results were used as the initial conditions for the transient simulation which had a duration of 54 hours corresponding with wave data measured by the offshore buoy (Figure 3-5). The simulation time was slightly less than the 60 hours of field data collected. This was because during the last 6 hours of monitoring the offshore wave height increased again but as the wind direction had shifted offshore the increase in

wave height was not observed at the field site. Automatic time step control was used in FEFLOW using the Forward Euler/Backward Euler predictor corrector scheme, which offers good stability for unsaturated flow models. The solution proved to be independent of grid size when running simulations with double and half the grid discretization.

3.3   Results and Discussion

3.3.1   Field observations

The offshore wave height was less than 0.5 m at the start of the monitoring period ($t = 0$ - 5 hours, Figure 3-5). Accordingly, conditions were calm with small unsteady swash action. Initially, the landward hydraulic gradient was 1.4% sloping towards the lake and the beach topography was non-planar with a berm and trough formation near the shoreline ($x = $ - $2.7 - 0$ m, Figure 3-6). Consistent with groundwater discharging upwards into the lake, negative vertical head gradients indicating upward flux were initially measured at pressure transducer arrays lakeward of the shoreline (A3 and A4; Figure 3-7c and d). The largest upward flux was measured directly adjacent to the shoreline at A3 (gradient = -0.01 – -0.015) with a lower flux measured further offshore at A4 (gradient = -0.001 – -0.004). Despite only small wave conditions over this period, wave run-up caused some downward flux lake water across the SWI slightly landward of the shoreline. This is indicated by small positive head gradients initially measured at A2 ($t = $ 2 and 4.75 hours, Figure 7b), in addition to localized water table mounding observed around the shoreline ($x = $ - $3.9 - $ - 1 m, Figure 3-6). A negligible vertical pressure gradient was measured at the most landward array A1 during this period consistent with lakeward horizontal groundwater flow through the beach aquifer (Figure 3-7a). The calm conditions over this period provided an ideal initial state to evaluate the subsequent perturbation in groundwater flows induced by the wave event.
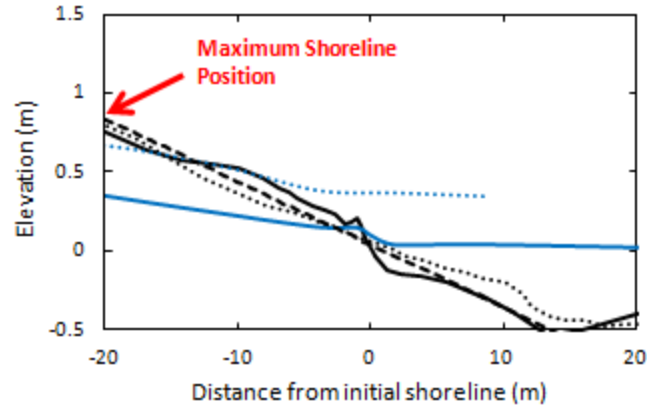
Figure 3-6 Beach surface pre-wave event (t = -4 hours, ▬), near peak of the wave event (t = 17.5 hours, •••), and planar beach surface implemented in model (▬ ▬). Initial groundwater and surface water levels (t = - 4 hours, ▬), and levels at peak of the wave event (t = 16 hours, •••) are also shown. It should be noted that the shoreline position at the peak of the wave event is not accurately depicted by the water level data due to the spatial resolution of the monitoring piezometers.

The offshore wave height increased sharply at approximately t = 5 hours and continued to increase with a peak wave height of 2.02 m occurring at t = 16 hours (Figure 3-5). The increasing wave height corresponded to an increase in the mean water surface near the shoreline and the shoreline position moved onshore from x = 0 m to x = - 20 m (Figure 3-6). Sand erosion landward of the initial shoreline and accretion offshore between t = 5 – 17.5 hours resulted in a more uniform beach slope (Figure 3-6). The beach groundwater table rose as the unsaturated portion of the beach was inundated by wave run-up and the shoreline moved onshore. Infiltration and filling of the beach was most evident at the landward array A1 where a strong downward flux (maximum gradient = 0.017) was measured between t = 5.75 to 10.8 hours (Figure 3-7a). This downward flux occurred when the shoreline was in the vicinity of the transducer array. Similar observations have been reported by *Kang, et al.* [1994] and *Robinson, et al.* [2006]. At the same time this strong downward flux was measured at A1, comparatively strong upward flux (maximum gradient = -0.017) was measured at A2 (Figure 3-7b). This indicates that a shallow wave-induced flow recirculation may have developed in the vicinity of these arrays over this time. As the wave height continued to increase and the shoreline moved further onshore,

the infiltration zone moved landward. Accordingly the downward flux measured at A1 decreased and transitioned into an upward flux at 10.8 hours. The upward flux at A2 and A3 decreased as the shoreline reached its maximum onshore excursion around $t = 16$ hours (Figure 3-7b and c). This may have been due to a weakening of the landward hydraulic gradient and thus groundwater discharge as the phase-averaged lake elevation increased (Figure 3-6). The vertical head gradient measured at A4 remained small (< -0.01) over the wave event. While the flux was generally upwards, consistent with groundwater discharge, reversals in the vertical flow direction were observed. This array was located near the wave breaking zone around the peak of the wave event and as such the downward flux may have been caused by wave setdown [*Bakhtyar, et al.*, 2011; *Li and Barry*, 2000].

The offshore wave height decreased steadily from $t = 16$ to 38 hours, followed by a slower rate of decrease until $t = 54$ hours after which time the wave height at the site remained low (Figure 3-5). The shoreline receded as the wave height decreased and the groundwater table elevation decreased as the beach drained. While seepage was intermittently observed between individual swashes, there was no clear decoupling of the groundwater table exit point from the wave run-up limit as the shoreline receded. The upward flux at A1 continued until $t = 28.5$ hours at which time the shoreline returned to this array location and a downward flux was again observed. This downward flux persisted until $t = 43$ hours, after which time, consistent with the pre-wave event conditions, the vertical gradient became negligible. As the shoreline receded and the beach drained, the upward flux at A2 also increased from $t = 12.5 - 48.5$ hours. The wave-induced recirculations may have become narrower and more focused around this location during this period contributing to the large upward flux observed. The large upward flux at A2 continued until approximately $t = 48.5$ hours after which time it also reduced as the shoreline continued to recede and the wave-induced recirculations became negligible. As the shoreline reached its final position ($x = -1$ m) the upward flux at A3 and A4 returned to the pre-wave event conditions. The final vertical head gradient distribution indicates that terrestrial groundwater discharge was once again the main driver of the vertical fluxes offshore. The offshore wave height at the end of the monitoring period was similar to $t = 0$ hours but the lake level remained slightly elevated

compared to its initial level – this resulted in the final shoreline position being 1 m landward of its initial location ($x = -1$ m). The upward flux observed at A2 at $t = 60$ hours (gradient = -0.005) may have been due to this slight movement of the shoreline and thus landward shift in the groundwater discharge zone.
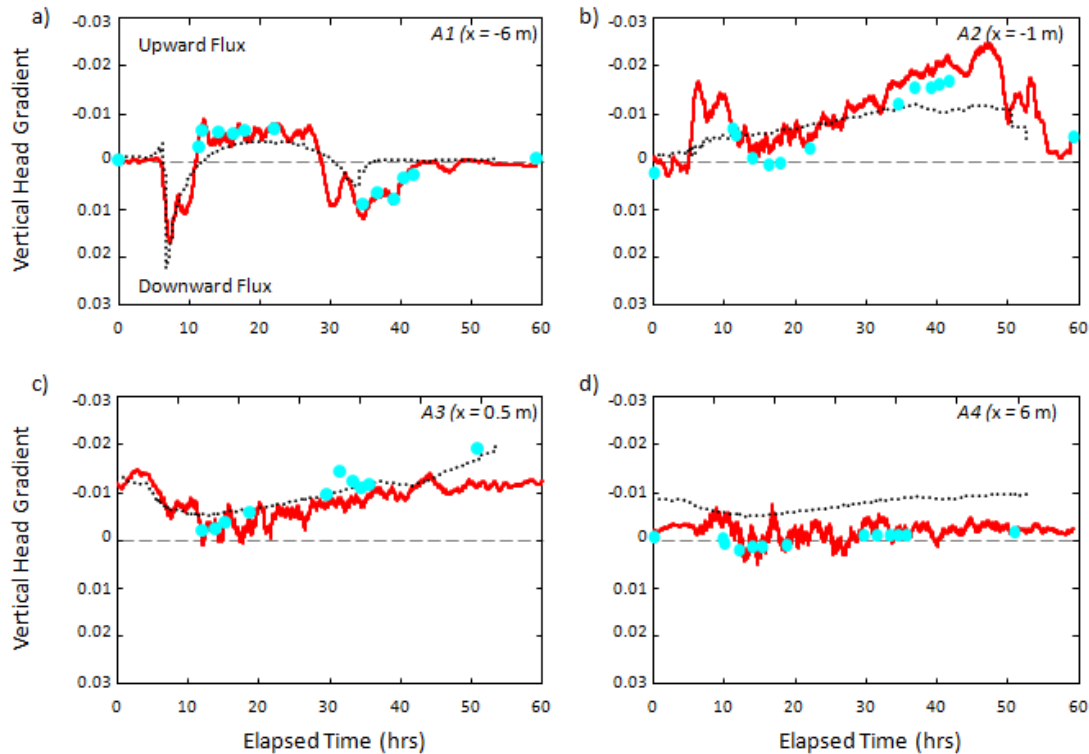
Figure 3-7 Vertical head gradients over the wave event calculated from pressure transducer arrays (—) and differential manometers (●) located at (a) A1, $x = -6$ m; (b) A2, $x = -1$ m, (c) A3, $x = 0.5$ m, and (d) A4, $x = 6$ m (see Figure 3-3). The simulated vertical pressure gradients for each location are also shown (••). A negative head gradient indicates upward flux and a positive gradient indicates downward flux.

3.3.2   Numerical simulation results

Simulated groundwater flow paths through the nearshore aquifer at discrete times over the wave event are shown in Figure 3-8. Particle tracking was used to generate the flow paths at each time with particles originating at 1 m depth intervals landward of the maximum shoreline, and at varying intervals along the saturated SWI. The coloured

contouring on the lines represents the travel time along each instantaneous flow path. To compare the simulated groundwater flow paths with the field data, vertical and horizontal gradients from the pressure transducer array data were used to calculate interpolated directional components of the groundwater flow at six locations. These measured flow directions are depicted by the red arrowheads in Figure 3-8. Magnitudes are not shown since the simulated flow streamlines only indicate flow direction. Measured and simulated vertical head gradients, and therefore the magnitude of the gradients, are directly compared in Figure 3-7.

The simulated groundwater flow paths at $t = 0$ hours show a classical groundwater discharge pattern and are in good agreement with the measured flow directions (Figure 3-8a). As the offshore wave height increased, the shoreline moved landward, the beach water table rose, and the wave-induced recirculation zone expanded. These simulated flow patterns over the wave event are consistent with the numerical results of *Robinson, et al.* [2014]. During the initial stages of the wave event ($t = 6$ hours), the simulated recirculation zone was relatively small (extending from $x = - 6 - 1.5$ m) with travel times for the recirculating water ranging from a few hours up to ten days (Figure 3-8b). The development of wave-induced recirculations caused the terrestrial groundwater flow to diverge – shallow flow paths were directed upwards landward of the recirculation zone contributing to a rise in the water table, whereas deeper flow paths were forced beneath the recirculation zone discharging further offshore.

At the peak wave height ($t = 16$ hours), the wave-induced recirculation zone extended from the maximum wave setup location ($x = -18.5$ m) to approximately 20 m offshore (Figure 3-8c). While the shallow flow recirculations had relatively short travel times (a few hours) the deeper recirculations, which extended to a depth of 9.2 m, had travel times exceeding 150 days. Given the finite duration of the wave event (~ 60 hours), the depth to which recirculating water would actually have being transported into the aquifer would have been limited. The measured flow directions at $t = 16$ hours are all in good agreement with the simulated results with the exception of the inferred flow direction at A4 ($x = 6$m). This discrepancy may be due to wave setdown which is not considered in the wave setup boundary of the model.
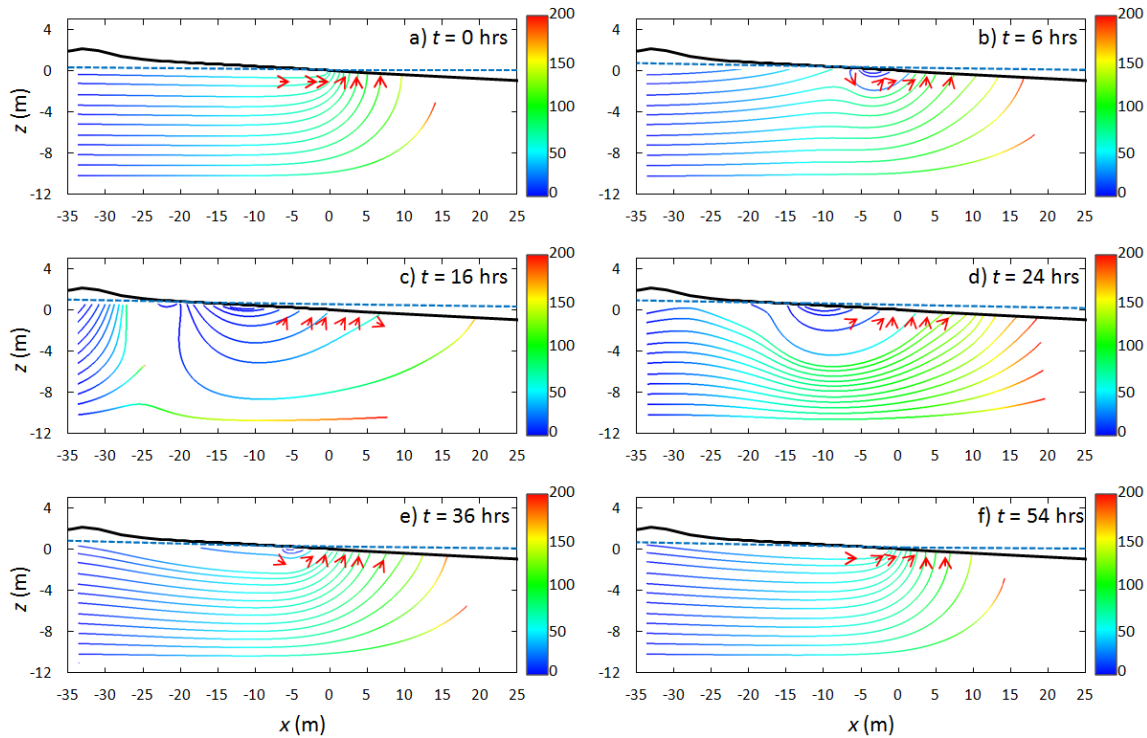
Figure 3-8 Instantaneous groundwater flow paths within the saturated zone of the beach aquifer for different times during the wave event. The coloured contouring represents the travel time along each flow path in days. The red arrowheads (>) depict the directional component of the groundwater flow measured by the pressure transducer arrays. The SWI (—) and instantaneous groundwater and surface water elevation are also shown (— —).

As the wave height declined and the shoreline receded, the simulated recirculation zone diminished and the water table dropped as the beach drained (Figure 3-8d-e). Comparison of the flow patterns over the wave event (e.g., 6 hours *c.f.* 36 hours) show that they vary depending on whether the wave heights are increasing or decreasing due to the effects of filling versus draining of the aquifer. At the final simulation time of $t = 54$ hours, the groundwater flow patterns had mostly returned to the pre-wave event conditions (Figure 3-8f). A small difference in the shallow terrestrial flow paths is evident since the aquifer was still draining at $t = 54$ hours.

The measured and simulated vertical head gradients generally match well at the four transducer array locations (Figure 3-7). The strong downward flux measured at A1 from t

= 5.75 to 10.8 hours as the shoreline passed this location was well captured by the model (Figure 3-7a). The model however did not capture the proportionately large upward flux measured at A2 over this period. Additional simulations conducted to evaluate if the large upward flux at A2 was due to the initial non-planar beach slope (berm-trough configuration) suggested that this did not account for the observed discrepancy. For the offshore transducer arrays, the measured vertical head gradient at A3 closely matched the simulated results over the entire simulation period, however the model over-predicted the vertical flux at A4 (Figure 3-7c, d). Simulations performed with varying aquifer depth (thickness = 7.5 m and 20 m) and hydraulic conductivity did not improve the match at A4. This discrepancy may be due to sediment heterogeneities and anisotropy producing lower vertical flux at this location. Alternatively, the assumption of an impermeable horizontal aquifer basement may be an oversimplification of field conditions. While the measured and simulated vertical head gradients match reasonably well at the peak of the wave event ($t = 16$ hours), the model was not able to capture the prolonged downward flux at A1 from $t = 28.5 - 42.5$ hours and large upward flux at A2 from $t = 32 - 50$ hours. This may be due to the empirical form of the wave set-up approximation used as small differences in the phased-averaged surface water level profile alter the configuration of the recirculation zone and thus the vertical fluxes. The discrepancy may also be because the wave conditions at the shore were slightly different than that recorded at the offshore buoy. All the measured gradients exhibited higher frequency fluctuations compared with the simulated gradients. This may be because localized wind gusts altered the wave characteristics (e.g. wave breaking depth, degree of non-linearity) near the shore relative to the offshore buoy.

Finally, total inflows and outflows across the SWI were extracted from the model results to evaluate the simulated water exchange over the wave event (Figure 3-9). Over the initial period ($t = 0 - 4$ hours) there was negligible inflow and the outflow, which was comprised of terrestrial groundwater discharge, was 1.63 m^3d^{-1} per m of shoreline. As the wave height, and thus wave-induced recirculations strengthened, the inflow increased to a maximum (2.73 m^3d^{-1} m^{-1}) at the peak of the wave event ($t = 16$ hours). The increase in outflow over the wave event was dampened and delayed relative to the inflow – this is consistent with the asymmetrical infiltration/ drainage behaviour of sloping beaches

[*Nielsen*, 1990]. Nevertheless, the outflow increased to 2.17 m^3d^{-1} m^{-1} due to the wave event indicating an increase of 33%. At the end of the simulation the inflow was again negligible but the outflow remained slightly higher relative to the initial conditions (1.84 $m^3m^{-1}d^{-1}$) – this suggests that the beach was still draining at this time.
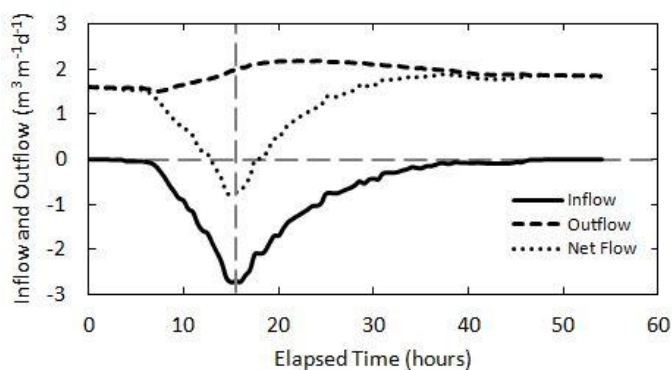
Figure 3-9 Simulated total inflow, outflow and net flow across the SWI through the wave event. The vertical dashed line indicates the time of the peak wave height. Positive values indicate outflow and negative values indicate inflow

3.3.3   Effect of wave-induced flows on nearshore geochemistry

Redox potential (ORP) and pH measurements obtained using four multi-parameter transducers installed near the shoreline illustrate the impact of the wave-induced water exchange and groundwater flows on the shallow beach groundwater chemistry (Figure 3-10). Multi-parameter transducers were installed to a depth of 0.2 m (M1, M2), and 0.5 m (M3, M4) below the SWI (Figure 3-3b). The surface water and terrestrial groundwater at the site represent two distinct end members. The surface water is generally moderately oxidized (ORP ~ 0.2 V) with pH around 8.25. High levels of particulate organic matter were also observed in the surface water over the first 24 hours of the monitoring period. In comparison, at $x = $ - 60 m, the groundwater at depths greater than 2 m below the water table is generally reduced (ORP ~ -0.18V) with a lower pH around 7.3.

The multi-parameter transducers were installed at $t = 0$ hours, but the first 12 hours of data was removed since the water initially used to fill the casings would have been equilibrating in-situ over this period. It is expected that the pH and ORP values measured

at t = 12 hours are consistent with pre-wave event (calm) conditions. Although measured vertical head gradients prior to t = 12 hours indicate periods of downward flux at A1 and A2 (Figure 3-7a, b), based on Darcy's Law, a sustained negative vertical head gradient of 0.03 for five hours would be required for surface water to be transported to a depth of 0.2 m below the SWI. Head gradients of this magnitude and duration were not observed (see Figure 3-7) and therefore pH and ORP measurements at t = 12 hours were likely not yet modified by surface water infiltration. A vertical redox gradient was observed at t = 12 hours with ORP lower at the deeper transducers (ORP ~ - 0.1 V at M3, M4) compared with the shallower transducers (ORP ~ 0.15 V at M1, M2 Figure 3-10a). A vertical pH gradient was also observed (pH ~7.5 at M3 $c.f.$ ~ 7.75 - 7.95 at M1, M2, Figure 3-10b). The pH data for M4 is not shown because this sensor malfunctioned. At t = 12 hours, the shallower groundwater (M1, M2) was similar to the surface water end member likely due to the regular occurrence of shallow recirculations with short residence times, whereas the pH and ORP for the deeper groundwater (M3, M4) was more consistent with the terrestrial groundwater end member.
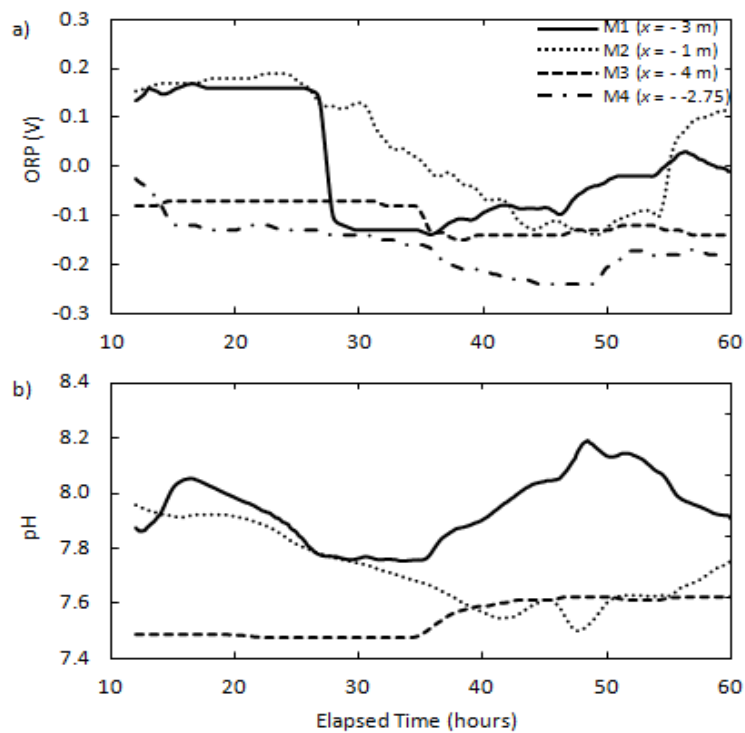
Figure 3-10 (a) ORP and (b) pH measured using multi-parameter transducers installed in shallow groundwater over the wave event.

The ORP and pH varied over the wave event in response to modified transport pathways, mixing of groundwater with recirculating surface water, and reactive processes. The variation in ORP observed at the shallower transducers (M1 and M2) was considerably greater than at the deeper transducers (M3 and M4, Figure 10a). Oxidizing conditions persisted at M1 and M2 until $t \approx 27$ hours at which time the ORP dropped rapidly at M1, and more gradually at M2. The rapid ORP drop at M1 suggests a sharp redox gradient, whereas the more gradual ORP decrease at M2 indicates a more diffuse redox gradient. The diffuse gradient may be due to more frequent enhanced groundwater-surface water mixing at this location just landward of the initial shoreline ($x = -1$ m). Measured vertical pressure gradients (Figure 3-7a, b), combined with simulated groundwater flows (Figure 8), indicate that in the period leading up to $t = 27$ hours, the wave-induced flow paths would have forced deeper terrestrial groundwater to the surface around the M1 and M2 transducer locations. While the instantaneous flow paths would suggest that the transducers are in the trajectory of recirculating surface water (Figure 3-8b-d), it is terrestrial groundwater that initially occupies the modified flow region. Therefore, the observed decrease in pH and ORP at M1 and M2 is consistent with the initial flushing of terrestrial groundwater through the measurement zone rather than recirculating surface water. The ORP at M1 and M2 began to increase and return to pre-wave event conditions around $t = 35.5$ and 50 hours, respectively. The observed increase in ORP is attributed to the influx of surface water into the shallow sediments at or just landward of the transducer locations as the waves receded – e.g., a prolonged strong downward flux (i.e., infiltration of surface water) was measured slightly landward at A1 from $t = 28.5 - 43$ hours (Figure 7a). Although the final pH and ORP at M1 and M2 are similar to their initial pre-wave event values, discrepancies observed (i.e., lower ORP at M2 and lower pH at M4) demonstrate the prolonged effect of the wave event on geochemical conditions in the aquifer. This is consistent with *Robinson, et al.* [2014].

There was less variability in pH and ORP at the deeper transducers (M3, M4) over the wave event. While reduced conditions at M3 and M4 persisted over the monitoring period there was a slight decrease in ORP at $t \approx 35$ hours. The pH was also relatively stable at M3 until $t \approx 35$ hours when it increased slightly from 7.47 to 7.60. It is possible that much like at M1 and M2, the change in geochemical conditions could be primarily

due to end member mixing; however, the simultaneous drop in ORP and increase in pH indicates reactive processes may also be occurring along the modified groundwater flow paths. For instance, enhanced influx of surface water as the waves increased would have delivered oxygenated but also organic-rich surface water into the aquifer mostly near the wave setup limit (e.g., Figure 7a). As the surface water moved along its subsurface recirculation flow path, decomposition of the organic matter may have produced stronger reducing conditions (i.e., drop in ORP) whilst maintaining a higher pH − this may explain the variability at M3 and M4.

The observed decrease in ORP measured by all transducers over the wave event may have important implications for redox-controlled processes that regulate transport of pollutants. For example, oxidized conditions in the shallow groundwater can promote precipitation of metal (hydr)oxides [*Charette and Sholkovitz*, 2002], and subsequent adsorption of chemicals including phosphate [*Anwar, et al.*, 2014; *Spiteri, et al.*, 2008] and arsenic [*Lee, et al.*, 2014]. The observed onset of reducing conditions during the wave event however may promote reductive dissolution of metal hydr(oxides) and an episodic release of adsorbed chemicals. The observed fluctuations in ORP and pH may also affect nitrogen cycling processes (denitrification-nitrification) occurring close to the SWI and thus alter the flux of nitrogen entering coastal waters. While the data presented provides valuable insight into the geochemical dynamics near the SWI over an isolated wave event, longer-term analysis of transient wave conditions as well as analysis of other chemical constituents in the groundwater is required in future field studies to definitively explain observed behaviours and their implications.

To illustrate the importance of wave events over a longer time-scale, offshore wave height and long-term groundwater levels were analyzed between July to October 2014 (Figure 3-11). Here a characteristic sharp increase and slower decrease in the inland groundwater level (W2, $x = - 38$ m) is observed in response to the offshore wave height indicating wave-driven infiltration during wave events. The data indicate $7 − 10$ wave events of varying magnitude and duration occurred during three months at a frequency that varied between as little as three days to up to two weeks. While the groundwater geochemistry was observed to fluctuate in response to the a single wave event (Figure 3-

10), the high frequency of wave events at Ipperwash beach suggests that waves may play an important role in controlling the nearshore aquifer's geochemical environment over long periods of time.
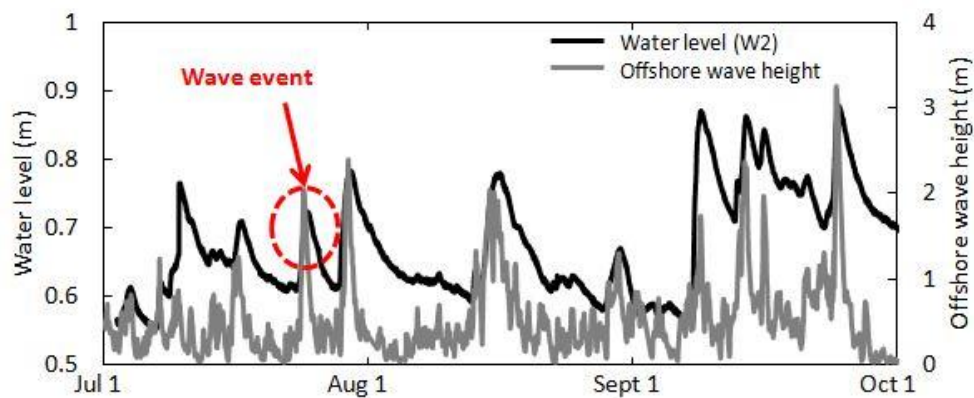
Figure 3-11 Comparison between groundwater level at monitoring piezometer W2 and offshore wave height. The wave event discussed in this chapter is highlighted with the red circle.

3.4 Conclusions

The data presented in this paper is the first time wave-driven groundwater flow dynamics have been captured in the field over an isolated wave event. Further, the data illustrate that the wave-induced water exchange and groundwater flows establish an active and dynamic mixing zone near the SWI with observed pH and ORP variations expected to impact the transport of reactive constituents and their ultimate flux to surface waters. Further work is required to determine the cause and also effect of the observed geochemical variations.

Combining the field data with numerical simulations provided validation of the simplified wave setup approach used in recent numerical studies to simulate wave effects on nearshore groundwater flows [e.g., *Anwar, et al.*, 2014; *Robinson, et al.*, 2014; *Xin, et al.*, 2014]. The numerical simulations also enabled interpretation of the measured wave-induced head gradients and their effects on geochemical conditions in the nearshore aquifer. While this study presents field and numerical results for a freshwater beach, the

findings are also directly applicable for marine shorelines. Shallow groundwater flow and transport in a wave-influenced marine beach are driven primarily by advective transport, rather than density-driven flow [*Robinson, et al.*, 2014]. Therefore the absence of density effects will not alter the general water exchange and flow patterns revealed here. Although the wave-induced phase-averaged groundwater flow behaviour described in this study underpins chemical transport in a wave-influenced beach aquifer, the impact of higher frequency phase-resolved wave-induced flows on geochemical and biological processes within the shallow layers (< 0.1 m) of the beach still remains unclear and should be examined in future studies.

3.5 References

Abarca, E., H. Karam, H. F. Hemond, and C. F. Harvey (2013), Transient groundwater dynamics in a coastal aquifer: The effects of tides, the lunar cycle, and the beach profile, *Water Resour. Res.*, *49*, 2473-2488, doi: 10.1002/wrcr.20075.

Alm, E. W., J. Burke, and E. Hagan (2006), Persistence and potential growth of the fecal indicator bacteria, Escherichia coli, in shoreline sand at Lake Huron, *J. Great Lakes Res.*, *32*, 401-405, doi: 10.3394/0380-1330(2006)32[401:PAPGOT]2.0.CO;2.

Anschutz, P., T. Smith, A. Mouret, J. Deborde, S. Bujan, D. Poirier, and P. Lecroart (2009), Tidal sands as biogeochemical reactors, *Estuar. Coast. Shelf S.*, *84*, 84-90, doi: 10.1016/j.ecss.2009.06.015.

Anwar, N., C. Robinson, and D. A. Barry (2014), Influence of tides and waves on the fate of nutrients in a nearshore aquifer: Numerical simulations, *Adv. Water Resour.*, *73*, 203-213, doi: 10.1016/j.advwatres.2014.08.015.

Bakhtyar, R., D. A. Barry, and A. Brovelli (2012), Numerical experiments on interactions between wave motion and variable-density coastal aquifers, *Coast. Eng.*, *60*, 95-108, doi: 10.1016/j.coastaleng.2011.09.001.

Bakhtyar, R., A. Brovelli, D. A. Barry, and L. Li (2011), Wave-induced water table fluctuations, sediment transport and beach profile change: Modeling and comparison with large-scale laboratory experiments, *Coast. Eng.*, *58*, 103-118, doi: 10.1016/j.coastaleng.2010.08.004.

Beck, A. J., J. K. Cochran, and S. A. Sañudo-Wilhelmy (2010), The distribution and speciation of dissolved trace metals in a shallow subterranean estuary, *Mar. Chem.*, *121*, 145-156, doi: 10.1016/j.marchem.2010.04.003.

Bitton, M., and M.-L. Byrne (2002), A volumetric analysis of coastal dune blowout morphology change, Pinery Provincial Park, paper presented at Parks Research Forum of Ontario Annual Meeting, Thunder Bay, Ontario.

Boufadel, M. C., H. Li, M. T. Suidan, and A. D. Venosa (2007), Tracer studies in a laboratory beach subjected to waves, *J. Environ. Eng-ASCE*, *133*, 722-732, doi: 10.1061/(asce)0733-9372(2007)133:7(722).

Bowen, J., K. Kroeger, G. Tomasky, W. Pabich, M. Cole, R. Carmichael, and I. Valiela (2007), A review of land–sea coupling by groundwater discharge of nitrogen to New England estuaries: Mechanisms and effects, *Appl. Geochem.*, *22*, 175-191, doi: 10.1016/j.apgeochem.2006.09.002.

Burnett, W. C., H. Bokuniewicz, M. Huettel, W. S. Moore, and M. Taniguchi (2003), Groundwater and pore water inputs to the coastal zone, *Biogeochemistry*, *66*, 3-33, doi: 10.1023/B:BIOG.0000006066.21240.53.

Carsel, R. F., and R. S. Parrish (1988), Developing joint probability distributions of soil water retention characteristics, *Water Resour. Res.*, *24*, 755-769, doi: 10.1029/WR024i005p00755.

Cartwright, N., L. Li, and P. Nielsen (2004), Response of the salt–freshwater interface in a coastal aquifer to a wave-induced groundwater pulse: Field observations and modelling, *Adv. Water Resour.*, *27*, 297-303, doi: 10.1016/j.advwatres.2003.12.005.

Charbonnier, C., P. Anschutz, D. Poirier, S. Bujan, and P. Lecroart (2013), Aerobic respiration in a high-energy sandy beach, *Mar. Chem.*, *155*, 10-21, doi: 10.1016/j.marchem.2013.05.003.

Charette, M. A., and E. R. Sholkovitz (2002), Oxidative precipitation of groundwater-derived ferrous iron in the subterranean estuary of a coastal bay, *Geophys Res. Lett.*, *29*, doi: 10.1029/2001gl014512.

Crowe, A. S., and G. A. Meek (2009), Groundwater conditions beneath beaches of Lake Huron, Ontario, Canada, *Aquat. Ecosyst. Health Management*, *12*, 444-455, doi: 10.1080/14634980903354825.

Diersch, H. (2005), *FEFLOW finite element subsurface flow and transport simulation system*.

Eyles, N., and T. Meulendyk (2012), Ground-penetrating radar stratigraphy and depositional model for evolving Late Holocene aeolian dunes on the Lake Huron coast, Ontario, *J. Great Lakes Res.*, *38*, 708-719, doi: 10.1016/j.jglr.2012.09.003.

Geng, X., and M. C. Boufadel (2015), Numerical study of solute transport in shallow beach aquifers subjected to waves and tides, *J. Geophys. Res.-Oceans*, *120*, 1409-1428, doi: 10.1002/2014JC010539.

Geng, X., M. C. Boufadel, Y. Xia, H. Li, L. Zhao, and N. L. Jackson (2014), Numerical study of wave effects on groundwater flow and solute transport in a laboratory beach, *J. Contam. Hydrol.*, 37-52, doi: 10.1016/j.jconhyd.2014.07.001.

Gibbes, B., C. Robinson, L. Li, and D. Lockington (2007), Measurement of hydrodynamics and pore water chemistry in intertidal groundwater systems, *J. Coastal Res.*, 884-894.

Haack, S. K., B. P. Neff, D. O. Rosenberry, J. F. Savino, and S. C. Lundstrom (2005), An evaluation of effects of groundwater exchange on nearshore habitats and water quality of western Lake Erie, *J. Great Lakes Res.*, *31*, 45-63, doi: 10.1016/S0380-1330(05)70289-6.

Heiss, J. W., and H. A. Michael (2014), Saltwater-freshwater mixing dynamics in a sandy beach aquifer over tidal, spring-neap, and seasonal cycles, *Water Resour. Res.*, *50*, 6747-6766, doi: 10.1002/2014WR015574.

Heiss, J. W., W. J. Ullman, and H. A. Michael (2014), Swash zone moisture dynamics and unsaturated infiltration in two sandy beach aquifers, *Estuar. Coast. Shelf S.*, 20-31, doi: 10.1016/j.ecss.2014.03.015.

Horn, D. P. (2002), Beach groundwater dynamics, *Geomorphology*, *48*, 121-146, doi: 10.1016/S0169-555X(02)00178-2.
International Joint Commission (2011), 15th Biennial Report on Great Lakes Water Quality, Ottawa.

Johannes, R. (1980), Ecological significance of the submarine discharge of groundwater, *Marine. Ecol.- Prog. Ser.*, *3*, 365-373.

Kang, H.-Y., P. Nielsen, and D. J. Hanslow (1994), Watertable overheight due to wave runup on a sandy beach, *Coastal Engineering Proc.*, *1*, 2115-2124, doi: 10.9753/icce.v24.%25p.

Kornelsen, K. C., and P. Coulibaly (2014), Synthesis review on groundwater discharge to surface water in the Great Lakes Basin, *J. Great Lakes Res.*, *40*, 247-256, doi: 10.1016/j.jglr.2014.03.006.

Kroeger, K., and M. Charette (2008), Nitrogen biogeochemistry of submarine groundwater discharge, *Limnol. Oceanogr.*, *53*, 1025-1039, doi: 10.4319/lo.2008.53.3.1025.

Krumbein, W., and G. Monk (1943), Permeability as a function of the size parameters of unconsolidated sand, *T. Am. Mining. Eng.*, *151*, 153-163, doi: 10.2118/943153-G.

Kuan, W. K., G. Jin, P. Xin, C. Robinson, B. Gibbes, and L. Li (2012), Tidal influence on seawater intrusion in unconfined coastal aquifers, *Water Resour. Res.*, *48*, doi: 10.1029/2011WR010678.

Lee, J., C. Robinson, and R.-M. Couture (2014), Effect of groundwater–lake interactions on arsenic enrichment in freshwater beach aquifers, *Environ. Sci. Technol.*, *48*, 10174-10181, doi: 10.1021/es5020136.

Li, L., and D. Barry (2000), Wave-induced beach groundwater flow, *Adv. Water Resour.*, *23*, 325-337, doi: 10.1016/S0309-1708(99)00032-9.

Longuet-Higgins, M. S. (1983), Wave set-up, percolation and undertow in the surf zone, *Proc. R. Soc. London*, *390*, 283-291, doi: 10.1098/rspa.1983.0132.

Longuet-Higgins, M. S., and R. Stewart (1964), Radiation stresses in water waves; a physical discussion, with applications, paper presented at Deep Sea Research and Oceanographic Abstracts, Elsevier.

Michael, H. A., A. E. Mulligan, and C. F. Harvey (2005), Seasonal oscillations in water exchange between aquifers and the coastal ocean, *Nature*, *436*, 1145-1148, doi: 10.1038/nature03935.

Moore, W. S. (1999), The subterranean estuary: a reaction zone of ground water and sea water, *Mar. Chem.*, *65*, 111-125, doi: 10.1016/S0304-4203(99)00014-6.

Moore, W. S. (2010), The effect of submarine groundwater discharge on the ocean, *Annu. Rev. Marine Sci.*, *2*, 59-88, doi: 10.1146/annurev-marine-120308-081019.

Nielsen, P. (1990), Tidal dynamics of the water table in beaches, *Water Resour. Res.*, *26*, 2127-2134, doi: 10.1029/WR026i009p02127.

Nielsen, P. (2009), *Coastal and Estuarine Processes*, World Scientific Publishing Co. Pt2. Ltd., Singapore.

O'Connor, A. E., J. L. Luek, H. McIntosh, and A. J. Beck (2015), Geochemistry of redox-sensitive trace elements in a shallow subterranean estuary, *Mar. Chem.*, *172*, 70-81, doi: 10.1016.jmarchem.2015.03.001.

Richards, L. A. (1931), Capillary conduction of liquids through porous mediums, *Journal of Applied Physics*, *1*, 318-333, doi: 10.1063/1.1745010.

Robinson, C., A. Brovelli, D. Barry, and L. Li (2009), Tidal influence on BTEX biodegradation in sandy coastal aquifers, *Adv. Water Resour.*, *32*, 16-28, doi: 10.1016/j.advwatres.2008.09.008.

Robinson, C., B. Gibbes, H. Carey, and L. Li (2007a), Salt-freshwater dynamics in a subterranean estuary over a spring-neap tidal cycle, *J. Geophys. Res.-Oceans*, *112*, doi: 10.1029/2006jc003888.

Robinson, C., B. Gibbes, and L. Li (2006), Driving mechanisms for groundwater flow and salt transport in a subterranean estuary, *Geophys Res. Lett.*, *33*, doi: 10.1029/2005GL025247.

Robinson, C., L. Li, and D. Barry (2007b), Effect of tidal forcing on a subterranean estuary, *Adv. Water Resour.*, *30*, 851-865, doi: 10.1016/j.advwatres.2006.07.006.

Robinson, C., L. Li, and H. Prommer (2007c), Tide-induced recirculation across the aquifer-ocean interface, *Water Resour. Res.*, *43*, doi: 10.1029/2006WR005679.

Robinson, C., P. Xin, L. Li, and D. A. Barry (2014), Groundwater flow and salt transport in a subterranean estuary driven by intensified wave conditions, *Water Resour. Res.*, *50*, 165-181, doi: 10.1002/2013WR013813.

Santos, I. R., W. C. Burnett, T. Dittmar, I. G. Suryaputra, and J. Chanton (2009), Tidal pumping drives nutrient and dissolved organic matter dynamics in a Gulf of Mexico subterranean estuary, *Geochem. Cosmochim. Acta*, *73*, 1325-1339, doi: 10.1016/j.gca.2008.11.029.

Santos, I. R., B. D. Eyre, and M. Huettel (2012), The driving forces of porewater and groundwater flow in permeable coastal sediments: A review, *Estuar. Coast. Shelf S.*, *98*, 1-15, doi: 10.1016/j.ecss.2011.10.024.

Slomp, C. P., and P. Van Cappellen (2004), Nutrient inputs to the coastal ocean through submarine groundwater discharge: controls and potential impact, *J. Hydrol.*, *295*, 64-86, doi: 10.1016/j.jhydrol.2004.02.018.

Sous, D., A. Lambert, R. Vincent, and H. Michallet (2013), Swash-groundwater dynamics in a sandy beach laboratory experiment, *Coast. Eng.*, 122-136, doi: 10.1016/j.coastaleng.2013.05.006.

Spiteri, C., C. P. Slomp, M. A. Charette, K. Tuncay, and C. Meile (2008), Flow and nutrient dynamics in a subterranean estuary (Waquoit Bay, MA, USA): field data and reactive transport modeling, *Geochem. Cosmochim. Acta*, *72*, 3398-3412, doi: 10.1016/j.gca.2008.04.027.

Turner, I. L. (1998), Monitoring groundwater dynamics in the littoral zone at seasonal, storm, tide and swash frequencies, *Coast. Eng.*, *35*, 1-16, doi: 10.1016/S0378-3839(98)00023-4.

Turner, I. L., and G. Masselink (1998), Swash infiltration-exfiltration and sediment transport, *J. Geophys. Res.-Oceans*, *103*, 30813-30824, doi: 10.1029/98JC02606.

Turner, I. L., and P. Nielsen (1997), Rapid water table fluctuations within the beach face: Implications for swash zone sediment mobility?, *Coast. Eng.*, *32*, 45-59, doi: 10.1016/S0378-3839(97)00015-X.

Valiela, I., K. Foreman, M. LaMontagne, D. Hersh, J. Costa, P. Peckol, B. DeMeo-Andreson, C. D'Avanzo, M. Babione, and C.-H. Sham (1992), Couplings of watersheds and coastal waters: sources and consequences of nutrient enrichment in Waquoit Bay, Massachusetts, *Estuaries*, *15*, 443-457, doi: 10.2307/1352389.

van Genuchten, M. T. (1980), A closed-form equation for predicting the hydraulic conductivity of unsaturated soils, *Soil Sci. Soc. Am. J.*, *44*, 892-898, doi: 10.2136/sssaj1980.03615995004400050002x.

Werner, A. D., M. Bakker, V. E. Post, A. Vandenbohede, C. Lu, B. Ataie-Ashtiani, C. T. Simmons, and D. A. Barry (2013), Seawater intrusion processes, investigation and management: recent advances and future challenges, *Adv. Water Resour.*, *51*, 3-26, doi: 10.1016/j.advwatres.2012.03.004.

Westbrook, S., J. Rayner, G. Davis, T. Clement, P. L. Bjerg, and S. Fisher (2005), Interaction between shallow groundwater, saline surface water and contaminant discharge at a seasonally and tidally forced estuarine boundary, *J. Hydrol.*, *302*, 255-269, doi: 10.1016/j.jhydrol.2004.07.007.

Whitman, R. L., V. J. Harwood, T. A. Edge, M. B. Nevers, M. Byappanahalli, K. Vijayavel, J. Brandao, M. J. Sadowsky, E. W. Alm, and A. Crowe (2014), Microbes in beach sands: integrating environment, ecology and public health, *Rev. Environ. Sci Bio/Tech.*, *13*, 329-368, doi: 10.1007/s11157-014-9340-8.

Xin, P., C. Robinson, L. Li, D. A. Barry, and R. Bakhtyar (2010), Effects of wave forcing on a subterranean estuary, *Water Resour. Res.*, *46*, doi: 10.1029/2010WR009632.

Xin, P., S. S. J. Wang, C. Lu, C. Robinson, and L. Li (2015), Non-linear interactions of waves and tides in a subterranean estuary, *Geophys Res. Lett.*, *42*, 2277–2284, doi: 10.1002/2015GL063643.

Xin, P., S. S. J. Wang, C. Robinson, L. Li, Y. G. Wang, and D. Barry (2014), Memory of past random wave conditions in submarine groundwater discharge, *Geophys Res. Lett.*, *41*, 2401-2410, doi: 10.1002/2014GL059617.

Chapter 4

4 Importance of Phase-Averaged Versus Phase-Resolved Effects of Waves for Contaminant Transport in Coastal Aquifers

4.1 Introduction

Water exchange across the sediment-water interface (SWI) in permeable nearshore environments impacts the flux of dissolved and particulate constituents such as nutrients, trace elements, organic matter (OM) and microbial bacteria to coastal waters [*Anschutz, et al.*, 2009; *Beck, et al.*, 2007; *McLachlan and Turner*, 1994; *Santos, et al.*, 2009; *Whitman, et al.*, 2014]. In the nearshore, water exchange across the SWI is driven by various forcing including the terrestrial groundwater hydraulic gradient, tides, waves and currents [*Santos, et al.*, 2012]. Water exchange not only increases groundwater discharge rates, but also impacts the biogeochemical conditions in a nearshore aquifer. These conditions control the transformation and fate of chemical and microbial constituents that are discharging as well as recirculating across the SWI [*Anwar, et al.*, 2014; *Charette and Sholkovitz*, 2006; *McAllister, et al.*, 2015; *Slomp and Van Cappellen*, 2004].

Waves are a major forcing along most permeable coastlines worldwide. The phase-averaged effects of waves causes an increase in the mean water surface elevation towards the shore referred to as wave setup [*Longuet-Higgins*, 1983]. The onshore hydraulic gradient produced by wave set up drives groundwater flow recirculations through the nearshore aquifer (Figure 4-1) that extend from the average wave run-up limit to the wave breaking zone [*Li and Barry*, 2000; *Longuet-Higgins*, 1983]. The depth of the recirculations are of a similar magnitude to their width [*Li and Barry*, 2000]. The residence time for coastal water to travel along the wave-induced recirculation flow paths depends on various factors (i.e., hydraulic conductivity, porosity, wave height) with numerical simulations indicating it may be on the order of days or months [e.g., *Robinson, et al.*, 2014; *Xin, et al.*, 2010]. This residence time has been shown to be sufficient for many geochemical transformations including the mineralization of OM and regeneration of inorganic nutrients [*Anschutz, et al.*, 2009; *McLachlan, et al.*, 1981;

Santos, et al., 2009]. As such, these phase-averaged flow recirculations and the associated water exchange have been shown to impact the fate and transport of dissolved constituents in nearshore aquifers and their subsequent flux to coastal waters [*Anwar, et al.*, 2014; *Lee, et al.*, 2014].
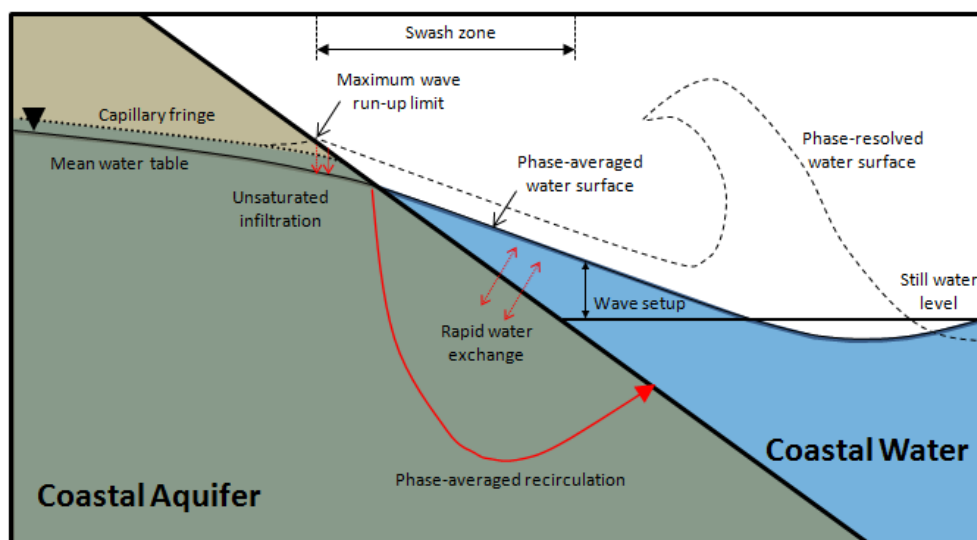
Figure 4-1 Conceptual diagram illustrating key wave phenomena in a nearshore coastal environment. The red arrows represent wave-induced mechanisms for water exchange across the SWI.

In addition to the phase-averaged effects of waves, phase-resolved (i.e., instantaneous) wave action induces rapid water exchange (infiltration/exfiltration, Figure 4-1) and complex groundwater flows in the shallow sediment beneath the swash zone [*Baldock, et al.*, 2001; *Horn, et al.*, 1998; *Sous, et al.*, 2013; *Turner and Nielsen*, 1997]. To date, few studies have investigated the influence of the phase-resolved wave effects on the behaviour of chemical and microbial constituents near the SWI. The potential importance of swash-driven processes was recently explored by *Heiss, et al.* [2014] who measured high frequency moisture dynamics in response to swash overtopping the unsaturated zone and used these measurements to calculate infiltration rates. They inferred that the observed moisture dynamics and subsequent water table response have important implications for transport of reactive constituents in the shallow nearshore aquifer. Aside from this study, most previous work involving phase-resolved wave effects at the SWI

has focused on the implications for sediment transport [e.g., *Elfrink and Baldock*, 2002; *Horn, et al.*, 1998; *Masselink and Hughes*, 1998; *Turner and Nielsen*, 1997]. The mobility and transport of sediment in the swash zone has been linked to the bed shear stresses induced by up-rush and backwash swash cycles [*Conley and Griffin*, 2004; *Nielsen*, 2002] and rapid infiltration/exfiltration across the SWI [*Bakhtyar, et al.*, 2012; *Turner and Masselink*, 1998]. Field studies have shown large swash-induced vertical hydraulic gradients ($\frac{dh}{dz}$ = 0.5 to 2.5) occurring in the shallow sediments below the SWI [e.g., *Baldock, et al.*, 2001; *Horn, et al.*, 1998; *Turner and Masselink*, 1998]. These hydraulic gradients and resulting groundwater velocities are $O(10^2 - 10^3)$ larger than gradients associated with wave-induced phase-averaged groundwater recirculations (see Chapter 3, Section 3.3.1) as well as terrestrial groundwater gradients typically observed at beaches [e.g., *Crowe and Meek*, 2009; *Heiss, et al.*, 2014; *Turner*, 1998].

Beach sediment behaves as a low pass filter where the high frequency, phase-resolved wave effects rapidly become attenuated with increasing distance (depth) away from the SWI [*Horn*, 2006; *Kang, et al.*, 1994; *Masselink and Puleo*, 2006]. Consequently, studies focused on evaluating the effect of waves on groundwater discharge rates and solute transport in nearshore aquifers often only consider the phase-averaged effects [e.g., *Anwar, et al.*, 2014; *Boehm, et al.*, 2006; *Li, et al.*, 1999; *Robinson, et al.*, 2014]. Simulation of the phase-resolved effects of waves acting on a sloping beach is computationally demanding, especially when combined with other forcing such as tides [*Bakhtyar, et al.*, 2013]. *Xin, et al.* [2010] showed numerically that there is little difference between the net groundwater flows and solute (salt) transport through a nearshore aquifer when phase-averaged (i.e., wave setup) compared with phase-resolved (i.e., instantaneous) wave effects were simulated. However, while consideration of only the phase-averaged effects may adequately simulate the net wave-induced groundwater flows and solute transport in the nearshore aquifer, this approach neglects the larger total volume of water and associated constituents that are filtered through the shallow sediments by rapid phase-resolved (swash) processes. For example, numerical simulations by *Geng, et al.* [2014] showed that the phase-resolved approach produced large volumetric infiltration and exfiltration across the SWI. While the larger water

volume filtered through the shallow sediments may not considerably impact the fate of dissolved constituents due to the short residence time, it may be important for the fate of particulates in the recirculating surface water that have a tendency to associate with sand grains. Mechanisms such as straining and attachment often govern the transport of particulates in porous media and may be important for controlling the fate of surface water-derived particulate OM (POM) and fecal bacteria (e.g., *E. coli*, enterococci) near the SWI [*Bradford, et al.*, 2014; *Huettel, et al.*, 1996]. The behaviour of OM and fecal bacteria near the SWI are of particular interest as they are important regulators of nutrient processing and nearshore recreational water quality, respectively. There is currently limited understanding of the physical transport mechanisms, including rapid swash-driven water exchange, controlling the fate of these constituents near the SWI.

To date, researchers have generally focused on either rapid phase-resolved effects of waves close to the SWI of the swash zone for better understanding sediment transport processes, or alternatively focused on deeper wave-induced phase-averaged groundwater flow recirculations to better quantify groundwater discharge and solute fluxes. There is a need to link these distinct research areas and in doing so explore the impact of wave-induced phase-resolved versus phase-averaged groundwater flow behaviours in controlling the fate and transport of dissolved and particulate constituents in permeable nearshore aquifers. To bridge the knowledge gap between these two research areas, measurements of wave-induced phase-resolved vertical fluxes close to the SWI were compared with net phase-averaged vertical fluxes measured deeper in the aquifer. Based on the understanding generated, the implications of the wave-induced phase-resolved flows and the phase-averaged groundwater recirculations for the fate and transport of nutrients and fecal bacteria are discussed.

4.2 Methodology

4.2.1 Field site

Field work was conducted from 22 – 25 July 2014 at Ipperwash Beach which is located on the southeast shoreline of Lake Huron, Ontario (43º12'46.6"N, 81º58'6.0"W). Measurements were made over a period of intensified wave conditions (herein called a

wave event). The monitoring period was approximately 60 hours in duration with calm conditions occurring at the beginning and end, effectively isolating the effects of the wave event. Ipperwash Beach is a uniform fine sand beach (Coefficient of Uniformity (C_u) = 2.18 and d_{50} = 0.16 mm) with an average beach slope of 0.035. The average hydraulic conductivity was estimated to be 10 md^{-1} using the method of *Krumbein and Monk* [1943]. Waves are the dominant coastal forcing at the site as tidal and density effects are negligible in this freshwater Great Lakes environment. During the monitoring period, the offshore wave height ranged from 0.2 – 2 m (Figure 4-2a). The reader is referred to Chapter 3 (Section 3.2.1) for further details about the study site.
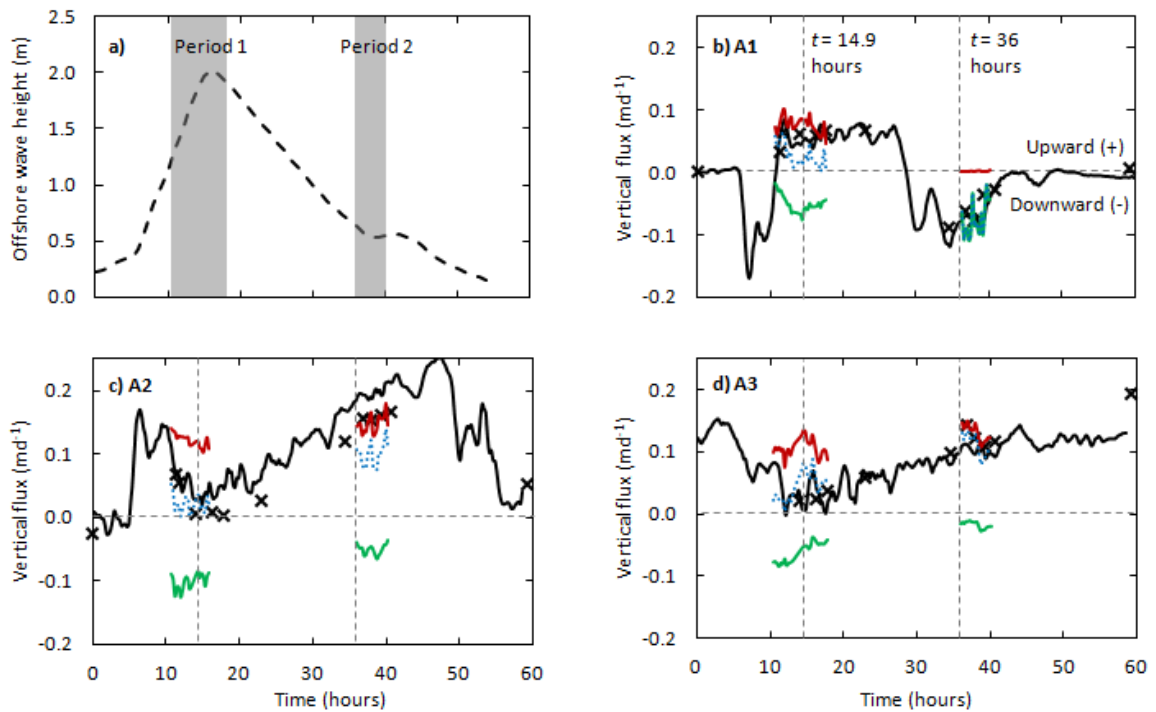
Figure 4-2 a) Offshore wave height over 60 hour monitoring period with Period 1 and Period 2 denoted by grey shading. b) – d) Deep net phase-averaged flux measured by nested pressure transducers (━) and nested piezometers (×), and shallow upward (━), downward (━) and net (•••) phase-averaged flux measured using miniature nested piezometers. Vertical dashed lines denote times for which simulated phase-averaged groundwater flows are shown in Figure 4-4 and the phase-resolved flux was analyzed and presented in Figure 4-6.

4.2.2 Field methods

High frequency vertical head gradients in the shallow nearshore aquifer were measured using three arrays of miniature vertically nested piezometers (ϕ 1.8 mm I.D. nylon tubing) installed at discrete cross-shore locations. Arrays A1 and A2 were landward of the initial still water shoreline (x = -6 m and x = -1 m respectively, Figure 4-3) and array A3 was installed lakeward of the initial still water shoreline (x = 0.5 m). The equipment setup was based on the design of *Baldock and Holmes* [1996] who used the setup to measure high frequency swash-induced vertical head gradients below the SWI in the field [e.g., *Baldock, et al.*, 2001]. Each array consisted of three miniature piezometers spaced vertically at 0.2 m intervals. The piezometers were secured to a ϕ 10 mm steel pole that was driven into the beach sediment. The array was positioned vertically so the upper piezometer opening was located directly below the SWI for initially submerged locations (A3) and directly below the water table for initially unsubmerged locations (A1 and A2). Due to erosion and accretion, small vertical adjustments were made at the start of each day as needed in order to maintain the desired positioning of the piezometers. Each piezometer was attached to a high resolution, low range pressure transducer (Honeywell FPG, 2 psi) and a constant head reservoir. The transducers and head reservoir were mounted to a secured wooden board. The head reservoir was used to purge the system of air bubbles in addition to facilitating field calibration of the pressure transducers. Measurements were recorded using a Campbell Scientific CR3000 datalogger at 5 Hz with the measurement frequency based on previous swash investigations [e.g., *Baldock, et al.*, 2001; *Turner and Masselink*, 1998; *Turner and Nielsen*, 1997]. The vertical head gradients in the shallow sediment were measured for two separate periods during the wave event with each period representing different wave conditions. Period 1 corresponds to a period of high wave height (t = 10.7 − 17.75 hours, offshore wave height = 1.25 − 2.02 m) with maximum wave run-up ranging between 15 - 20 m landward of the initial still water shoreline (x = 0 m; Figure 4-3). Period 2 corresponds to a period of declining wave height (t = 36 − 40.25 hours, offshore wave height = 0.5 − 0.6 m) with maximum wave run-up between 5 - 7 m landward of the initial shoreline (Figure 4-3). The high frequency vertical gradients were separated into positive and negative components for individual analysis. A 15 minute moving average was applied to obtain

the phase-averaged gradient for both positive and negative directions. The directional components were then summed to provide a shallow net phase-averaged vertical head gradient. Groundwater fluxes were calculated as the product of the hydraulic gradient ($-\frac{dh}{dz}$) and the hydraulic conductivity (K) where positive values represent upward flux and negative values represent downward flux (Figure 4-2b – d).
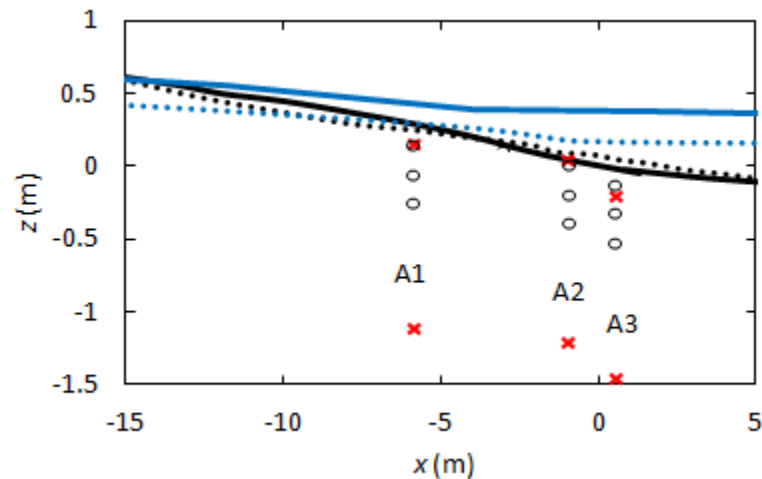
Figure 4-3 Layout of equipment for measuring vertical fluxes near the SWI including locations of nested pressure transducers (×) and miniature nested piezometer openings (○). Beach surface elevations (—) and phase-averaged water levels (—) during Period 1 (t = 14.9 hours), and beach surface elevations (•••) and phase-averaged water levels (•••) during Period 2 (t = 36 hours) are also shown. Note that (×) also marks the location of the nested piezometer openings used to validate the deep phase-averaged pressure transducer data.

Deep net phase-averaged vertical head gradients in the nearshore aquifer were measured by two methods. The first method consisted of three arrays of self-logging pressure transducers (In-Situ Inc. LevelTROLL 700) installed at the same cross-shore locations as the shallow miniature vertically nested piezometers (A1, A2 and A3, Figure 4-3). Each array consisted of two pressure transducers nested vertically (1.25 m spacing) inside ϕ 25 mm screened PVC casings (see *Gibbes, et al.* [2007]). The screen of the top transducer was positioned 0.1 m below the submerged SWI (A3) or directly below the water table within the unsaturated swash zone (A1 and A2) depending on the cross shore location of

the array relative to the initial shoreline. A sampling frequency of 0.1 Hz was used. The deep net phase-averaged vertical hydraulic gradients were calculated over the 60 hour monitoring period by applying a 15 minute moving average to pressure data from these vertically nested transducer arrays. Fluxes were calculated for comparison with the shallow phase-averaged measurements (Figure 4-2b – c). The second measurement method consisted of three sets of vertically nested piezometers (ϕ 10mm) installed in pairs with openings spaced 1.25 m vertically. These were installed directly adjacent to each vertical pressure transducer array. Vertical head gradients were obtained from the nested piezometers by connecting each pair to a differential manometer (see *Gibbes, et al.* [2007]). Manometer readings were taken every two hours over the 60 hour monitoring period while the site was occupied. Although the sampling frequency used for the deeper self-logging pressure transducers (0.1 Hz) was not sufficient to capture the full phase-resolved pressure signal induced by waves, applying a 15 minute moving average smoothed sampling bias leaving only the net phase-averaged flux behaviour. The vertical flux calculated with the deep transducer array data matched well with the vertical flux manually measured using the differential manometers, thus verifying the measurement technique (Figure 4-2b – d). Manometers only detect the low-frequency phase-averaged effects of waves as viscous effects within the manometer tubes dampen the frequency response [*Nielsen and Dunn*, 1998].

Groundwater table elevations were measured with piezometers (ϕ 50 mm PVC) installed in a cross shore transect at $8 - 20$ m intervals from the initial shoreline to the landward extent of the beach. Surface water elevations were measured with 4 stilling piezometers installed (ϕ 50 mm clear polycarbonate) offshore of the initial shoreline at $5 - 10$ m intervals. Stilling piezometers were secured to metal posts hammered into the lake bed. Groundwater and surface water elevations were recorded at each piezometer and stilling piezometer every two hours along with the manometer readings. Piezometers and instrumented pressure transducer arrays were installed below the water table using a hand auger and a casing system. Equipment locations and elevations were surveyed relative to a local benchmark.

4.2.3　Numerical groundwater model

A two-dimensional, variably-saturated groundwater flow model was used to simulate the transient wave-induced phase-averaged groundwater flows in the beach aquifer over the 60 hour monitoring period as described in Chapter 3 (Section 3.3.2). While the simulation results, including model performance are not the focus of this chapter, the results are shown to provide insight into the transient wave-induced groundwater flows over the monitoring period and assist with the interpretation of the field data.

Details of the model set up are provided in Chapter 3 (Section 3.2.3). Briefly, the simulated aquifer was homogeneous and isotropic with a saturated hydraulic conductivity (K) of 10 md^{-1} and porosity (ϕ) of 0.3. Unsaturated groundwater flow was simulated using the head-based form of the Richards Equation [*Richards*, 1931]. The *van Genuchten* [1980] model was used to determine the pressure-saturation relationship and relative hydraulic conductivity in the unsaturated zone. Fitting parameters α and *n* were chosen as 14.5 m^{-1} and 2.68 respectively from *Carsel and Parrish* [1988]. The model domain was 125 x 15 m representing a vertical slice of the nearshore aquifer. The landward boundary was assigned as a constant head based on measured groundwater table elevations. The effect of waves on the groundwater flow was simulated by considering wave setup acting on the sloping SWI (phase-averaged effects only). A time series of the offshore wave height over the monitoring period was used in an empirical formula describing wave setup [*Nielsen*, 2009] to derive a time-dependent boundary condition. This boundary condition was applied for all submerged nodes along the SWI. No flow boundaries were assigned to the bottom and top of the model domain.

4.3　Results

4.3.1　Comparison of deep and shallow phase-averaged groundwater fluxes

The phase-averaged vertical fluxes in the nearshore aquifer were perturbed in response to the wave event (Figure 2-2). The measured deep phase-averaged fluxes over the monitoring period were shown in Chapter 3 (Section 3.3.2) to correspond well with numerical simulations of the phase-averaged groundwater recirculations driven by wave

setup. Wave conditions were calm for the first 6 hours of the monitoring period with the measured and simulated results during this time indicating a classical groundwater discharge flow configuration (Figure 4-4a). The initial terrestrial hydraulic gradient across the beach was 1.4% with groundwater flow towards the lake. Landward of the shoreline at A1 ($x = -6$ m), the vertical flux was negligible, indicating horizontal terrestrial groundwater flow through the beach (Figure 4-2b). Weak downward flux initially observed at A2 (Figure 4-2c), located slightly landward of the shoreline ($x = -0.5$ m), was due to unsaturated infiltration (See Figure 1). Lakeward of the shoreline at A3, the strong upward flux measured was consistent with vertical discharge of terrestrial groundwater (Figure 4-2d). The increasing wave height caused the shoreline to advance landward and led to the development of phase-averaged groundwater recirculations. This is evident, for instance, by the strong downward flux observed at A1 and proportionately large upward flux observed at A2 when the shoreline reached the location of A1 ($t = 6 - 11$ hours, Figure 4-2b, c). As the wave height continued to increase, the downward flux at A1 transitioned to an upward flux just after $t = 11$ hours. After this time the three arrays measured an upward flux as all arrays were located in the lower part of the recirculation zone that was dominated by upward flow. This is illustrated by the simulated groundwater flow paths at $t = 14.9$ hours (Figure 4-4b). Although the wave setup and subsequent groundwater recirculation were greatest from approximately $t = 11 - 16$ hours, the upward vertical flux at A2 and A3 weakened over this period. This behaviour is attributed to the increase in phase-averaged water surface relative to the landward water table weakening the lakeward-directed hydraulic gradient. The opposite was observed after $t = 16$ hours with the upward flux at A2 and A3 increasing as the wave height and MWS decreased. Seepage face formation was negligible as the water table dropped at a similar rate to the decline in wave height and subsequent offshore retreat of the shoreline. From $t = 28.5 - 45$ hours, the wave run-up limit was in the vicinity of A1 and again a strong downward flux was observed at this location during this period. The simulated flow paths indicate that the groundwater recirculations diminished as the wave height decreased (Figure 4-4c). As the conditions became calm the measured vertical fluxes returned to their approximate pre-wave event conditions.
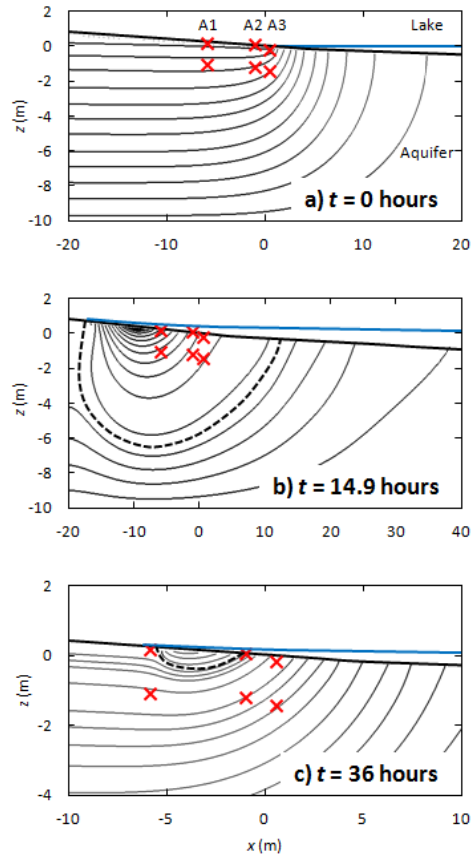
Figure 4-4 Simulated groundwater flow paths for a) initial calm conditions ($t = 0$ hours), b) during Period 1 ($t = 14.9$ hours) and c) during Period 2 ($t = 36$ hours). The black dashed line represents the divide between the terrestrial groundwater flow paths and the wave-induced recirculation flow paths. The simulated surface water elevation (—) and the nested pressure transducers (×) are also shown.

During Period 1 ($t = 10.7 - 17.75$ hours), all monitoring arrays were located in the lower region of the swash zone due to the large wave run-up. Here, the surface sediments remained fully saturated between individual swash events. While the deep and shallow net phase-averaged vertical fluxes over this measurement period are similar, some interesting features are apparent (Figure 2-2). All net phase-averaged vertical flux measurements indicate upward flux with simulation results suggesting that this was because the arrays were located in the lower portion of the recirculation zone where the groundwater flow is upward (Figure 4-4b). The shallow net vertical fluxes measured at A1 and A2 however were slightly lower than the deeper vertical fluxes (Figure 2-2b, c).

Assuming one-dimensional vertical flow, this discrepancy violates continuity; however, Figure 6 shows that the simulated flows at the array locations have a considerable horizontal component. For A3 where the vertical shallow and deep net phase-averaged fluxes were similar, the simulated horizontal fluxes were uniform with depth (Figure 4-5c). However, similar phase-averaged horizontal fluxes with depth were also measured at A1 and A2 during Period 1, thus not explaining the differences between the vertical shallow and deep net phase-averaged fluxes. It is therefore thought that near the SWI, where the groundwater flows are more complex, the assumption that the phase-averaged effects adequately represent the groundwater flow processes may be invalid.
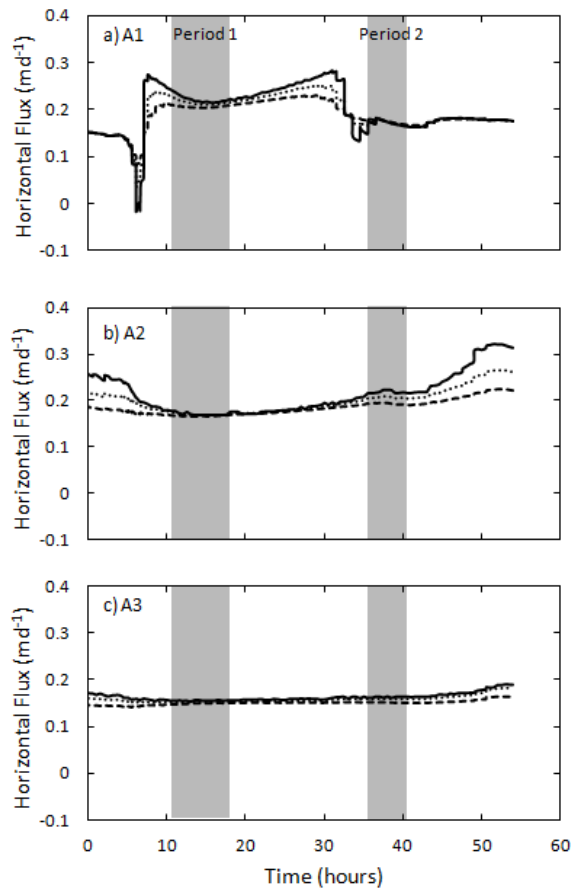
**Figure 4-5 Simulated horizontal flux at monitoring array locations (a) A1, (b) A2, and (c) A3 at depths 0.25 m (—), 0.875 m (•••) and 1.5 m (— —) below the SWI. The grey shading denotes Period 1 and Period 2. Note that a positive flux indicates lakeward flow and negative flux denotes landward flow.**

The directional components of the shallow phase-averaged flux (upwards and downwards) during Period 1 are also shown in Figure 4-2. It can be seen that over Period 1 the shallow directional fluxes were considerably larger than the net fluxes, sometimes by over an order of magnitude. This behaviour was consistently shown at all three arrays during this time period. These high shallow directional fluxes, when integrated over the entire monitoring period, indicate that large volumes of surface water are filtered through the shallow sediments relative to the net exchange volume. The impact of this larger volume of water filtering through the shallow sediments on chemical and microbial constituents is discussed in Section 4.4.

During Period 2, A1 was located at the top of the swash zone in a region of intermittent saturation at the surface while A2 and A3 were located in the mid-lower and bottom of the swash zone, respectively, where the sediments remained fully saturated due to regular overtopping of swash. Only the largest wave run-up overtopped the sand surface at A1 during this period, resulting in downward-directed shallow net flux of a similar magnitude to the deeper net flux (Figure 4-2b). The intermittency of the wave run-up resulted in the sand surface at this location being partially saturated or saturated by the capillary fringe intersecting the surface. Unsaturated infiltration is driven downward by gravity and thus there was negligible upward flux. Both the shallow and deep net phase-averaged flux at A2 were upward during Period 2 (Figure 4-2c). However, the deep net phase-averaged flux at A2 did not fall within the envelope of the shallow upward/downward flux components during Period 2 suggesting a discontinuity between the deep and shallow groundwater flow behaviour. This may be due to the flow having a stronger horizontal (lakeward) component near the SWI compared to deeper in the aquifer over this period (Figure 4-5b). In addition, the simulated groundwater flows suggest that the deeper measurements were within the terrestrial groundwater discharge zone whereas the shallow measurements were within the wave-induced groundwater recirculation zone (Figure 4-4c). Nevertheless, the shallow flux had large components of both upward and downward flux indicating a larger total volume of water exchanged across the SWI in comparison to either the shallow or deep net phase-averaged flux. Both shallow and deep net phase-averaged measurements at A3 also indicate strong upward flux. Here, while the shallow flux was bidirectional the upward flux was dominant. The

net shallow and deep upward flux measured is consistent with simulation results which showed upward terrestrial groundwater discharge at this location over this period (Figure 4-4c).

4.3.2   Shallow phase-resolved groundwater flux

The high frequency pressure data used to generate the shallow phase-averaged flux also provide insight into the rapid shallow flux induced by the phase-resolved wave effects. Data are presented in Figure 4-6 for short representative time intervals during Period 1 (t = 14.9 hours) and Period 2 (t = 36 hours). Swash was generated by wind waves, thus resulting in irregular swash period (between 4 and 7 seconds) and depth. At t = 14.9 hours, individual swash events produced large rapidly reversing upward and downward vertical groundwater flux at the three measurement locations. The magnitude of the shallow phase-resolved flux in the upper 0.20 m below the SWI was between approximately 10 – 80 times larger than the shallow net phase-averaged flux (Figure 6a-c). Measurements between 0.20 and 0.40 m depth show, as expected, the dampening of the vertical flux with depth below the SWI. Although attenuated at depth, the magnitude of these rapidly reversing fluxes near the SWI may play a critical role in the transport of particulates, particularly in their attachment and detachment to sand grains – this is discussed further in Section 4.4.

The wave conditions at t = 36 hours, during Period 2, provide insight into the shallow phase-resolved groundwater flow behaviour at different regions in the swash zone. At the start of the time period shown, the water table at A1 was initially located approximately 5 cm below the sand surface and thus the phase-resolved flux was different to that at A2 and A3 where the surface sediments remained saturated between swash events. Only the largest wave run-up overtopped the SWI at the location of A1. During the period when the wave run-up did not reach this location, the vertical flux was negligible (t = 0 – 20 seconds, Figure 6d). When overtopping occurred (t = 23 seconds) an instantaneous downward flux of approximately 0.5 md^{-1} was measured. This type of behaviour was also observed by *Turner and Nielsen* [1997] in nearshore sediments where the capillary fringe intersected the beach surface. They suggested that the large instantaneous downward flux was due to capillary effects where only a small amount of infiltration caused a transition

from negative to positive pore pressure within the capillary fringe, resulting in a near instantaneous increase water table elevation. The downward flux remained present, albeit decreasing, while the surface sediments drained or returned to capillary saturation between individual swash events. The behaviour at A2 and A3 during this period was similar to Period 1 with large rapidly reversing fluxes (Figure 6e, f). The maximum upward and downward phase-resolved fluxes at A2 of 0.96 md^{-1} and 1.97 md^{-1} respectively were 10 – 20 times larger than the shallow phase-averaged flux of 0.102 md^{-1} upward. The magnitudes of the phase-resolved vertical flux at A3 during Period 2 were slightly smaller than during Period 1 which is attributed to the reduced swash depth associated with the declining wave height. Both upward and downward phase-resolved fluxes at A3 reached a maximum of 0.5 md^{-1}, a magnitude approximately 4 times larger than the shallow net phase-averaged flux of 0.131 md^{-1} upward.
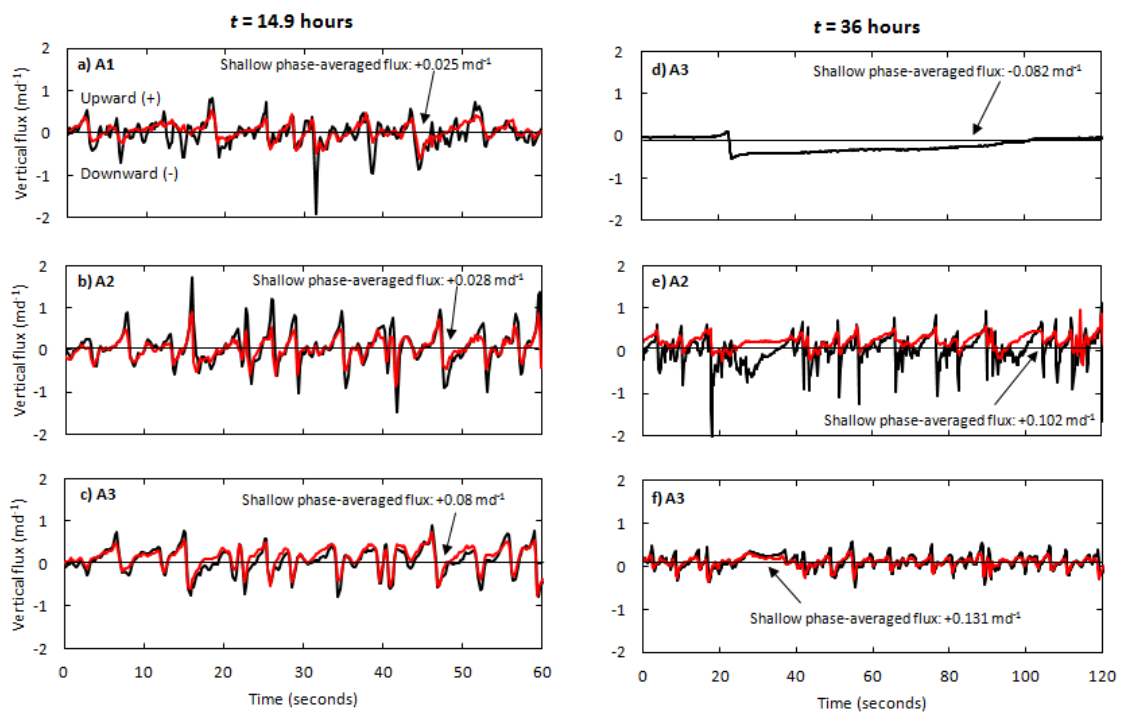
Figure 4-6 Phase-resolved (instantaneous) shallow vertical flux measurements during Period 1 at *t* = 14.9 hours (a – c) and Period 2 at *t* = 36 hours (d – f). Gradients are calculated over depths 0 – 0.2 m (──) and 0.2 – 0.4 m (──) below the SWI or water table. The black horizontal line represents the shallow net phase-averaged flux.

4.4 Discussion

4.4.1 Implications for nutrient cycling and transport

It is well recognized that permeable nearshore aquifers act as important biogeochemical reactors for regenerating inorganic nutrients (nitrate [NO_3^-], ammonium [NH_4^+], phosphate [PO_4^{3-}]) by organic matter mineralization (decomposition) as well as controlling the exit conditions for terrestrial groundwater nutrients discharging to coastal waters [*Anwar, et al.*, 2014; *Charbonnier, et al.*, 2013; *Spiteri, et al.*, 2008]. The cycling of nutrients in a nearshore aquifer and thus the ultimate flux of nutrients to coastal waters depends on the specific chemical species, groundwater velocities and flow paths including the residence time, and the geochemical conditions along the groundwater flow paths [*Slomp and Van Cappellen*, 2004]. Waves deliver surface water and associated dissolved and particulate constituents including dissolved oxygen (DO), dissolved organic matter (DOM) and particulate organic matter (POM) into the nearshore aquifer [*Anwar, et al.*, 2014; *McLachlan, et al.*, 1985; *McLachlan and Turner*, 1994]. The availability of these species strongly influences the redox and pH conditions in the nearshore aquifer and thus nutrient transformations [*Charbonnier, et al.*, 2013; *Kroeger and Charette*, 2008; *Reckhardt, et al.*, 2015; *Santos, et al.*, 2008; *Santos, et al.*, 2009]. Mineralization of OM, whether DOM or POM, converts organic nitrogen and phosphorous back into it its dissolved inorganic forms (i.e., NH_4^+, PO_4^{3-}). The dissolved inorganic nutrients may then be transported back to coastal waters via groundwater discharge. Oxic zones near the SWI have been shown to stimulate nitrification (conversion of NH_4^+ to NO_3^-) as well as trigger the precipitation of ferric hydroxides which tend to adsorb PO_4^{3-} [*Anwar, et al.*, 2014; *Charette and Sholkovitz*, 2002; *Lee, et al.*, 2014; *Spiteri, et al.*, 2008]. OM decomposition also consumes oxygen and other electron acceptors leading to anoxic conditions that are favourable for denitrification [*Kroeger and Charette*, 2008; *Slomp and Van Cappellen*, 2004].

Although the phase-resolved (instantaneous) effects of waves cause large quantities of coastal water to filter across the SWI, the rapid flow reversals shown in Figure 4-6 suggest that the residence time for coastal-derived dissolved constituents (i.e., DOM, DO, nutrients etc.) in the shallow sediments may not be sufficient for mineralization or

reaction to take place in the aquifer. Considering the phase-resolved groundwater flux measured during Period 1 (Figure 4-6a – c) and assuming one-dimensional vertical advective transport, it is estimated that the residence time for infiltrating water particles and associated dissolved constituents would be between < 1 – 70 seconds. This is considerably shorter than the residence time required for OM mineralization. For instance, *Anschutz, et al.* [2009] observed a residence time of about 7 tidal cycles (3.7 days) to be sufficient for mineralization of OM. Column experiments by *McLachlan, et al.* [1981] suggest this process may be slightly faster, wherein they determined that 35% of organic N was mineralized within a 50 cm partially saturated sand column. Based on the flow rate used, this equates to a residence time on the order of several hours. While these residence times are much larger than those associated with the phase-resolved fluxes, they are of similar magnitude to those associated with the wave-induced phase-averaged water exchange and flow processes. Simulated flow paths previously shown in Chapter 3 (Section 3.3.2) indicate that at peak wave conditions, residence times for the recirculating groundwater ranged from 4 hours to 160 days with an average residence time of 44 days. Thus, the fluxes induced by the phase-averaged effects of waves are likely more important for the processing of dissolved constituents including OM in the aquifer. The phase-averaged effects of waves are also likely more important for controlling the fate of terrestrially-derived nutrients discharging through the nearshore aquifer. The phase-averaged wave effects cause water to recirculate deeper into the aquifer than the phase-resolved effects and this enhances mixing between terrestrial groundwater and recirculating surface water [*Robinson, et al.*, 2014]. Redox gradients set up by this mixing have been shown to considerably modify the fate and ultimate flux of nutrients to coastal waters [*Anwar, et al.*, 2014]. Deep phase-averaged recirculations also increase the residence time of terrestrially-derived constituents by increasing dispersion as well as moving the terrestrial discharge zone further offshore [*Bakhtyar, et al.*, 2013; *Geng, et al.*, 2014]. This longer residence time may allow for increased transformation of species within the aquifer prior to discharge.

While it is expected that the phase-resolved wave-induced recirculations may be more important for the fate and transport of dissolved constituents in the nearshore aquifer, the phase-resolved rapid water exchange may be important for processing particulates such

as POM. The considerably larger total volume of water filtered through the shallow sediments by rapid phase-resolved, wave-driven exchange may be important for the transport of POM as sediment interactions including attachment, straining and electrostatic attraction may trap particles in the shallow sediment [*Molnar, et al.*, 2015]. For illustration, the 15 minute moving average of the shallow flux was integrated with time at A1 over the full duration of Period 1. Assuming upward flux equates entirely to exfiltration and downward flux to infiltration, the cumulative shallow net phase-averaged flux indicates $7 \times 10^{-3} \ m^3m^{-2}$ of exfiltration whereas the upward and downward flux components indicate $1.8 \times 10^{-2} \ m^3m^{-2}$ of exfiltration and $1.1 \times 10^{-2} \ m^3m^{-2}$ of infiltration, respectively. Thus, consideration of the unidirectional net flow neglects the input of constituents associated with infiltration. While the short residence time associated with rapid water exchange estimated above ($< 1 - 70$ seconds) is not sufficient for OM mineralization, trapping of POM in the shallow sediment may result in sufficiently long residence times for mineralization to occur.

4.4.2   Implications for fate of fecal bacteria at the SWI

Recreational use of nearshore waters is often impaired due high levels of fecal bacteria derived from human (e.g., wastewater, storm water) and non-human (e.g., gulls, dogs) sources [*International Joint Commission*, 2011]. Studies have shown that the occurrence of fecal indicator bacteria (FIB, e.g., *E. coli* and enterococci) positively correlate with harmful pathogens known to cause gastrointestinal illness in humans [*Cabelli, et al.*, 1982; *Wade, et al.*, 2003]. Although current water quality standards are based on FIB concentrations in the surface water, shallow sand and groundwater in the swash zone accumulate FIB with concentrations often several orders of magnitude larger than in the adjacent surface water [*Edge and Hill*, 2007; *Whitman and Nevers*, 2003]. The bacteria in the sand, while in itself is a potential health risk, may also act as a non-point source of contamination for the surface waters [e.g., *Edge and Hill*, 2007; *Phillips, et al.*, 2014; *Yamahara, et al.*, 2007]. Bacterial surface water quality has been shown to be closely related to the adjacent FIB concentrations in the sand indicating the transfer of FIB back-and-forth between the surface water and the sand [e.g., *Alm, et al.*, 2003; *Beversdorf, et al.*, 2007; *Ge, et al.*, 2010]. It is unclear whether it is a result of water exchange or

sediment resuspension; however, it is likely a combination of both [*Whitman, et al.*, 2014]. The accumulation and fate of FIB in beach sand is controlled by complex and interacting physical, chemical and microbial processes occurring at the SWI. While there has been considerable research regarding the survival and potential replication of FIB within beach sand, there is currently limited understanding of the physical mechanisms that control the accumulation of FIB in the beach sands and its subsequent release, although this understanding is required to predict the fate of fecal bacteria in a beach environment. Here field data was used to evaluate the potential importance of rapid wave-induced water exchange on the fate of FIB in the beach sand based on current understanding of microbial transport in saturated and unsaturated porous media.

The processes governing the transport of FIB in sand are similar to POM in that their mobility is influenced by sediment interactions including attachment and detachment. The large shallow groundwater velocities driven by phase-resolved wave effects likely play an important role in controlling the accumulation and later release of FIB in the shallow beach sands. For instance, the intermittent strong downward flux observed at A1 during Period 2 (Figure 4-6d) would deliver surface water and associated FIB into the beach sand via saturated and unsaturated infiltration. *Russell, et al.* [2012] inferred from column experiments conducted with high porewater velocities (10^0 cm/s) that swash infiltration may result in the detachment of FIB from unsaturated sediments, transporting them downward to the water table. They did not however attribute the high mobility to the large pore water velocity but rather, it was thought to be due to scouring from the wetting front. Shallow phase-resolved flux measurements at A1 indicate much lower velocities than used in the column experiments by *Russell, et al.* [2012] (on the order of 10^{-3} cm/s). Further, the downward flux that was measured may have been associated with minimal infiltration and caused rather by capillarity effects [*Turner and Nielsen*, 1997]. Nevertheless, FIB transport into the sand will still occur at A1 as the net flow was into the aquifer as indicated by both the net shallow and deep phase-averaged fluxes (Figure 2a). As the pore water velocity decreases, the relative strength of the attraction between bacteria and sand increases – thus increasing the likelihood of attachment. The characteristic rapid drop in FIB concentration with increasing depth below the water table

[e.g., *Alm, et al.*, 2003; *Whitman and Nevers*, 2003; *Whitman, et al.*, 2006] may therefore be attributed in part to the attenuation of the velocity with depth.

Although FIB concentrations are generally highest in sands in the upper regions of the swash zone where wave-induced infiltration dominates, FIB concentrations in sand are often still elevated relative to surface waters in the lower region of the swash zone and in some cases in shallow offshore sediments [*Whitman and Nevers*, 2003]. Although the phase-averaged measurements indicate that the net flow is upwards, resulting in exfiltration in the lower regions of the swash zone (i.e., Period 1 at A1-3 and Period 2 at A2 and A3), the large rapidly reversing phase-resolved groundwater fluxes may govern the exchange of bacteria to and from the sand. The large volume of water filtered through the shallow sediments due to phase-resolved wave effects provides more opportunity for bacteria to contact sand grains and become attached. On the other hand, the large phase-resolved groundwater flux measured near the SWI (e.g., Figure 7a-c) may also be favourable for detachment as high velocities increase shear forces acting on attached bacteria [*Bergendahl and Grasso*, 2000]. Once detached, the FIB may then be delivered to surface water via groundwater exfiltration [*Boehm, et al.*, 2004; *Russell, et al.*, 2012]. Steady flow column experiments by *Phillips, et al.* [2011] observed little detachment of enterococci at pore water velocities of 10^{-2} cm/s which by comparison was much larger than the shallow velocities we measured in the field of $10^{-4} - 10^{-3}$ cm/s (Period 1, A1-A3). While this result suggests that the magnitude of the velocities may not be sufficient for detachment to occur, detachment not only depends on pore-scale hydrodynamics, but also the solution chemistry [*Bradford, et al.*, 2014; *Torkzaban, et al.*, 2007]. For instance, studies have reported that attachment and detachment of different strains of *E. coli* and enterococci are influenced by solution pH and ionic strength [e.g., *Chen and Walker*, 2012; *Kim, et al.*, 2009; *Torkzaban, et al.*, 2008]. This may be important during large wave events where the mixing of groundwater and surface water end members via wave-induced recirculations may alter geochemical conditions near the SWI (as shown in Section 3.3.3). It is also important to note that shallow hydraulic gradients of similar magnitude to those measured in this study have also been measured near the SWI at coarser grained beaches – this would result in pore water velocities orders of magnitude larger that may therefore better promote detachment [e.g., *Turner and Masselink*, 1998].

The duration of attachment is also important as bacteria detachment rates decrease the longer they spend attached to sand grains due to increased adhesion [*Kumar, et al.*, 2013]. Thus there may be asymmetry in the attachment/detachment process.

4.5 Summary

Until recently, there has been little effort to understand the importance of waves at the phase-resolved frequency as it relates to the transport and fate of dissolved and particulate constituents and their flux to coastal waters [*Heiss, et al.*, 2014]. The data presented in this chapter explores the relationship between the phase-resolved and phase-averaged vertical fluxes in a permeable nearshore aquifer and illustrates the potential importance of these fluxes for the fate and transport of dissolved and particulate constituents. While the phase-averaged and phase-resolved wave effects are ultimately driven by the same wave forcing, they respectively manifest in low-frequency, deep groundwater recirculations and high-frequency shallow water exchange. Based on this, several key inferences were made:

- Residence times associated with phase-averaged groundwater recirculations are on the order of hours - months, providing sufficient time for reactive processes including OM decomposition to occur.
- Due to the attenuation of the rapid phase-resolved wave fluxes with depth in the aquifer, phase-averaged groundwater recirculations are likely more important for controlling the fate of terrestrially-derived pollutants that are transported deeper in the aquifer.
- While the phase-resolved wave-induced water exchange causes large volumes of surface water to filter through the shallow sediments, the fluxes are rapidly reversing and thus associated with short residence times ($<1 - 70$ seconds). The high fluxes may be important for particulates such as POM and fecal bacteria which have a tendency to become attached or strained in porous media. The attachment of POM may result in sufficient time for mineralization and subsequent regeneration of dissolved inorganic nutrients. Likewise, asymmetry associated with the rapidly

reversing fluxes may contribute to the accumulation of fecal bacteria in shallow beach sand.

- Large velocities associated with the phase-resolved wave-induced water exchange may also be important for the detachment of POM and bacteria. Thus a better understanding of the attachment/detachment processes near the SWI is required in order to effectively assess the fate of these particulate constituents.

4.6 References

Alm, E. W., J. Burke, and A. Spain (2003), Fecal indicator bacteria are abundant in wet sand at freshwater beaches, *Water research*, *37*, 3978-3982, doi: 10.1016/S0043-1354(03)00301-4.

Anschutz, P., T. Smith, A. Mouret, J. Deborde, S. Bujan, D. Poirier, and P. Lecroart (2009), Tidal sands as biogeochemical reactors, *Estuar. Coast. Shelf S.*, *84*, 84-90, doi: 10.1016/j.ecss.2009.06.015.

Anwar, N., C. Robinson, and D. A. Barry (2014), Influence of tides and waves on the fate of nutrients in a nearshore aquifer: Numerical simulations, *Adv. Water Resour.*, *73*, 203-213, doi: 10.1016/j.advwatres.2014.08.015.

Bakhtyar, R., D. A. Barry, and A. Brovelli (2012), Numerical experiments on interactions between wave motion and variable-density coastal aquifers, *Coast. Eng.*, *60*, 95-108, doi: 10.1016/j.coastaleng.2011.09.001.

Bakhtyar, R., A. Brovelli, D. A. Barry, C. Robinson, and L. Li (2013), Transport of variable-density solute plumes in beach aquifers in response to oceanic forcing, *Adv. Water Resour.*, *53*, 208-224, doi: 10.1016/j.advwatres.2012.11.009.

Baldock, T. E., A. J. Baird, D. P. Horn, and T. Mason (2001), Measurements and modeling of swash-induced pressure gradients in the surface layers of a sand beach, *Journal of Geophysical Research: Oceans (1978–2012)*, *106*, 2653-2666, doi: 10.1029/1999JC000170.

Baldock, T. E., and P. Holmes (1996), Pressure gradients within sediment beds, *Coastal Engineering Proc.*, *1*, doi: 10.9753/icce.v25.%25p.

Beck, A. J., Y. Tsukamoto, A. Tovar-Sanchez, M. Huerta-Diaz, H. J. Bokuniewicz, and S. A. Sanudo-Wilhelmy (2007), Importance of geochemical transformations in determining submarine groundwater discharge-derived trace metal and nutrient fluxes, *Appl. Geochem.*, *22*, 477-490, doi: 10.1016/j.apgeochem.2006.10.005.

Bergendahl, J., and D. Grasso (2000), Prediction of colloid detachment in a model porous media: hydrodynamics, *Chemical Engineering Science*, *55*, 1523-1532, doi: 10.1016/S0009-2509(99)00422-4.

Beversdorf, L., S. Bornstein-Forst, and S. McLellan (2007), The potential for beach sand to serve as a reservoir for Escherichia coli and the physical influences on cell die-off, *Journal of applied microbiology*, *102*, 1372-1381, doi: 10.1111/j.1365-2672.2006.03177.x.

Boehm, A. B., A. Paytan, G. G. Shellenbarger, and K. A. Davis (2006), Composition and flux of groundwater from a California beach aquifer: Implications for nutrient supply to the surf zone, *Continental shelf research*, *26*, 269-282, doi: 10.1016/j.csr.2005.11.008.

Boehm, A. B., G. G. Shellenbarger, and A. Paytan (2004), Groundwater discharge: potential association with fecal indicator bacteria in the surf zone, *Environ. Sci. Technol.*, *38*, 3558-3566, doi: 10.1021/es035385a.

Bradford, S. A., Y. Wang, H. Kim, S. Torkzaban, and J. Šimůnek (2014), Modeling microorganism transport and survival in the subsurface, *Journal of environmental quality*, *43*, 421-440, doi: 10.2134/jeq2013.05.0212.

Cabelli, V. J., A. P. Dufour, L. McCabe, and M. Levin (1982), Swimming-associated gastroenteritis and water quality, *Am. J. Epidemiol.*, *115*, 606-616.

Carsel, R. F., and R. S. Parrish (1988), Developing joint probability distributions of soil water retention characteristics, *Water Resour. Res.*, *24*, 755-769, doi: 10.1029/WR024i005p00755.

Charbonnier, C., P. Anschutz, D. Poirier, S. Bujan, and P. Lecroart (2013), Aerobic respiration in a high-energy sandy beach, *Mar. Chem.*, *155*, 10-21, doi: 10.1016/j.marchem.2013.05.003.

Charette, M. A., and E. R. Sholkovitz (2002), Oxidative precipitation of groundwater-derived ferrous iron in the subterranean estuary of a coastal bay, *Geophys Res. Lett.*, *29*, doi: 10.1029/2001gl014512.

Charette, M. A., and E. R. Sholkovitz (2006), Trace element cycling in a subterranean estuary: Part 2. Geochemistry of the pore water, *Geochem. Cosmochim. Acta*, *70*, 811-826, doi: 10.1016/j.gca.2005.10.019.

Chen, G., and S. L. Walker (2012), Fecal Indicator Bacteria Transport and Deposition in Saturated and Unsaturated Porous Media, *Environ. Sci. Technol.*, *46*, 8782-8790, doi: 10.1021/es301378q.

Conley, D. C., and J. G. Griffin (2004), Direct measurements of bed stress under swash in the field, *Journal of Geophysical Research: Oceans (1978–2012)*, *109*, doi: 10.1029/2003JC001899.

Crowe, A. S., and G. A. Meek (2009), Groundwater conditions beneath beaches of Lake Huron, Ontario, Canada, *Aquat. Ecosyst. Health Management*, *12*, 444-455, doi: 10.1080/14634980903354825.

Edge, T. A., and S. Hill (2007), Multiple lines of evidence to identify the sources of fecal pollution at a freshwater beach in Hamilton Harbour, Lake Ontario, *Water Research*, *41*, 3585-3594, doi:10.1016/j.watres.2007.05.012.

Elfrink, B., and T. Baldock (2002), Hydrodynamics and sediment transport in the swash zone: a review and perspectives, *Coast. Eng.*, *45*, 149-167, doi: 10.1016/S0378-3839(02)00032-7.

Ge, Z., M. B. Nevers, D. J. Schwab, and R. L. Whitman (2010), Coastal loading and transport of Escherichia coli at an embayed beach in Lake Michigan, *Environ. Sci. Technol.*, *44*, 6731-6737, doi: 10.1021/es100797r.

Geng, X., M. C. Boufadel, Y. Xia, H. Li, L. Zhao, and N. L. Jackson (2014), Numerical study of wave effects on groundwater flow and solute transport in a laboratory beach, *J. Contam. Hydrol.*, 37-52, doi: 10.1016/j.jconhyd.2014.07.001.

Gibbes, B., C. Robinson, L. Li, and D. Lockington (2007), Measurement of hydrodynamics and pore water chemistry in intertidal groundwater systems, *J. Coastal Res.*, 884-894.

Heiss, J. W., W. J. Ullman, and H. A. Michael (2014), Swash zone moisture dynamics and unsaturated infiltration in two sandy beach aquifers, *Estuar. Coast. Shelf S.*, 20-31, doi: 10.1016/j.ecss.2014.03.015.

Horn, D. P. (2006), Measurements and modelling of beach groundwater flow in the swash-zone: a review, *Continental shelf research*, *26*, 622-652, doi: 10.1016/j.csr.2006.02.001.

Horn, D. P., T. E. Baldock, A. J. Baird, and T. E. Mason (1998), Field measurements of swash induced pressures within a sandy beach, *Coastal Engineering Proc.*, *1*, doi: 10.9753/icce.v26.%25p.

Huettel, M., W. Ziebis, and S. Forster (1996), Flow-induced uptake of particulate matter in permeable sediments, *Limnol. Oceanogr.*, *41*, 309-322, doi: 10.4319/lo.1996.41.2.0309.

International Joint Commission (2011), 15th Biennial Report on Great Lakes Water Quality, Ottawa.

Kang, H.-Y., P. Nielsen, and D. J. Hanslow (1994), Watertable overheight due to wave runup on a sandy beach, *Coastal Engineering Proc.*, *1*, 2115-2124, doi: 10.9753/icce.v24.%25p.

Kim, H. N., S. A. Bradford, and S. L. Walker (2009), Escherichia coli O157: H7 transport in saturated porous media: Role of solution chemistry and surface macromolecules, *Environ. Sci. Technol.*, *43*, 4340-4347, doi: 10.1021/es8026055.

Kroeger, K., and M. Charette (2008), Nitrogen biogeochemistry of submarine groundwater discharge, *Limnol. Oceanogr.*, *53*, 1025-1039, doi: 10.4319/lo.2008.53.3.1025.

Krumbein, W., and G. Monk (1943), Permeability as a function of the size parameters of unconsolidated sand, *T. Am. Mining. Eng.*, *151*, 153-163, doi: 10.2118/943153-G.

Kumar, D., S. Bhattacharya, and S. Ghosh (2013), Weak adhesion at the mesoscale: particles at an interface, *Soft Matter*, *9*, 6618-6633, doi: 10.1039/c3sm00097d.

Lee, J., C. Robinson, and R.-M. Couture (2014), Effect of groundwater–lake interactions on arsenic enrichment in freshwater beach aquifers, *Environ. Sci. Technol.*, *48*, 10174-10181, doi: 10.1021/es5020136.

Li, L., and D. Barry (2000), Wave-induced beach groundwater flow, *Adv. Water Resour.*, *23*, 325-337, doi: 10.1016/S0309-1708(99)00032-9.

Li, L., D. Barry, F. Stagnitti, and J. Y. Parlange (1999), Submarine groundwater discharge and associated chemical input to a coastal sea, *Water Resour. Res.*, *35*, 3253-3259, doi: 10.1029/1999WR900189.

Longuet-Higgins, M. S. (1983), Wave set-up, percolation and undertow in the surf zone, *Proc. R. Soc. London*, *390*, 283-291, doi: 10.1098/rspa.1983.0132.

Masselink, G., and M. Hughes (1998), Field investigation of sediment transport in the swash zone, *Continental shelf research*, *18*, 1179-1199, doi: 10.1016/S0278-4343(98)00027-2.

Masselink, G., and J. A. Puleo (2006), Swash-zone morphodynamics, *Continental shelf research*, *26*, 661-680, doi: 10.1016/j.csr.2006.01.015.

McAllister, S. M., J. M. Barnett, J. W. Heiss, A. J. Findlay, D. J. MacDonald, C. L. Dow, G. W. Luther, H. A. Michael, and C. S. Chan (2015), Dynamic hydrologic and biogeochemical processes drive microbially enhanced iron and sulfur cycling within the intertidal mixing zone of a beach aquifer, *Limnol. Oceanogr.*, doi: 10.1002/lno.10029.

McLachlan, A., A. Dye, and B. Harty (1981), Simulation of the interstitial system of exposed sandy beaches, *Estuar. Coast. Shelf S.*, *12*, 267-278, doi: 10.1016/S0302-3524(81)80124-7.

McLachlan, A., I. G. Eliot, and D. J. Clarke (1985), Water filtration through reflective microtidal beaches and shallow sublittoral sands and its implications for an inshore ecosystem in Western-Australia, *Estuarine Coastal and Shelf Science*, *21*, 91-104, doi: 10.1016/0272-7714(85)90008-3.

McLachlan, A., and I. Turner (1994), The interstitial environment of sandy beaches, *Marine Ecology*, *15*, 177-212, doi: 10.1111/j.1439-0485.1994.tb00053.x.

Molnar, I. L., W. P. Johnson, J. I. Gerhard, C. S. Willson, and D. M. O'Carroll (2015), Predicting colloid transport through saturated porous media: A critical review, *Water Resour. Res.*, doi: 10.1002/2015WR017318.

Nielsen, P. (2002), Shear stress and sediment transport calculations for swash zone modelling, *Coast. Eng.*, *45*, 53-60, doi: 10.1016/S0378-3839(01)00036-9.

Nielsen, P. (2009), *Coastal and Estuarine Processes*, World Scientific Publishing Co. Pt2. Ltd., Singapore.

Nielsen, P., and S. L. Dunn (1998), Manometer tubes for coastal hydrodynamics investigations, *Coast. Eng.*, *35*, 73-84, doi: 10.1016/S0378-3839(98)00021-0.

Phillips, M. C., Z. Feng, L. J. Vogel, A. J. Reniers, B. K. Haus, A. A. Enns, Y. Zhang, D. B. Hernandez, and H. M. Solo-Gabriele (2014), Microbial release from seeded beach sediments during wave conditions, *Marine pollution bulletin*, *79*, 114-122, doi: 10.1016/j.marpolbul.2013.12.029.

Phillips, M. C., H. M. Solo-Gabriele, A. J. Reniers, J. D. Wang, R. T. Kiger, and N. Abdel-Mottaleb (2011), Pore water transport of enterococci out of beach sediments, *Marine pollution bulletin*, *62*, 2293-2298, doi: 10.1016/j.marpolbul.2011.08.049.

Reckhardt, A., M. Beck, M. Seidel, T. Riedel, A. Wehrmann, A. Bartholomae, B. Schnetger, T. Dittmar, and H.-J. Brumsack (2015), Carbon, nutrient and trace metal cycling in sandy sediments: A comparison of high-energy beaches and backbarrier tidal flats, *Estuarine Coastal and Shelf Science*, *159*, 1-14, doi: 10.1016/j.ecss.2015.03.025.

Richards, L. A. (1931), Capillary conduction of liquids through porous mediums, *Journal of Applied Physics*, *1*, 318-333, doi: 10.1063/1.1745010.

Robinson, C., P. Xin, L. Li, and D. A. Barry (2014), Groundwater flow and salt transport in a subterranean estuary driven by intensified wave conditions, *Water Resour. Res.*, *50*, 165-181, doi: 10.1002/2013WR013813.

Russell, T. L., K. M. Yamahara, and A. B. Boehm (2012), Mobilization and transport of naturally occurring enterococci in beach sands subject to transient infiltration of seawater, *Environ. Sci. Technol.*, *46*, 5988-5996, doi: 10.1021/es300408z.

Santos, I. R., W. C. Burnett, J. Chanton, B. Mwashote, I. G. N. A. Suryaputra, and T. Dittmar (2008), Nutrient biogeochemistry in a Gulf of Mexico subterranean estuary and groundwater-derived fluxes to the coastal ocean, *Limnol. Oceanogr.*, *53*, 705-718, doi: 10.4319/lo.2008.53.2.0705.

Santos, I. R., W. C. Burnett, T. Dittmar, I. G. Suryaputra, and J. Chanton (2009), Tidal pumping drives nutrient and dissolved organic matter dynamics in a Gulf of Mexico

subterranean estuary, *Geochem. Cosmochim. Acta*, *73*, 1325-1339, doi: 10.1016/j.gca.2008.11.029.

Santos, I. R., B. D. Eyre, and M. Huettel (2012), The driving forces of porewater and groundwater flow in permeable coastal sediments: A review, *Estuar. Coast. Shelf S.*, *98*, 1-15, doi: 10.1016/j.ecss.2011.10.024.

Slomp, C. P., and P. Van Cappellen (2004), Nutrient inputs to the coastal ocean through submarine groundwater discharge: controls and potential impact, *J. Hydrol.*, *295*, 64-86, doi: 10.1016/j.jhydrol.2004.02.018.

Sous, D., A. Lambert, R. Vincent, and H. Michallet (2013), Swash-groundwater dynamics in a sandy beach laboratory experiment, *Coast. Eng.*, 122-136, doi: 10.1016/j.coastaleng.2013.05.006.

Spiteri, C., C. P. Slomp, M. A. Charette, K. Tuncay, and C. Meile (2008), Flow and nutrient dynamics in a subterranean estuary (Waquoit Bay, MA, USA): field data and reactive transport modeling, *Geochem. Cosmochim. Acta*, *72*, 3398-3412, doi: 10.1016/j.gca.2008.04.027.

Torkzaban, S., S. A. Bradford, and S. L. Walker (2007), Resolving the coupled effects of hydrodynamics and DLVO forces on colloid attachment in porous media, *Langmuir*, *23*, 9652-9660, doi: 10.1021/la700995e.

Torkzaban, S., S. S. Tazehkand, S. L. Walker, and S. A. Bradford (2008), Transport and fate of bacteria in porous media: Coupled effects of chemical conditions and pore space geometry, *Water Resour. Res.*, *44*, doi: 10.1029/2007WR006541.

Turner, I. L. (1998), Monitoring groundwater dynamics in the littoral zone at seasonal, storm, tide and swash frequencies, *Coast. Eng.*, *35*, 1-16, doi: 10.1016/S0378-3839(98)00023-4.

Turner, I. L., and G. Masselink (1998), Swash infiltration-exfiltration and sediment transport, *J. Geophys. Res.-Oceans*, *103*, 30813-30824, doi: 10.1029/98JC02606.

Turner, I. L., and P. Nielsen (1997), Rapid water table fluctuations within the beach face: Implications for swash zone sediment mobility?, *Coast. Eng.*, *32*, 45-59, doi: 10.1016/S0378-3839(97)00015-X.

van Genuchten, M. T. (1980), A closed-form equation for predicting the hydraulic conductivity of unsaturated soils, *Soil Sci. Soc. Am. J.*, *44*, 892-898, doi: 10.2136/sssaj1980.03615995004400050002x.

Wade, T. J., N. Pai, J. N. Eisenberg, and J. M. Colford Jr (2003), Do US Environmental Protection Agency water quality guidelines for recreational waters prevent

gastrointestinal illness? A systematic review and meta-analysis, *Environ. Health Persp.*, *111*, 1102.

Whitman, R. L., V. J. Harwood, T. A. Edge, M. B. Nevers, M. Byappanahalli, K. Vijayavel, J. Brandao, M. J. Sadowsky, E. W. Alm, and A. Crowe (2014), Microbes in beach sands: integrating environment, ecology and public health, *Rev. Environ. Sci Bio/Tech.*, *13*, 329-368, doi: 10.1007/s11157-014-9340-8.

Whitman, R. L., and M. B. Nevers (2003), Foreshore sand as a source of Escherichia coli in nearshore water of a Lake Michigan beach, *Appl. Environ. Microbio.*, *69*, 5555-5562, doi: 10.1128/AEM.69.9.5555-5562.2003.

Whitman, R. L., M. B. Nevers, and M. N. Byappanahalli (2006), Examination of the watershed-wide distribution of Escherichia coli along southern Lake Michigan: an integrated approach, *Appl. Environ. Microbio.*, *72*, 7301-7310, doi: 10.1128/AEM.00454-06.

Xin, P., C. Robinson, L. Li, D. A. Barry, and R. Bakhtyar (2010), Effects of wave forcing on a subterranean estuary, *Water Resour. Res.*, *46*, doi: 10.1029/2010WR009632.

Yamahara, K. M., B. A. Layton, A. E. Santoro, and A. B. Boehm (2007), Beach sands along the California coast are diffuse sources of fecal bacteria to coastal waters, *Environ. Sci. Technol.*, *41*, 4515-4521, doi: 10.1021/es062822n.

Chapter 5

5 Summary and Recommendations

5.1 Summary

Wave-induced groundwater flows in permeable nearshore aquifers play an important role in regulating the transport and fate of pollutants discharging and recirculating across the groundwater-coastal water interface. In this thesis, field work conducted at Ipperwash Beach over a wave event was combined with numerical modelling to address two distinct research objectives.

The first objective focused on quantifying the impact of a wave event on groundwater flows and geochemical conditions in a permeable beach aquifer and using field data to validate a simplified numerical modeling approach for simulating wave effects. Field data of phase-averaged vertical hydraulic gradients indicate that nearshore groundwater flow behaviour is strongly perturbed by a wave event. Data, combined with the numerical simulation results indicate the development of a wave-induced groundwater recirculation cell that grew in response to increased wave height. The water exchange across the sediment-water interface (SWI) also increased as the wave height increased. The groundwater recirculations then diminished as the wave height subsided with the groundwater flow behaviour rapidly returning to the pre-event calm conditions. A comparison of the measured and modelled vertical hydraulic gradients indicates that the simplified wave setup modelling approach adopted is able capture the phase-averaged effects of waves on nearshore groundwater flows. This is the first field data set that captures the phase-averaged effects of waves and in doing so supports the wave setup modeling approach used in several other numerical studies.

Field measurements of redox (ORP) and pH over the wave event illustrated the influence of unsteady wave conditions and subsequent groundwater recirculations on the geochemistry in the shallow permeable beach aquifer. While groundwater 0.2 m below the SWI was initially oxidizing it transitioned to reducing conditions during the wave event. Conversely, at 0.5 m depth, the initially reducing conditions became more reduced.

The simulated groundwater flow paths and the measured hydraulic gradients indicate that the observed changes in redox and pH may have been due in part to the upwelling of deeper and potentially more reducing groundwater. In addition, the increased influx of surface water into the aquifer is a potential source of organic matter. Organic matter mineralization may have contributed to the onset of reducing conditions near the SWI. The wave-induced geochemical dynamics in the shallow aquifer may have important implications for various reactive processes including Fe redox cycling and nitrification/denitrification, and thus impact the ultimate flux of pollutants such as nutrients and metals to coastal waters. Unlike the groundwater flow patterns, the measured geochemical parameters did not return to pre-wave event conditions after the waves subsided suggesting that unsteady wave forcing may have longer lasting effects on geochemical conditions and reactive constituents in a nearshore aquifer.

The second objective was to evaluate the potential importance of high frequency (i.e., phase-resolved) wave effects at the SWI on chemical and microbial fluxes in a nearshore aquifer. Phase-resolved wave effects near the SWI are generally overlooked by researchers examining contaminant transport in coastal aquifers. This objective was addressed by measuring deep phase-averaged vertical hydraulic gradients which represent the groundwater recirculations driven by wave setup and comparing these with high frequency shallow vertical hydraulic gradient measurements near the SWI. Field data indicate that the phase-resolved wave effects result in large shallow groundwater velocities and account for considerably higher flux of water to exchange across the SWI in comparison to the net phase-averaged flux. However, the phase-resolved fluxes are rapidly reversing, resulting in short residence times (estimated between $< 1 - 70$ seconds). While the short residence time may not be sufficient for processing dissolved constituents in the aquifer [e.g., *Anschutz, et al.*, 2009; *McLachlan, et al.*, 1981], particulates may become attached or strained in the beach sediment. This may have important implications for particulate organic matter (POM). For instance, sediment interactions increases the residence time of the particles relative to the rapid water exchange and consequently may allow more time for mineralization and the subsequent regeneration of dissolved nutrients. Similarly, the fate of fecal bacteria in a beach environment is strongly influenced by attachment and detachment to and from sand. It is

proposed that the rapid water exchange across the swash zone coupled with the attenuation of groundwater velocity with depth may result in the accumulation of bacteria in the shallow swash zone sediments. Conversely the high velocities near the SWI may also important for the detachment and subsequent release of bacteria to adjacent surface waters.

5.2   Recommendations

The work presented in Chapter 3 advances the understanding of the role of transient wave forcing on groundwater flow and geochemistry in a permeable unconfined nearshore aquifer. The field data was able to support the phase-averaged modelling approach adopted to simulate the effects of waves on the groundwater flows. A more quantitative analysis of the geochemical dynamics would be beneficial for understanding the mechanisms by which waves affect chemical transport and transformation. The following recommendations are aimed at addressing this gap:

- While links were proposed between the groundwater flows and the geochemical conditions over the wave event, further quantitative analysis is required. In future studies, it would be beneficial to monitor not only basic physico-chemical parameters but also concentrations of chemical constituents that are known to affect the geochemical conditions such as dissolved oxygen (DO), Fe^{2+}, organic matter etc. This would provide more quantitative evidence of how transient wave forcing influence the transport and fate of chemicals discharging to coastal waters through a nearshore aquifer.

- This study only examined the effect of a single isolated wave event on the groundwater flows and shallow geochemistry. Previous work, however, has shown that the antecedent conditions (i.e., historical wave effects) are important for groundwater and solute transport in coastal aquifers [*Xin, et al.*, 2014]. While the groundwater flows were observed to return rapidly to pre-event conditions following the wave event, the long term effects on the geochemical conditions in a nearshore aquifer remains unclear. It is therefore recommended that redox and pH be monitored in addition to chemical constituents (e.g., organic matter, DO, nutrients, Fe^{2+}) for a

longer time period, prior to and after the wave event, to assess the full impact a wave event may have on the fate of coastal groundwater pollutants.

Chapter 4 of this thesis explored the relative importance of phase-averaged and phase-resolved wave effects on the fate of chemical and microbial constituents transported through the shallow beach sediments. Implications for particulate constituents including POM and fecal bacteria were discussed because these constituents are important for nutrient cycling in coastal environments and recreational water quality, respectively. While the measurement of phase-resolved and phase-averaged groundwater fluxes provided important insight into the wave-induced processes that may govern the fate of these particulate constituents, the analysis was mostly qualitative. For further understanding of the importance of the different flow characteristics (i.e., phase-resolved or phase-averaged) the following is recommended:

- Quantifying the phase-averaged and phase-resolved effects of waves require different approaches for field monitoring and also numerical simulation. For instance if one is interested in quantifying the phase-averaged effects of waves in the field, only simple instrumentation is required (i.e., nested piezometers). On the other hand, capturing the phase-resolved effects of waves in the field requires the collection of large amounts of data at a high sampling frequency, thus requiring a more sophisticated monitoring strategy. Similarly, numerical simulations adopting the phase-averaged approach require considerably less computational effort than the phase-resolved approach. This study has shown that there are instances for which using one approach over the other may be required or more appropriate. Given the attenuation of the phase-resolved wave effects in the aquifer it is recommended that the phase-averaged wave effects be considered for the transport of dissolved constituents through a nearshore aquifer. In many cases this is already the status quo [e.g., *Anwar, et al.*, 2014; *Robinson, et al.*, 2014; *Xin, et al.*, 2014]. However, near the SWI the flows are considerably more complex and therefore the phase-resolved approach should be considered when investigating the fate of particulate constituents transported through the shallow nearshore sediments.

- A more quantitative analysis of the conditions that promote the attachment and detachment of particulates in beach sediment subject to wave-driven water exchange is needed. While some experimental and numerical studies exist that assess the transport of particulates through saturated and unsaturated porous media none have examined the high frequency, high velocity effects, such that are produced by the phase-resolved wave effects. It is recommended that a pore-scale force balance [e.g., *Bergendahl and Grasso*, 2000] be conducted using the groundwater flux datasets presented in this study to assess the conditions favourable for attachment and detachment. Findings would be applicable to POM and microbial bacteria as both exhibit colloidal properties.

5.3 References

Anschutz, P., T. Smith, A. Mouret, J. Deborde, S. Bujan, D. Poirier, and P. Lecroart (2009), Tidal sands as biogeochemical reactors, *Estuar. Coast. Shelf S.*, *84*, 84-90, doi: 10.1016/j.ecss.2009.06.015.

Anwar, N., C. Robinson, and D. A. Barry (2014), Influence of tides and waves on the fate of nutrients in a nearshore aquifer: Numerical simulations, *Adv. Water Resour.*, *73*, 203-213, doi: 10.1016/j.advwatres.2014.08.015.

Bergendahl, J., and D. Grasso (2000), Prediction of colloid detachment in a model porous media: hydrodynamics, *Chemical Engineering Science*, *55*, 1523-1532, doi: 10.1016/S0009-2509(99)00422-4.

McLachlan, A., A. Dye, and B. Harty (1981), Simulation of the interstitial system of exposed sandy beaches, *Estuar. Coast. Shelf S.*, *12*, 267-278, doi: 10.1016/S0302-3524(81)80124-7.

Robinson, C., P. Xin, L. Li, and D. A. Barry (2014), Groundwater flow and salt transport in a subterranean estuary driven by intensified wave conditions, *Water Resour. Res.*, *50*, 165-181, doi: 10.1002/2013WR013813.

Xin, P., S. S. J. Wang, C. Robinson, L. Li, Y. G. Wang, and D. Barry (2014), Memory of past random wave conditions in submarine groundwater discharge, *Geophys Res. Lett.*, *41*, 2401-2410, doi: 10.1002/2014GL059617.

Appendices

Appendix A: Governing equations for numerical model

FEFLOW was used to simulate variably saturated groundwater flow in an unconfined coastal aquifer. FEFLOW is a finite element model developed by *Diersch* [2005]. The following equations govern groundwater flow in saturated and unsaturated media.

Unconfined saturated groundwater flow:

The following equation is based on the assumption of a homogeneous, isotropic aquifer with flow occurring in two dimensions (*x, z*).

$$S_s \frac{\partial h}{\partial t} = K\left[\frac{\partial}{\partial x}\left(\frac{\partial h}{\partial x} \right) + \frac{\partial}{\partial z}\left(\frac{\partial h}{\partial z} \right) \right] \qquad (A1)$$

Ss is the specific storage [L^{-1}], *t* is time [T], *K* [LT^{-1}] is the hydraulic conductivity, *h* is the hydraulic head [L].

Unsaturated groundwater flow:

FEFLOW resolves unsaturated groundwater flow using the two dimensional (*x, z*) head-based form of the Richards Equation:

$$C(\psi) \frac{\partial \psi}{\partial t} = \frac{\partial}{\partial x}\left[K(\psi)\left(\frac{\partial \psi}{\partial x} \right) \right] + \frac{\partial}{\partial z}\left[K(\psi)\left(\frac{\partial \psi}{\partial z} + 1 \right) \right] \qquad (A2)$$

where $C(\psi) = \dfrac{\partial \theta}{\partial \psi}$ refers to the specific moisture capacity function, θ is the volumetric moisture content [-], ψ [L] is the pressure head, *t* is time [T], *z* is the coordinate in the vertical direction [L]

The specific moisture capacity function requires estimation of the pressure, saturation relationship unique to each soil type. The van Genuchten model [*van Genuchten*, 1980]

(A3) was chosen because it is one of the most commonly used approaches and data for parameter inputs are widely available. The relationship is as follows:

$$s_e = \frac{(s - s_r)}{(s_s - s_r)} = \begin{cases} [1 + (-\alpha \psi)^n]^{-m}, \psi < 0 \\ 1, \psi \geq 0 \end{cases} \quad \text{(A3)}$$

$$m = 1 - \frac{1}{n}$$

$$K_r = s_e^{0.5}[1 - (1 - s_e^{\frac{1}{m}})^m]^2 \quad \text{(A4)}$$

where s is the saturation [-], s_r is the residual saturation [-], s_s is the maximum saturation [-], s_e is the effective saturation, ψ is the pressure head [L], K_r is the relative hydraulic conductivity [LT^{-1}], m [-], n [-], α [L^{-1}] are fitting parameters. In FEFLOW, the van Genuchten model is paired with the relative hydraulic conductivity (K_r, A4) approximation from *Mualem* [1976].

References

Diersch, H. (2005), *FEFLOW finite element subsurface flow and transport simulation system*.

Mualem, Y. (1976), A new model for predicting the hydraulic conductivity of unsaturated porous media, *Water Resour. Res*, *12*, 513-522, doi: 10.1029/WR012i003p00513.

van Genuchten, M. T. (1980), A closed-form equation for predicting the hydraulic conductivity of unsaturated soils, *Soil Sci. Soc. Am. J.*, *44*, 892-898, doi: 10.2136/sssaj1980.03615995004400050002x.

Curriculum Vitae

Name:	Spencer Saron Malott
Post-secondary Education and Degrees:	University of Western Ontario London, Ontario, Canada 2009 – 2013 BESc.
Honours and Awards:	Natural Science and Engineering Research Council of Canada Undergraduate Student Research Award 2012
	Ontario Graduate Scholarship 2013 – 2014
	Natural Science and Engineering Research Council of Canada Canadian Graduate Scholarship (Masters) 2014 – 2015
Related Work Experience	Teaching Assistant The University of Western Ontario 2013 – 2015